The effects of ultrasound on the spread of intramuscularly injected formulations

Kuo Zhang

A Thesis submitted for the degree of
Master of Science
at the University of Otago, Dunedin,
New Zealand

July 2019

ABSTRACT

Context: The intramuscular (IM) injection is an important route of drug administration. Some researchers have suggested that the erratic rate of drug absorption from oil-based IM injections is due to variability in the spread of the formulations from the injection site. Recently, the application of ultrasound (US) has been investigated as a possible strategy to enhance the spread of IM injected formulations and thereby reduce variability in drug absorption.

Objective: The aim of the research reported in this thesis was to investigate the effects of US on the spread of IM injected formulations.

Methods: For in vitro experiments, transparent agarose gel was used as the matrix. Both Nile blue(aqueous) solution (0.001% w/w) and Nile red(oily) solutions (0.01% w/w) were prepared and injected into gels. The area of spread of injected formulations was photographically recorded and measured immediately after injection. US (1.1 MHz, 3 W/cm^2) was then applied to the injection site using a 6 min on-off working cycle for 60 min after which the area of spread was measured again. Areas of spread determined as mean ± standard deviation before and after US treatment were compared. For in vivo experiments, three Wether lambs (6 to 8 months old, 32 kgs approx.) were subjected to IM injections post-mortem. Three different types of formulation (Lipiodol: ethyl esters of iodized fatty acid of poppy seed oil, 48% w/v iodine; oily suspension: barium sulfate in Miglyol 812, 30% w/w; and a self-emulsifying drug delivery system (SEDDS): mixture of Lipiodol, Maisine and Miglyol, 40:20:40%, w/w)) were prepared and two different injection volumes (1.5 and 4.5 mL) injected into muscle. US (1.1 MHz, 3 W/cm^2, 100% working cycle) was applied for 0, 5 and 10 min at the injection site and the spread of formulations visualized by CT scan and measured before and after US application. The collected data was analysed using two-way ANOVA and Tukey test for post -hoc statistical analysis. Muscle tissue containing injected formulations was frozen in liquid nitrogen and subsequently examined by dissection.

Results: In the in vitro study, 60 minutes after injection, the spread of both aqueous and oily solutions remained unchanged after application of US. In the post-mortem study,

the initial spread showed no significant difference between either type of formulation or injection volume. After application of US for 5 min, a significant increase in spread was observed for the oily suspension and SEDDS using an injection volume of 4.5 mL; after exposure to US for 10 min, significant increases in spread were found for the oily suspension and SEDDS at both 1.5 and 4.5 mL injection volumes. The subsequent dissection revealed a large amount of injected formulation outside the injected muscle bundle resulting from spread along the fat layer and into the inter-muscle space.

Conclusion: There is no effect of US on the spread of formulations injected into agarose gel. In the post-mortem study, the CT scan proved to be suitable to visualize the spread of IM injected formulations. The initial spread of the IM injected oil formulations showed high variation. US-induced spread was observed for the oil suspension and SEDDS. The mechanism behind the enhanced spread needs further investigation but could be related to the ability of applied US to reduce the viscosity of the injected formulations or to the transfer of the mechanical energy of US to surface energy.

ACKNOWLEDGEMENT

This thesis was carried in both School of Pharmacy and Applied Science Department, University of Otago, Dunedin, New Zealand, over the period September 2015 to July 2019. I would like to take this special opportunity to express my sincere thanks and appreciation to my supervisors, Dr. Olaf Bork, Professor Ian Tucker and Dr. Rohit Jain. It has been a unique experience about not only gaining knowledge but also how to become an independent researcher. It is a gift and I am grateful. Also my appreciation goes to many people who have offered their time, effort and knowledge to help me. Paricularly, Dr. Himang Mujoo for his expertise in ultrasound and drug delivery, Dr. Paul Fawcett for this experience and knowledge in pharmacy and scientific writing. As a part-time research thesis, it is difficult to balance life, work and research. I could have never done this without their patience, guidance and support.

I am also grateful to the technical and academic staff in both School of Pharmacy and Applied Science Department, University of Otago, Dr. Azam Ali and Kevin Crump for their consistent support and assistance.

A very special gratitude goes out to my parents, Ms. Lin Jiang and Mr. Yibin Zhang, for their continuous support and unconditional love. And finally, to my girlfriend Miss Zhen Wang, my eternal cheerleader, your voice brings me courage.

TABLE OF CONTENTS

LIST OF FIGURES

LIST OF TABLES

LIST OF ABBREVIATIONS

A	Absorbance
ADME	Absorption, distribution, metabolism and excretion.
ANOVA	Analysis of the variance
cm	centimeter
CT	Computed tomography
dB	Decibel
Df	Degree of freedom
F	formulation
g	gram
Hz	Hertz
IM	Intramuscular
kHz	Kilohertz
L	length
λ	wavelength
m	meter
mg	Milligram

MHz	Million hertz
min	Minute
mL	Millilitre
MRI	Magnetic resonance imaging
MS	Mean squared error
nm	Nanometer
o/w	Oil in water
PA	pascal
SEDDS	Self-emulsifying drug delivery system
s	Second
SS	Sum of squares
US	Ultrasound
V	volume
W	Work
WC	Working cycles
w/o	Water to oil
w/v	Weight to volume
w/w	Weight to weight

°C	Celsius degree
μg	microgram
μL	microliter

CHAPTER ONE
INTRODUCTION

1.1 BACKGROUND

The intramuscular (IM) injection is an important means of drug administration for vaccines, antibiotics and hormones. The sites of IM injection include the deltoid, lateral gluteal, vastus lateralis and posterior gluteal muscles (Morrissey 2011). Unfortunately the rate of IM drug absorption is somewhat erratic (Zuidema et al. 1994) leading to highly variable arterial drug concentrations (Zuidema et al. 1994). A satisfactory explanation for this variable rate of IM absorption has yet to be found although research suggests it arises due to variability in the spread of IM injected formulations (Gehling et al. 2018).

Absorption, distribution, metabolism, and excretion (ADME) have been the main focus of research into the pharmacokinetics of drugs delivered by IM injection. In most situations, absorption is described as the process by which a drug moves from the injection site into surrounding blood capillaries. However, some literature indicates that spread of the injectate must take place before absorption begins and has a significant effect on the subsequent absorption (Darville et al. 2016). In clinical practice, the process of injection pushes the injectate into the targeted muscle bundle to create and fill a cavity often described as the injection depot. Spread then follows the pressure gradient and depends on the injection site and injection volume. Due to the elasticity of muscle, sometimes the injectate can be lost from the muscle by being squeezed back along the needle track and/or spreading outside the muscle bundle i.e. there is intra- and extra-muscular spread. Whatever the case, spread is usually finished quickly and is followed by absorption of drug into the surrounding capillaries.

Descriptions of spread based on observational studies have varied. Brown et al. 1944 stated that IM injected oils tend to accumulate along fascial sheaths and, to some extent, between muscle bundles. Later, Berton 1968 compared the spreading of oil and water-based formulations and found the latter spread immediately whereas the former tended to form a sphere-shaped deposit around the needlepoint. Svendesen 1979 showed that IM injections of low viscosity oil spread between muscle fibers and around fascicles and Howard, 1983 showed that arachis oil given by IM injection to rabbits spreads more slowly, probably due to its higher viscosity, than ethyl oleate. More recently, it was again reported that IM injected formulations can squeeze back along the

track of the needle eventually leading to leakage into extra-muscular tissue (Bjerregaard et al. 2001, Gehling et al. 2018).

The main problem of administration of drugs by IM injecction is the erratic nature of the spread of their formulations. A few attempts have been made to overcome this erratic spread particularly as it relates to formulations in an oily medium. One researcher suggested that using deep, firm massage of the tissue around the injection site would facilitate more consistent absorption (Zelman 1961). Recently, the application of ultrasound (US) has been suggested as a potentially useful strategy to improve the uniformity of spread of various types of formulation in tissue (Frenkel et al. 2000a).

Medical research has shown that US usually gives rise to both thermal and non-thermal effects on human tissue (Baker et al. 2001, O'Brien Jr 2007). To study the thermal effect, Draper 1995 determined the temperature 30 mm under the skin during application of 1 MHz, 1.5 W/cm^2 US to the skin of the human upper arm. They found that after 10 min of continuous US exposure the temperature increased by 5°C (Draper et al. 1995). Robinson et al, 1995 observed an increased blood flow in the skeletal muscle of healthy human volunteers after application of 1.5 W/cm^2 US for 5 min. Also Frenkel et al, 2001 showed that US can increase the mass transport of silver particles in the tissue of fish. The non-thermal effects of US are related to its mechanical effects, in particular the process of cavitation. However, it is well known that cavitation is very difficult to induce in vivo without the use of a gas bubble agent (Miller et al. 2002). Although US has the potential to enhance spread, there is no direct evidence that it actually enhances the spread of formulations in muscle tissue.

In this thesis, the spreads of various types of formulations administered by IM injection were studied in vitro in gels and muscle pieces and in vivo in animals immediately post-mortem. The influence of exposure to 1.1 MHz US for various lengths of time on the spread of the formulations was also studied. In this Chapter, aspects of muscle structure relevant to the spread of IM injections (Section 1.2), the mechanisms suggested for their spreading (Section 1.3), US and its effects (Section 1.4), the challenges of visualizing the spread (Section 1.5) and formulation considerations

(Section 1.6) are described. Research questions and the hypotheses of the thesis are then given in Section 1.7.

1.2 ANATOMY OF MUSCLE

As shown in Figure 1-1, skeletal muscle is surrounded by a connective tissue layer called the fascia. Epimysium is specialized fascia and ensheaths the entire muscle. The muscle contains multiple bundles called fascicles each of which is surrounded by another connective tissue layer called the perimysium. Within each fascicle, individual muscle cells take the form of fibres which are surrounded by the endomysium, the third layer of connective tissue (Fratzl 2008). All above connective tissue layers contain capillaries, nerves and lymph (Robert Schleip 2012). The thickness of the perimysium is reported to be 30-40 µm in human muscle (Fang et al. 1999) whereas the thickness of the endomysium is in the range 0.2-1.0 µm (Schmalbruch et al. 1974).

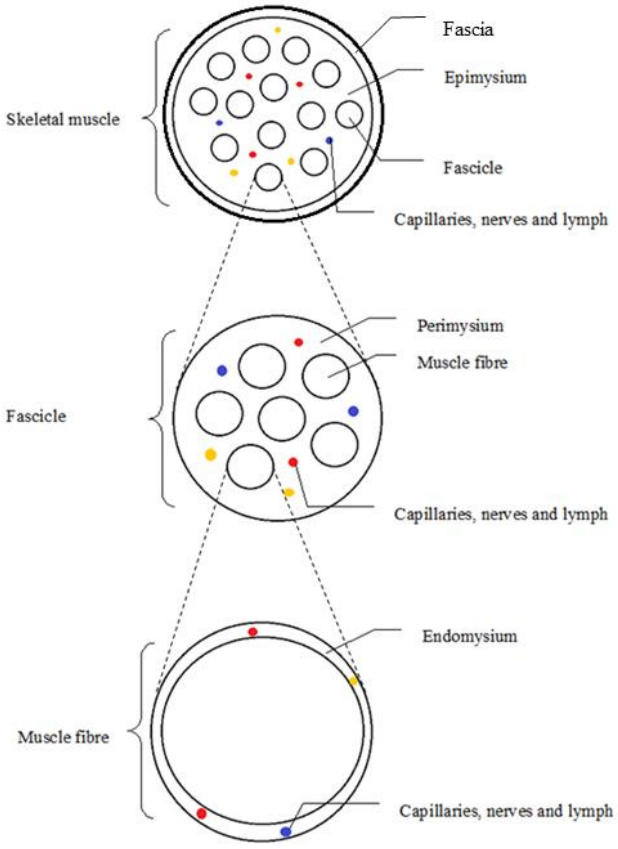

Figure 1-1Schematic diagram of a cross section of muscle tissue.

Although the microanatomy of muscle tissue is not the main focus of this thesis, a few important points are worth mentioning because they relate to the spread of IM injected formulations. First, the water content and its distribution in muscle have an influence on the spread of an IM injected formulation because water can act as a solvent (Zuidema et al. 1988). Lean muscle contains approximately 75% water (Rajanayagam et al. 1991), most of which (85%) is located within the muscle fibre (Pearce et al. 2011) with only some 15% being found between the muscle fibres and the inter-fascicular space (Offer et al. 1983). Secondly, the thickness and length of the intermuscular fat layer can affect spread since they vary depending on the percentage of body fat and the injection site.

1.3 MECHANISM OF SPREAD

1.3.1 General mechanics of IM Injection

From a mechanical point of view, the spread of a formulation administered by IM injection is a simple process (Figure 1.2). In using a syringe, injectate receives both pushing force and shear force. The shear force comes from the wall of the syringe and needle. The shear force increases while the injectate is being pushed through the needle due to the diameter of needle being much smaller than syringe. After the needle has pierced through the skin and subcutaneous tissue, it reaches the target muscle. The injectate is pushed out from the needle, then forms an injection depot. The injection depot experiences a force of resistance resulting from elasticity of the muscle. After the injection is finished and the pushing force from the syringe is no longer present, the injectate is pushed by the elasticity of muscle into tissue with less resistance, such as the needle hole and connective tissue layers. In the muscle the depot, once formed, is surrounded by a matrix filled with water.

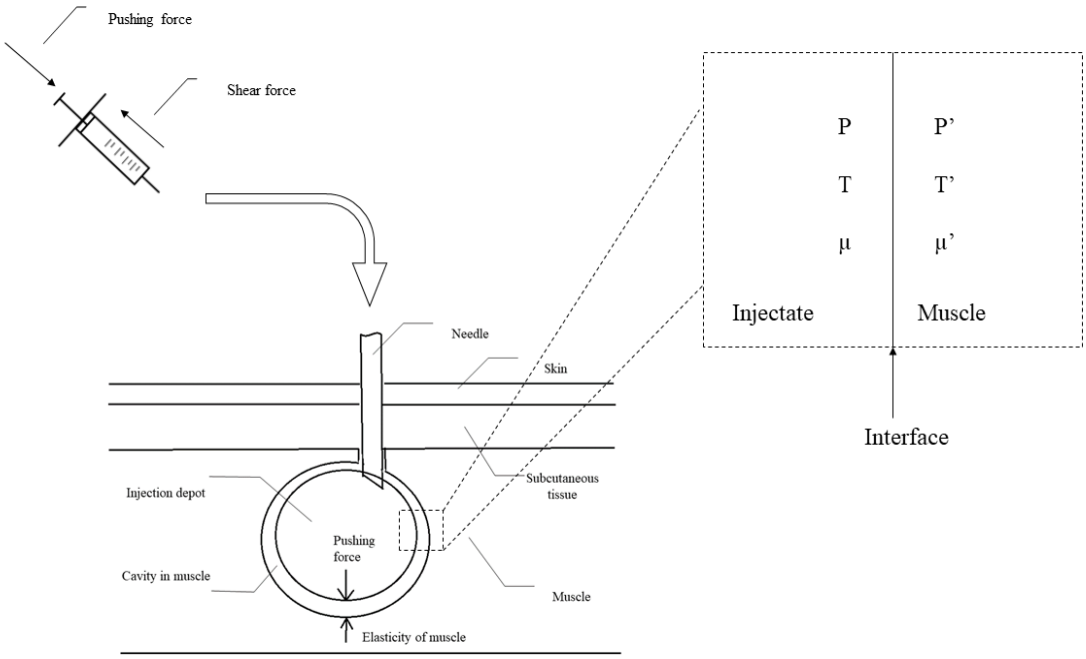

Figure 1-2 Diagram shows basic mechanics of IM injection.

Depending on the type of formulation injected, there can then be various types of interface between the depot and the surrounding matrix. If the formulation is aqueous, a water-water interface is formed whereas if it is oily, an oil-water interface is formed. The following behaviour of the injection depot can be explained in two theories: mass transfer (Section 1.3.2), free surface energy and surface tension (Section 1.3.3).

1.3.2 Mass transfer

In this thesis, mass transfer is the movement of molecules of a fluid in muscle. In general, mass transfer is a kinetic process, occurring in systems that are not at equilibrium. In order to understand the thermodynamic basis of mass transfer, consider an isolated system shown in Figure 1-3.

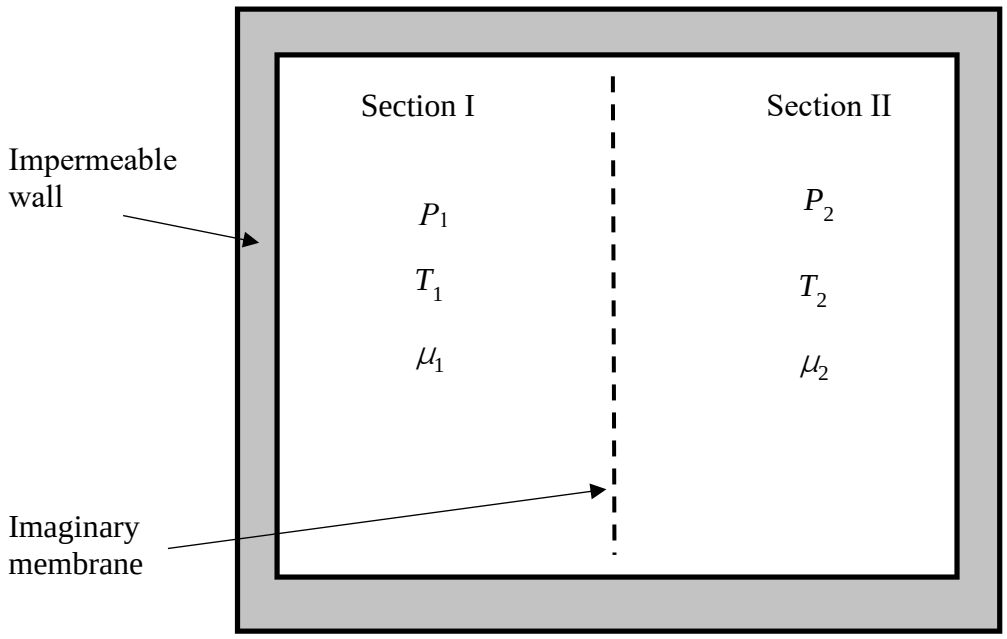

Figure 1-3 Isolated system consisting of two sections separated by an imaginary permeable membrane. At equilibrium, the temperature (T), pressure (P), and chemical potentials of each of the species in the system are equal in the two sections (Gordon L. Amidon 2000)

The isolated system is bounded by an impermeable wall which stops the transfer of matter, heat, or mechanical energy. The system is separated into two sections of equal volume, as labelled I and II in Figure 1-3. The sections are separated by an imaginary membrane, which is permissive to the transfer of mass, heat, and mechanical energy. At equilibrium, the temperatures, T, pressures, P, and chemical potentials, μ, of the species are equal in two sections.

If this isolated system is unperturbed, it will remain at this thermodynamic equilibrium indefinitely. Suppose that the pressure in section I is increased, which means $P_1 > P_2$, while the temperatures and all chemical potentials remain equal in the two sections. Thermodynamics asserts that as a result of this perturbation the system will change in an attempt to establish a new equilibrium condition (Gordon L. Amidon 2000). One of the simplest changes that can be imagined is the re-equilibration of the two pressures P_1 and P_2, with no change in the values of the temperatures or chemical potentials. If the imaginary membrane is fully permeable to the fluids in the system, the re-equilibration of the pressures will occur through the flow of fluid from section I to section II, which

will continue until the values of P_1 and P_2 are again equal. This flow of fluid in response to a spatial gradient in pressure is called convection (Gordon L. Amidon 2000).

Suppose that the chemical potential of one the species, A, is now increased in section I so that $\mu_1 > \mu_2$. The system is perturbed from equilibrium and will change in order to establish a new equilibrium. One of the simplest changes is the re-equilibration of the chemical potentials of species A, without change in the other variables. If the imaginary membrane is permeable to species A, the re-equilibration will occur through the movement of A from section I to section II, which will continue until the chemical potentials are equal again. This movement of mass in response to a spatial gradient in chemical potential, and as the result of the random thermal motion of molecules, is called diffusion (Gordon L. Amidon 2000).

Thus an injection depot may spread caused by pressure from the elasticity of muscle. This is convectional movement. Absorption of drug, or solvents, from the depot is thought to occur by diffusion (Hirano et al. 1981c).

1.3.3 Free surface energy and surface tension

If the surface of a liquid increases, as occurs when a depot of oil breaks into droplets, the free energy of the liquid increases in proportion to the increase in the surface area (Martin 2006). Surface tension is a force that contracts the surface of a liquid and reduces the area of the interface. Thus when the interfacial tension between liquid of the depot and the surrounding material is decreased, it is easier to break the depot liquid into smaller droplets or for it to spread (Howard et al. 1983). Surface free energy (and surface tension) can be affected by factors such as the presence of surfactant and temperature as well as US. US does not only affect the free surface energy of injectate, but also applies mechanical and thermal effects on the tissue of injection site.

1.4 US AND ITS EFFECTS

1.4.1 US and acoustic/thermal properties of human tissues

US is an acoustic wave with a frequency higher than 20 kHz (Lele et al. 1975) although most medical applications utilise a frequency range of 1 MHz -15 MHz. Therapeutic

US works around 1 MHz but most diagnostic applications are in the frequency range 2.5 MHz -7.5 MHz (ter Haar 2007). US can propagate in various media including gases, liquids and solids.

The ultrasonic wave is classified into either longitudinal or shear waves depending on the type of motion induced in the medium by the propagating sound wave (O'Brien Jr 2007). Longitudinal waves occur when particles of the medium move back and forth in the direction of the wave thereby creating areas of high and low pressure in the medium. Shear waves occur when the particles move at right angles to the direction of the wave. Longitudinal waves can travel through all kinds of material whether gas, liquid or solid, but shear waves can only occur in solid materials. Thus shear waves have only limited ability to propagate through soft tissue because of its high percentage of liquid but can exist in harder biological materials such as bones (Baker et al. 2001).

The propagation of US is therefore highly influenced by the physical properties of the medium. The acoustic and thermal properties of water and human tissues (i.e. how they respond to sound waves and heat) are listed in Table 1-1 (López-Haro et al. 2015, Nowak et al. 2015).

Table 1-1 Acoustic and thermal properties of water and human tissues at 37˚C.

	Acoustic properties		**Thermal properties**	
	Speed (m/s)	Attenuation (dB/m at 1MHz)	Heat capacity (J/kg/°C)	Thermal conductivity (W/m/°C)
Water	1527	0.22	4178	0.6
Skin	1540	230–470	3898	0.209
Fat	1420	6–52	3221	0.402
Muscle	1529	48–100	3807	0.618

As regards the acoustic properties, attenuation is inversely proportional to the frequency of the applied US (Hayes et al. 2004). In previous studies, a frequency range of 1.5 MHz –10 MHz has been tested in human liver (Gammell et al. 1979, Hynynen et al. 2005) whereas a frequency of 0.69 MHz was tested in rabbits (Wells 1977). Generally a frequency of 1 MHz -3 MHz is used in both human and animal studies (Hayes et al. 2004, Miller et al. 2012). As for thermal properties, the skin has a higher heat capacity than either fat or muscle. It also has a lower thermal conductivity meaning that heat induced by US in skin has only limited ability to pass to the underlying tissue. The heat capacity of muscle is similar to that of skin, but fat has a lower heat capacity and higher thermal conductivity.

In biological applications, the propagation of US is a process of transferring energy to tissues. The effects of US are divided into either thermal effects or non-thermal mechanical effects.

1.4.2 Thermal effects of US

When ultrasonic energy is propagated in tissues, around 80% of the energy is converted into heat (López-Haro et al. 2015, Nowak et al. 2015). The temperature of the tissue may then increase depending on whether the rate at which heat is produced exceeds that at which it is removed. Depending on the parameters of US, the thermal effects result in various effects from mild warm to lesion in muscle. Based on the literature, exposure of bovine skeletal muscle to 1.03 MHz, 2 W/cm^2 US for 4 min caused a temperature increase from 37°C to 46.2°C at a depth of 20 mm (Cortela et al. 2016). In human muscle exposed to 3 MHz, 1.5 W/cm^2 US for 3.4 min, the temperature increased from 35.5°C to 40°C at a depth of 2.5 cm (Hayes et al. 2004). Another study in human medial triceps surae showed that application of 1 MHz, 2 W/cm^2 US for 10 min increased the temperature by 4°C at 2.5 cm depth (n=24) (Draper et al. 1995). This US-induced local hyperthermia can result in increased blood flow to the muscle (Wust et al. 2007).

1.4.3 Non-thermal effects of US

Non-thermal effects of US include cavitation, acoustic radiation force, and acoustic streaming (Dayton et al. 1999, Frenkel 2008). In clinical applications, cavitation is

usually induced due to injection of US contrast agents or gas microbubbles. However, there is no experimental evidence to suggest that inertial cavitation occurs in mammalian parenchymal tissue i.e. endogenous cavitation appears to be rare in most tissues (O'Brien Jr 2007).

The acoustic radiation force is calculated using the following equation:

$$F_{rad} = \frac{W}{c} = \frac{2\alpha I}{c} \qquad \text{equation 1.1}$$

where W is the acoustic power, c is the propagation speed and α is the absorption coefficient, I is the temporal average intensity of the acoustic wave at the given location in W/cm^2. If the radiation force is large enough, it is capable of causing local displacement of tissue (Torr 1984).

Acoustic streaming results from attenuation of an acoustic wave by the medium (Frenkel et al. 2001). The velocity of acoustic streaming is proportional to the intensity of the US, the surface area to which it is applied and the attenuation coefficient of the medium; it is inversely proportional to the bulk viscosity and the speed of sound in the medium (Barnett 1998). The radiation force and acoustic streaming demonstrate the ability to move or redistribute agents from the luminal space towards the walls of the vessels at a velocity of 0.5 m/s (Dayton et al. 2002). Frenkel et al. carried out a series of studies showing that non-cavitation US (3MHz, 2.2W/cm^2) can increase mass transport into skin and non-destructive widening of the intercellular spaces between epithelial cells at the fluid-tissue interface (Frenkel et al. 2000b). The authors explained that the above phenomena were caused by a steep gradient in shear force created by ultrasonic waves.

The non-thermal effects of US produce extra pressure or shear force which possibly influence the convective spread of formulations administered by IM injection. To date, there is no mathematical model or theory that can describe how US affects the spread of IM injected formulations. Furthermore, the challenge of this research is not only to describe how US affects the spread of IM injections but also how to visualize and measure spread.

1.5 THE CHALLENGE TO VISUALIZE SPREAD

Based on the literature, the spread of an IM injection is usually visualized by adding a fluorescent dye or contrast medium (the agent) to the formulation and using the appropriate detection system to capture images during the spread(Nguyen et al. 2011, Zhang et al. 2013, Dauffenbach et al. 2014, Seo et al. 2015). Each captured image consists of many pixels each representing a small area which is usually processed in a binary mode where the pixels are either black or white. The muscle then appears black and the injectate white due to the agent in it. However, if the concentration of agent is below a certain threshold, the pixel shows black and appears like muscle or fat. As the agent is released from the injection depot into the surrounding capillaries, its concentration in the depot drops while that in the surrounding capillaries rises. It is then possible for the concentrations of agent in both injection depot and capillaries to be higher than the threshold and for an erroneously large spread to be observed. With current image processing technology, it is difficult to completely avoid this erroneous measure of spread.

1.6 FORMULATION CONSIDERATIONS

Suspensions and solutions are commonly used as injectable pharmaceutical formulations that are convenient to use and active immediately. Emulsions have received attention in recent years as a vehicle for drug delivery by injection. An emulsion can be defined as a mixture of two (or more) immiscible phases with a third component, usually an emulsifier, added to stabilize the dispersed droplets (Davis et al. 1987). By the nature of the dispersed and continuous phases, emulsions can be classified as either oil-in-water (o/w) or water-in-oil (w/o) systems. The self-emulsifying drug delivery system (SEDDS) has been shown to improve the solubility and absorption of poorly water-soluble drugs (Neslihan Gursoy et al. 2004) and reduce pain on injection (Westrin et al. 1992). However, research into the spread of SEDDS given by IM injection is very limited. One study showed a w/o emulsion containing small ellipsoid droplets (radius 150 μm – 350 μm) spread beneath the epimysial, fascial sheaths and within the perimysial septa (Bjerregaard et al. 2001). The interaction between different types of formulation and US remains unclear.

1.7 RESEARCH QUESTIONS AND HYPOTHESIS

Although the IM injection is widely used in both human and animal healthcare, there is an awareness that absorption of injected formulations is highly variable due to uneven and inconsistent spread. This has led to interest in the potential of US to improve the spread of IM formulations. However, it remains unclear which factors or physicochemical properties are critical for the spread of IM formulations leading to the need for greater understanding of the interaction between US and spread in artificial and real muscle.

Considering this situation, the following research questions are of interest:

- Does US influence the spread of formulations administered by IM injection?
- Which factors are critical for the spread of injected formulations in artificial and real muscle?

The following factors have the potential to influence spread and are of particular interest:

Table 1-2 Factors potentially able to influence the spread of an intramuscular injection

Factor		
Formulation	**Ultrasound**	**Other**
Hydrophilic vehicle Lipophilic vehicle Viscosity Surfactant Injection volume Particle size of suspended solids	Duration of exposure Frequency Intensity	Temperature

The hypothesis of this study is therefore:

Formulation factors and physical and thermal effects of US can influence the spread of liquid formulations at the IM injection site.

1.8 AIMS OF THE THESIS

The aim of this thesis was to study formulation properties and the effects of US on the spread of formulations administered by IM injection to artificial and real muscle. Specifically, the objectives were:

i) To carry out in vitro experiments to study the spread of an injected formulation in agarose gels with and without the application of US (Chapter Two);
ii) To carry out post-mortem animal experiments in wether lambs using a balanced factorial design to study the effects of US on the spread of IM injected formulations, in particular investigating the influence of the duration of application of US, the type of formulation and the volume of the injection on the spread (Chapter Three);
iii) To compare and discuss the results of both in vitro and post-mortem studies in order to understand the influence of US on intramuscular spread and suggest future research in the field (Chapter 4).

CHAPTER TWO

EFFECT OF ULTRASOUND ON THE SPREAD OF FORMULATIONS INJECTED INTO GEL PHANTOMS

2.1 INTRODUCTION

This Chapter describes studies of the effect of US on the spread of aqueous and oily solutions of dyes in gel phantoms. Gel phantoms or tissue-mimicking phantoms are transparent gels suitable for use in US studies since they possess similar acoustic and thermal properties to those of muscle (Takegami et al. 2004). In the literature, two types of gel phantoms prepared using agarose gel and polyacrylamide gel and both containing egg white have been widely used (McCabe 1972, Zhi-Jian et al. 2002, Divkovic et al. 2007). In this study agarose gels were used because:

1) They have similar thermal and acoustic properties to muscles. As noted in section 1.4.1, the attenuation of muscle is from 48 dB/m to 100 dB/m at 1 MHz. The attenuation of 2.5% agarose gel is from 31 dB/m to 68 dB/m at 1 MHz. For acoustic speed, similar results were measured in muscle (1529 m/s) and 2.5% (w/v) agarose gel (1519 m/s to 1560 m/s) (Ortega et al. 2010). Another study (Pilkington et al. 2010) showed that thermal conductivity of 1% agarose gel is 0.55 W/m/°C, which is similar to muscle (0.618 W/m/°C). Unlike muscle, agarose gel is transparent.

2) Polyacrylamide gels containing egg white, although they too have similar properties to those of muscle, they are not considered in this study as their major component egg white causes a colour change from transparent to milky white (Divkovic et al. 2007) with rise in temperature caused by ultrasound.

Agarose gels have been used in studies of drug diffusion and the spread of drugs administered by injection. There are reports from Chen and Ye describing the injection of aqueous and oily dye solutions into 1% (Chen et al. 2008) or 0.5% agarose gels (Ye et al. 2012) using injection pumps. In the study by Chen (2008), an injection volume of 26 µL aqueous dye was injected at a rate of 0.27 µL/min. In the study by Ye (2012), an injection volume of 3 µL oily solution of dye (at injection rate of 0.3 µL/min) was injected into an 0.5% (w/v) agarose gel. In these studies, the gel provided a suitable model of muscle for studying the diffusion of the injected formulations. However, the injection volumes employed were much lower than those required for studies of IM injections in humans (2 ml) and cattle (5 ml) and much lower in injection rate than required in clinical applications (>2 ml/min). Some researchers

have attempted to improve the suitability of the model by introducing pre-made cavities into phantom gels to create space for the injected formulations (Behrendt et al. 2008, Foroughi et al. 2011).

The frequency of US used in the medical field varies from kHz to MHz. Lower frequency US is less attenuated than higher frequency and therefore penetrates tissue to greater depths (Gammell et al. 1979). Liu found that US of 1 MHz frequency enhanced drug transport and distribution in rat brain (Liu et al. 2010). As regards thermal effect, Draper et al. (1995) showed that the temperature of human muscle 30 mm below the skin surface increased by 5°C after exposure to 1 MHz, 1.5 W/cm^2 US for 10 min (Draper et al. 1995).

For the power of US used on human, an in vivo study in mice indicated it was necessary to increase US intensity from up to 3 W/cm^2 to achieve increases in the temperature of skin and deeper tissue (ter Haar 2007) although other in vivo studies showed 1.5 W/ cm^2 US was sufficient to raise the temperature of human muscle tissue (Hayes et al. 2004).

The work described in this Chapter involved (1) the use of a transparent agarose gel phantom to visualise the spread of a dye formulation injected into premade cavities with and without exposure to US and (2) the application of US using a US device (TSG US-7c Canine Ultrasound) commonly used for physiotherapy on dogs.

2.2 CHAPTER AIMS

The aims of the work described in this Chapter were the following:

- to develop an agarose gel system to study the spread of formulations;
- to determine how the nature of a formulation (aqueous or oily) affects its spread in the gel phantom; and
- to study the influence of US on the spread of formulations in the gel phantom.

2.3 MATERIALS

Analytical grade Nile blue powder was purchased from Sensient Technologies, Auckland, New Zealand, Analytical grade Nile red powder was purchased from Sigma Aldrich, New Zealand. Granulated agar powder (BD® Difco TM Agar) was purchased from BD, USA. Medium chain triglyceride (Miglyol 812N) was purchased from Sasol, Hamburg, Germany. Milli-Q water (Millipore Corporation, Bedford, MA, USA) was used for gel and dye sample preparation. The US device (TSG US-7c Canine Ultrasound) setting with 1.1 MHZ and 3 W/cm^2 maximum output was purchased from TGS Electronics Pty. Ltd, Australia.

2.4 METHODS

2.4.1 Preparation of agarose gel phantom

Initially, both oily and aqueous dye solutions were injected directly into gels. However, with a large injection volume (0.4 mL), most of the injected solution flowed back up the needle track and occasionally the gel cracked and caused more leakage. After several attempts, it was decided to use gels with premade cavities.

An agarose gel (1%) with premade cavities was prepared by the following procedure (McCabe, 1972). In a beaker, 250 mL Milli-Q water was stirred at 1500 rpm and heated to 100°C on a magnetically stirred heating plate (ARE heating magnetic stirrer, VELP Scientific). Once the water began to boil, 2.5 g of Agar powder was added with continuous stirring until a clear solution was obtained. The solution was then poured into a container (length 90 mm, width 65 mm, height 40 mm) for casting and left undisturbed at room temperature for 2 h to solidify. Two cavities, each with diameter 6 mm and depth 20 mm, were produced in the upper surface of the gel during the casting by inserting needle caps (BD® PrecisionGlide needle, 21G 1 1/2TW). The volume of the cavities was approximately 0.57 mL. The dimensions of the phantom gels and cavities are shown in Figure 2-1

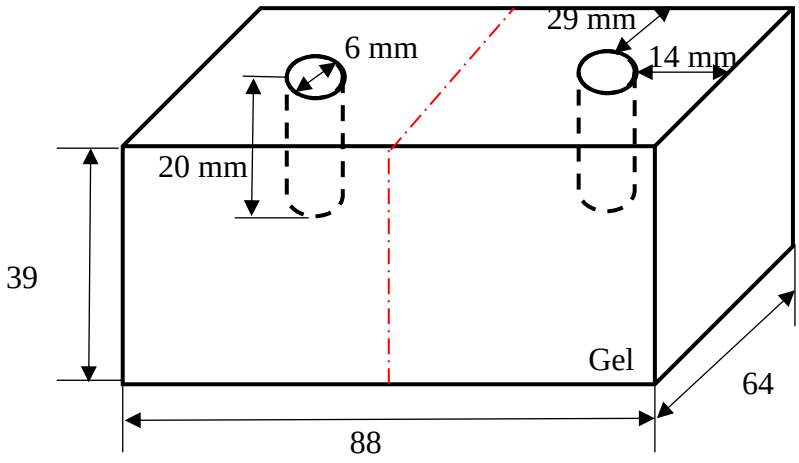

Figure 2-1 Dimensions of the agarose gel phantom and the positions and dimensions of the two premade cavities.

After the phantom gel was solid, it was cut into half (shown as red dotted line in Figure 2-1) so that each half contained one cavity in the top surface of the phantom gel.

2.4.2 Preparation of dye formulations

Nile blue solution (0.001% w/w) was prepared by mixing 0.1g Nile Blue powder and making up to 10 g Milli-Q water and then diluting (1-1000) to the final concentration with Milli-Q water. Nile Red solution (0.01% w/w) was made by mixing 0.1g Nile Red powder up to 10 g with Miglyol 812 then diluting to the final concentration with Miglyol 812.

2.4.3 Working cycle of the US transducer

The US device used in this study had a crystal diameter of 26 mm, a 1.1 MHz working frequency and an output intensity range of 0-3 W/cm^2. The output of the US wave was set to continuous mode and the “off-on” working cycle (WC) to 6 min (Figure 2-2). This means the WC constitutes no US for the first 6 min, followed by switching to the

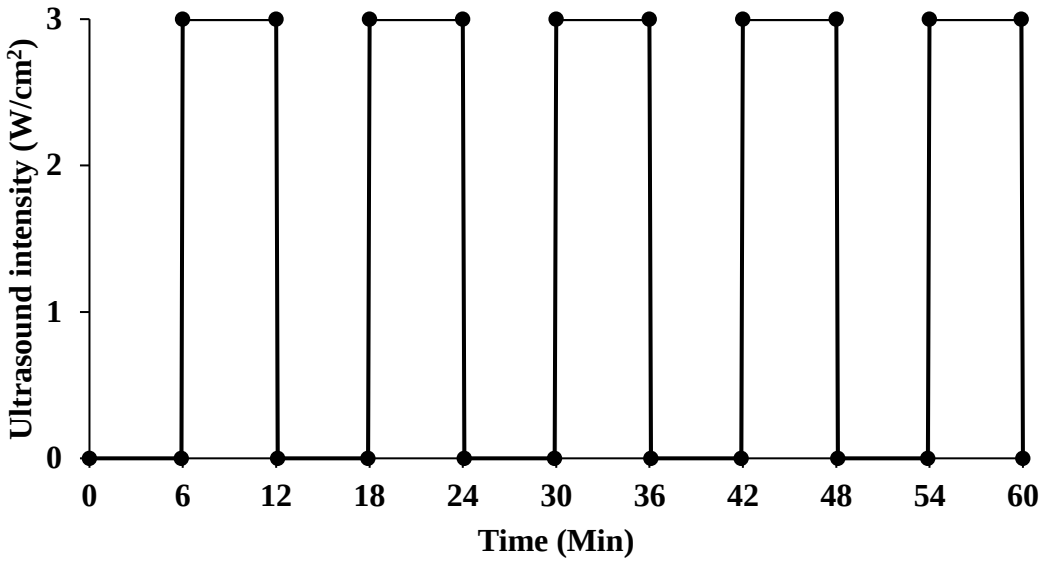

Figure 2-2 The 6 mins "off-on" ultrasound (1.1 MHz, 3W/cm^2) working cycle.

maximum output (3 W/cm^2) for the next 6 min. The US was applied for 60 min i.e. for 5 WC. The reason for a 6 min "off-on" WC was to avoid melting the gel phantom.

2.4.4 Injection of formulations

The formulations were designated 1-4 as follows: (1) aqueous solution of Nile Blue with US; (2) aqueous solution of Nile Blue without US; (3) oily solution of Nile Red with US and (4) oily solution of Nile Red without US. Aliquots of formulations (0.4 mL) were injected into the cavities after which the cavities were sealed with US coupling gel (AllCare Products Pty Ltd, Auckland, New Zealand). The US probe was placed closely connecting to the upper surface of gel in order to apply US to the formulations (1 MHz using the 6 min "off-on" WC).

Images were captured from the side of the gel phantoms using an iPhone 6 camera (Apple, USA) placed in a fixed position 20 cm from the gel. Photos were taken every 6 min over the 60 min of the 5 WC.

2.4.5 Analysis of spread of injected formulations

Image analysis was carried out using Image J software (Version 1.49, National Institutes of Health, USA). Cavities filled with formulation were set to scale, the

background noise removed and the threshold adjusted to measure the area of interest (Figure 2-3).

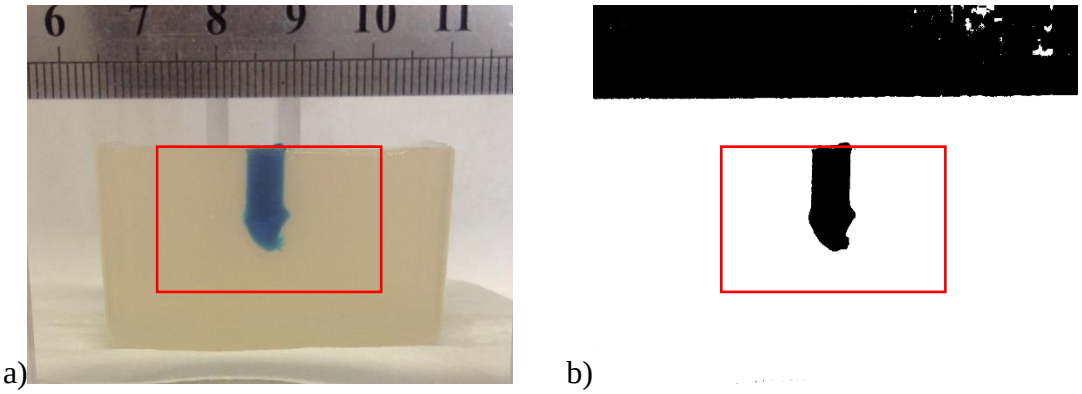

Figure 2-3 a) The original image shows the gel phantom with visible distribution pattern of the Nile Blue formulation; b) Processed image - the background was removed and turned to black/white image (binary) for measuring the region of interest (ROI, shown as red box)

The spreading area of injection was measured by the Region of interest (ROI) function of Image J software. ROI were measured at time 0 then at every 6 min up to 60 min. The ratio of changing area of spread were calculated by the following equation:

$$\%\ \text{change in the area of spread} = \frac{Area_{T=n}}{Area_{T=0}} \times 100\% \qquad \text{equation 2.1}$$

where, n = time 0, 6, 12…60 min. The data were then plotted in Excel. More details of the image processing are shown in Appendix-1.

2.4.6 Effect of ultrasound on temperature inside the agarose gel

A thermocouple (Digitech QM1323, China) was placed inside each cavity to monitor the temperature of formulations during experiments. A second thermocouple was placed on the bench near gel phantoms to monitor the surrounding temperature. Temperature was measured every 6 min, over the 60 min of the 5 WC.

2.4.7 Pore size of agarose gels

The pore size of agarose gels was measured based on the change in turbidity of their clear solutions during solidification (Aymard et al. 2001). Briefly, a clear solution of agar (1%, 2% and 3%) prepared as described in Section 2.4.1 was transferred into a 3 mL glass cuvette and placed in the beam of a UV-Vis spectrophotometer (Ultrospec 2100 pro spectrophotometer, GE Healthcare, MO, USA). The absorbance was then measured every 10 nm in the range 700-800 nm at time zero and every 20 min thereafter until a solid gel was formed. The experiment was carried out in triplicate. The turbidity and pore size were calculated using Aymard's method:

$$\tau(\lambda) = 2.3\, A(\lambda)/L \qquad \text{equation 2.2}$$

where τ is the turbidity, A is the absorbance, λ is wavelength and L is the optical path length. Turbidity spectra were calculated from the absorbance spectra and used to calculate the wavelength exponent (WLE) using the equation

$$\text{WLE} = \frac{d \log \tau(\lambda)}{d \log \lambda} \qquad \text{equation 2.3}$$

The plot (Figure 2-4) of WLE corresponding to pore size values of 1 nm to 100 µm is given by Aymard:

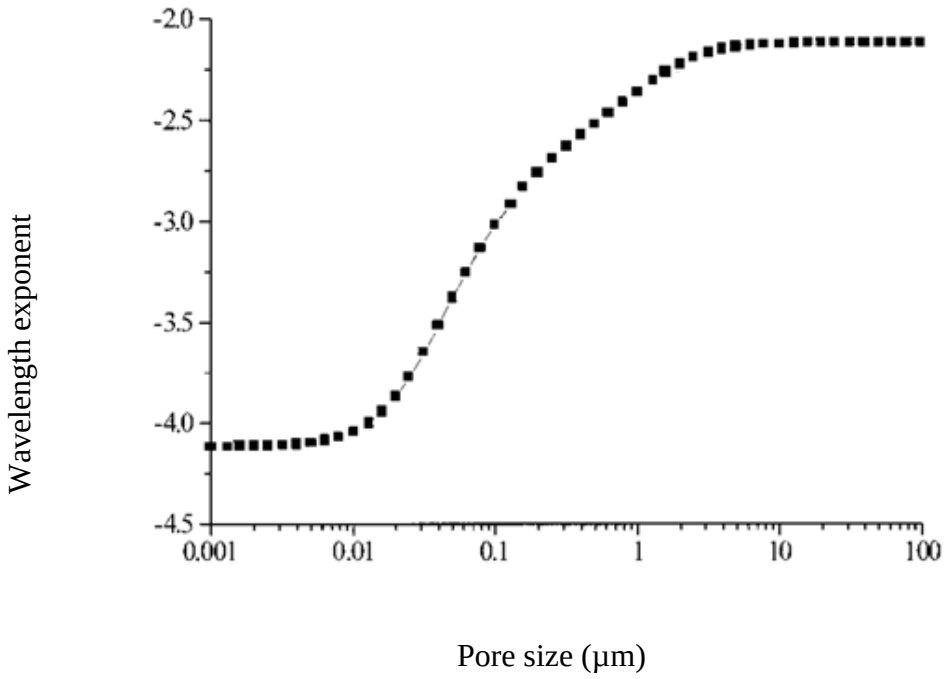

Figure 2-4 Dependence of the wavelength exponent (WLE) calculated between 700 nm and 800 nm on the correlation length (Aymard et al. 2001).

Aymard's method provides an accurate estimation of the pore size of agarose gels for pore sizes in the range 30 nm -2000 nm (Narayanan et al. 2006). Considering the typical pore size of agarose gels is in the range 80-500 nm (Pernodet et al. 1997), Aymard's method provides a fast and convenient method for pore size determination.

2.5 RESULTS

2.5.1 Analysis of spread of formulations from gel cavities

The changes in area of spread for the four groups are shown in Figure 2-5.

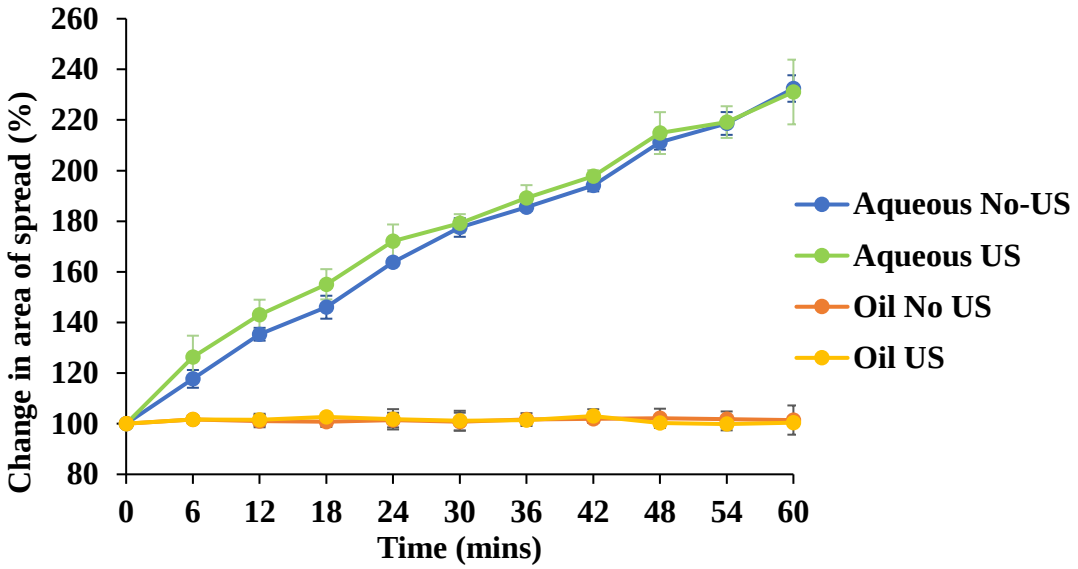

Figure 2-5 Percentage change in area of spread of Nile blue dye in oily and aqueous solutions in agarose gel (1%) phantoms with and without the application of ultrasound (data points are means ± SD, n=3).

A large increase in area of spread (~230%) was observed for the aqueous formulations irrespective of the application of US. The rate of spread decreased slightly over time as shown by the curvature of the graph. The oily formulations showed no evidence of spread both with and without US.

2.5.2 Effect of US on temperature inside gels

After exposure to 60 min of off/on US, the temperature of the gel increased from 20.4°C to 45.5°C in a stepwise manner (Figure 2-6). The rate of increase of temperature in successive 6 min on periods tended to decrease slightly. The decrease in temperature during the off periods was due to equilibration of the gel with the surrounding (room) temperature (25°C).

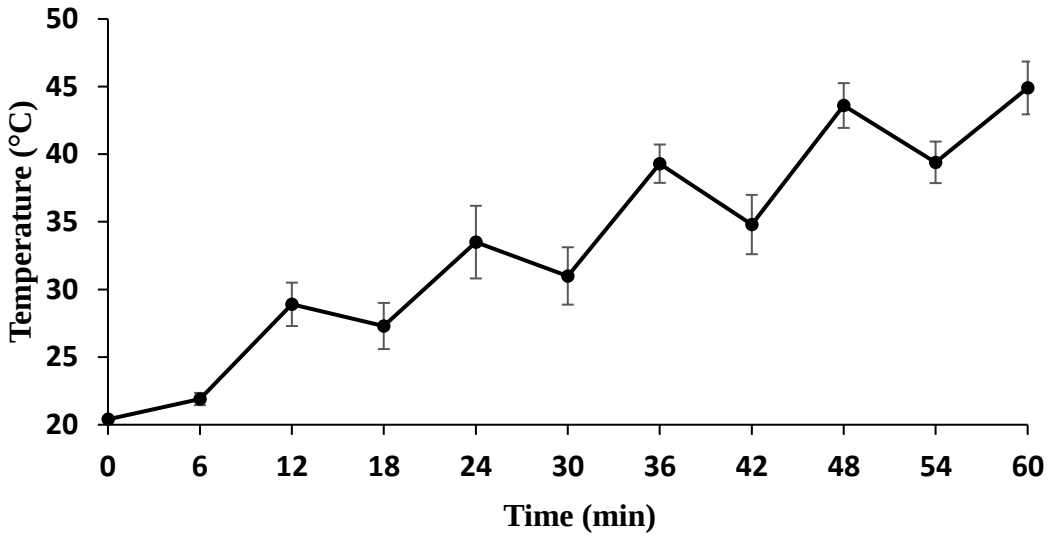

Figure 2-6 Increase in temperature of a 1% (w/w) agarose gel during exposure to 60 min of an off/on ultrasound (1.1 MHz, 3 W/cm^2) working cycle (data are means ± SD, n = 3; the first 6 min are off).

2.5.3 Determination of gel pore size

The agarose gel remained in the liquid state during the first 40 min of cooling in cuvettes so no pore size could be measured. The pore size then decreased for gels of all concentrations to an equilibrium size by 60 min (Figure 2-7).

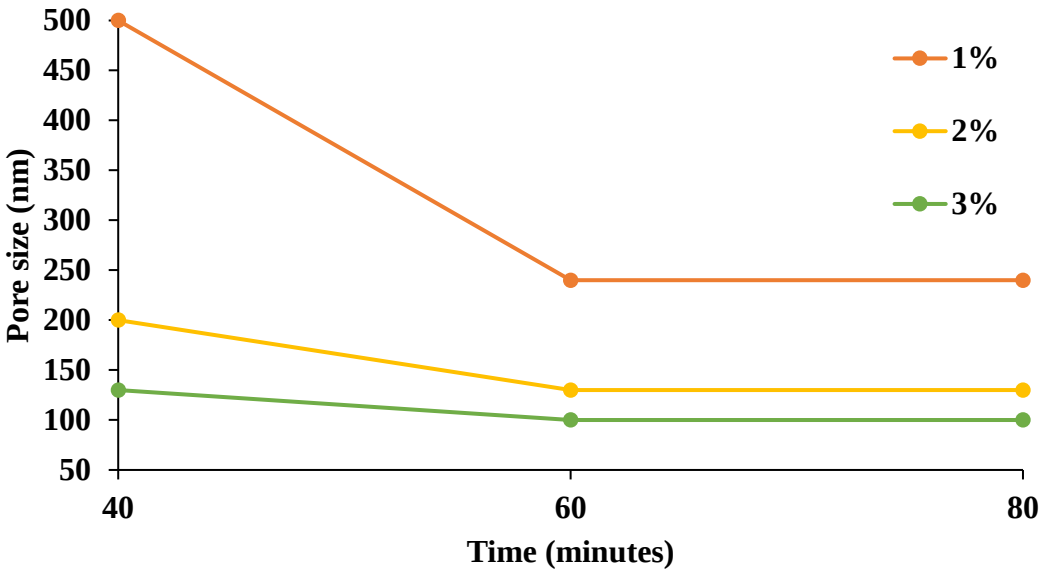

Figure 2-7 Pore size of 1%, 2% and 3% agarose gels during the gel solidification process (gels were liquid during the first 40 min of cooling).

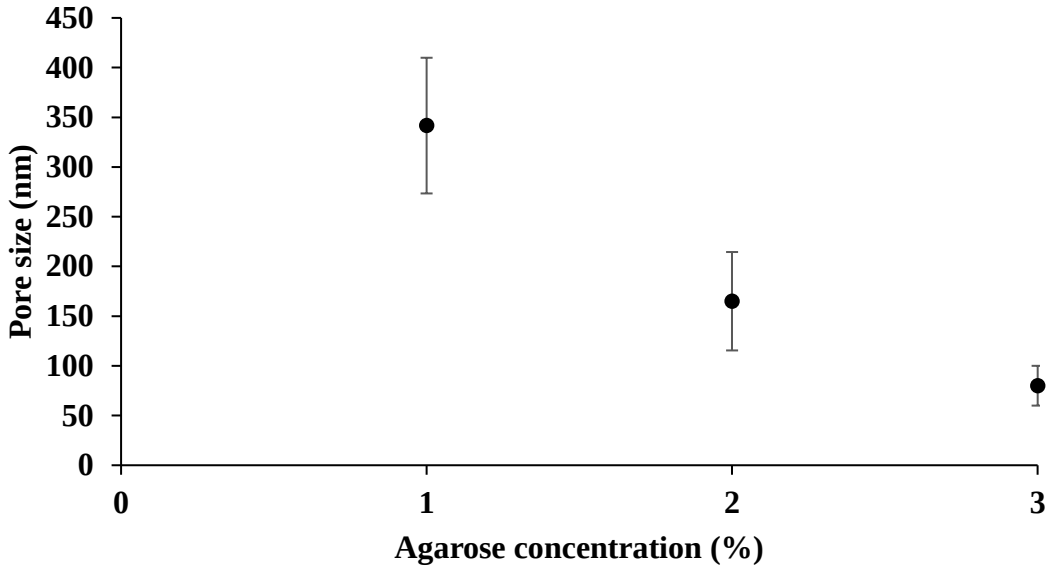

Figure 2-8 Pore size of 1%, 2% and 3% agarose gels after cooling for 80 min (data are means ± SD, n=6 for 1%, n=3 for 2% and 3% gels).

After cooling for 60 min, agarose gels solidified and stable pore size measurements could be obtained. As Figure 2-8 shows, pore size decreased as the gel concentration increased. The mean pore size of the 1% agarose gel was around 350 nm with a large variation (270 nm-430 nm).

2.6 DISCUSSION

Before discussing the spread of formulations placed in pre-made cavities in agarose gels, it is pertinent to consider the situation during direct injection into a gel phantom. In this case the injectate is pushed into the gel to create its own cavity as occurs during an IM injection into animal tissue. The elasticity of the gel then works to close the cavity and squeeze the injectate out. The routes that liquid flows out will depend on the resistances of the various routes of escape. The opposing forces eventually reach a balance at which point a small amount of injectate remains in the gel as a depot and the rest returns to the tissue surface through the injection hole. This series of events has been observed in animal studies. For example, injection of 200 µL of an oily solution into the caudal thigh muscle of mice was followed by massive leakage to the outside of the targeted muscle bundle (Gehling et al. 2018). The result reveals that the elasticity of muscle is more than sufficient to eject all but a small volume of an IM injection.

In experiments involving injection into premade cavities in gel phantoms, a major drawback of the method is that the injectate is not under pressure when introduced into the cavity. Therefore there is no pushing force to counteract the elasticity of the gel and facilitate spread. In fact the spreading shown in Section 2.5.1 is actually the result of diffusion of the dye into the gel matrix and not a true reflection of spread. However, the terms “spread” and “area of spread” are still used here for the sake of consistency.

Interestingly, the results obtained for injection of aqueous and oily solutions are very different. Of particular interest is the fact that there was no spreading of the oily solution even after 60 min. This is consistent with the findings of Larsen et al. 2001 who showed that the clearance of an oily vehicle from injection site can take from hours to days. In our experiment, the absence of spread from the oily solution can be ascribed to the insolubility of Nile red in water and its inability to partition from the oil into the aqueous phase of the matrix of the gel. In contrast, the spreading of the water soluble Nile blue dye into the agarose gel requires no phase transfer and occurs efficiently irrespective of the application of US.

Based on the work of Zuidema et al (1988), diffusion plays an important role in the absorption of drugs when aqueous solutions are administered by IM injection. The diffusion coefficient is defined as follows:

$$D = D_0 e^{-E_A}/kT \qquad \text{equation 2.4}$$

where D_0 is the maximum diffusion coefficient at infinite temperature, E_A is the activation energy T is the absolute temperature and k is the Boltzmann constant. Since in the experiments described here D_0, E_A and k are constants, the relationship between e and D can be simplified to:

$$D \propto e^{-\frac{1}{T}} \qquad \text{equation 2.5}$$

Given that T refers to absolute temperature, it is clear that D does not change a great deal for the temperature increase of 25°C resulting from the application of US to the gel.

While the temperature change has little effect on diffusion, this is not the case for pore size which is critical for the absorption of an IM injection. The pore size of the 1% agar gel used in this study of 340 ± 75 nm is within the range reported in previous studies. According to the results of a study by Pluen et al,1999 molecules with a hydrodynamic radius < 30 nm have little or no interaction with the gel matrix(Pluen et al. 1999). Since the hydrodynamic radius of Nile blue is only about 0.5 nm (Dutt et al. 1991), it is clear it does not interact with the polymer matrix of the phantom gel and spreads without resistance. Thus although the increase in temperature has the potential to increase pore size (Aymard et al. 2001), its influence on the spread of Nile blue is also negligible. For the oily solution where the Nile red must first partition into the aqueous gel before undergoing diffusion(Larsen et al. 1998), the small temperature increase will cause only a negligible change in its partition coefficient. Also, the temperature increased by US, as observed in gel experiment, is not likely to occur in vivo since heat would dissipate into the flowing blood.

In summary, the study of the spread of dyes from aqueous and oily injectates into phantom gels was restricted to the use of premade cavities. This did not reflect the true

situation of IM injections which are administered under pressure. Only dye in aqueous solution showed apparent spread which occurred by diffusion and was not affected by the application of US despite the increase in the temperature of the gel it caused. Further work will be restricted to studies of spread subsequent to IM injections into the muscle of post-mortem animals.

CHAPTER THREE

EFFECT OF US ON THE SPREAD OF INTRAMUSCULAR INJECTIONS IN PORCINE MUSCLE AND POST-MORTEM SHEEP

3.1 Introduction

Following an IM injection, the injectate spreads from the site of injection and is subsequently absorbed into the peripheral circulation. Characterizing the spread depends on understanding the nature of the formulation, selecting an appropriate tissue model and developing a technique to measure the spread. Only a few studies have been done about quantifying the spread of IM injections. One group injected iohexol into thigh muscle of mice (injection volume up to 200 μL), then the spread of injection was measured by coned beam computed tomography (CT) (Gehling et al. 2018). However, there are drawbacks to the use of small animals such as their small body mass, large ratio of injection volume to muscle mass and differences in physiological factors from those in large mammals. Accordingly, sheep were used in this study to better understand the pattern of spread of IM injections in large livestock animals. In this chapter, formulations were IM injected immediately after euthanasia of sheep. The fact that blood flow and muscle movements are absent in the dead animal is a limitation of this method.

A major challenge in researching the spread of IM injectates lies in choosing an appropriate imaging technique. This is mainly because of the scarcity of relevant literature. However, a recent study showed that CT could be used to examine the spread of aqueous formulations containing an iodinated, water soluble contrast agent (Dauffenbach et al. 2014). Application of the technique to study the spread of IM injections in unembalmed corpses showed that detailed images could be obtained with sufficient resolution to delineate the spreading pattern. CT imaging was therefore used in the present study to examine the effect of US on the spreading behaviour of oily formulations after IM injection into the muscle of post-mortem sheep. In this chapter, preliminary study-I was carried out firstly to prove the concept of US affecting the spread of IM injected formulations by injecting aqueous and oily formulation containing fluorescent dye in porcine muscle (Section 3.4.1). After the concept was tested, preliminary study-II was carried to determine the suitable type and concentration of contrast agent for CT scans (Section 3.4.2). In Section 3.4.3, The experiment on post-mortem sheep was then carried out. The statistical analysis of the post-mortem sheep study data is described in Section 3.4.4. Particle size and viscosity of the formulation used in post-mortem experiments were also analysed (Section 3.4.5).

Characteristics of muscle dissected from around the injection site (Section 3.4.6) and surface temperature (Section 3.4.7) were recorded as well.

3.2 Chapter aims

The aims of the research reported in this Chapter were to determine:

- the effects of US on the spread of formulations injected into a piece of porcine muscle; and
- the effects of US on the spread of formulations injected into the muscle of post-mortem sheep (wethers).

3.3 Materials

Materials [suppliers] were as follows: MF-fluoRed (particles) [Microparticles GmbH, Germany]; Nile blue powder and MilliQ water [see Section 2.3.1]; Boneless cuts of porcine muscle (300 g each) were purchased from a local supermarket. Lipiodol® (ethyl esters of iodized fatty acids of poppy seed oil containing 48% w/v iodine, NDC 67684-1901-1) [Guerbet, USA], barium sulfate (analytical grade) and Oil Blue N dye [Sigma-Aldrich, New Zealand], Miglyol 812 [Sasol, Hamburg, Germany], Cremophor EL [BASF, Germany], Maisine 35-1 (glyceryl monolinoleate) [Gattefosse, France].

3.4 Methods

3.4.1 Preliminary study I: Spread in porcine muscle phantoms

3.4.1.1 Formulations

The aqueous formulation was an 0.001% (w/w) solution of Nile blue in MilliQ water. The oily formulation was a suspension of MF-FluoRed (0.1% w/w) prepared by adding 0.1 g MF-FluoRed to 100 g Miglyol 812. Formulations were mixed well by vortexing for 1 min (IKA® Minishaker, Sigma-Aldrich, New Zealand).

3.4.1.2 Experimental setup

The spread of IM injections in porcine muscle phantoms was visualized using a Bruker FX pro imager (Bruker, USA), an automated multifunctional imaging platform. Fluorescence images detecting the dyes were obtained using excitation and emission wavelengths of 630 nm and 790 nm. In each experiment, two pieces of porcine rump muscle were placed in the FX pro imager as shown in Figure 3-1. One piece was treated with US while the other acted as control.

Figure 3-1 Image of two pieces of porcine rump muscle (1 & 2) in the FX pro imager.

Muscle 1 (control) was not exposed to US whereas Muscle 2 (test) was exposed at the injection site to 1 MHz 3 W/cm^2 US for 3 min on 100% duty cycle after injection.

Aqueous and oily formulations were studied in separate pieces of muscle each with a respective control. Aliquots of 0.5 mL and 0.3 mL of aqueous and oily formulations respectively were injected into muscle. In both cases a 1 mL syringe (needle size 21G 1 1/2 TW) was used to deliver injectates to a depth of 15 mm below the muscle surface. Test muscle was then exposed to 3 min, 1 MHz 3 W/cm^2 US, 100% duty cycle at the injection site. Images were captured immediately after injection and at the end of the US application. Captured images were analyzed using FX image pro software.

3.4.2 Preliminary study II: Contrast agent concentration in the post-mortem sheep study

3.4.2.1 Formulations:

To determine the most suitable concentration of contrast agent in formulations to be studied in the post-mortem sheep study, a series of solutions and suspensions of the contrast agent were prepared. Lipiodol concentrations of 24% and 12% were prepared by diluting the commercial 48% solution with Miglyol. Barium sulfate powder (1, 2, 3 and 4 g respectively) was added into Miglyol 812 (10 g final weight) to make 10%, 20%, 30% and 40% (w/w) barium sulfate suspensions. Oil blue N dye (0.02% w/w) was added to each formulation. The criteria for the most suitable concentration of contrast agent included ease of injection, lack of interaction with the Oil blue N dye, good contrast of muscle.

3.4.2.2 Experimental setup

Formulation spread was evaluated by FX pro imager (Bruck Corporation, USA) based on observations of 4 x 0.1 mL IM injections into sheep muscle (lamb loin chops with 80g of average weight from local supermarket) using a 21G 1 1/2TW sized needle. The needle was left inside the muscle after injection to indicate the site. Each concentration was tested in duplicate.

3.4.3 Spread in post-mortem sheep

3.4.3.1 Preparation of formulations

There were three different formulation types used in post-mortem experiment: oily solution, oily suspension and self-emulsifying system (SEDDS).

Lipiodol at original concentration (48%, w/v) was used as oil soluble contrast.

The oily contrast suspension (30% w/w) was prepared by adding barium sulfate (30 g) to Miglyol 812 (70 g) with continuous stirring on a magnetic stirrer set at 550 rpm. Stirring of the suspension was then continued for 30 min to achieve homogeneity after which the suspension was milled in a planetary ball mill (Retsch® Planetary Ball Mill PM 200, Germany) using zirconium oxide beads (1 mm) and a zirconium oxide milling jar (4 kg). The operating protocol involved a total milling time of 40 min at 400 rpm with 5 min intervals and 2 min breaks.

The SEDDS was prepared by mixing Lipiodol, Maisine and Miglyol 812 in the ratio 40:20:40 w/w on a magnetic stirrer (ARE heating magnetic stirrer, VELP Scientifica) set at 550 rpm for 10 min.

3.4.3.2 Animals

Experiments were carried out in July 2015 using 3 male wether lambs (age 6 months-8 months; weight 32 kg). The animals had free access to food and water and were housed in a pen at the animal facility of AgResearch NZ, Invermay Agricultural Centre, Dunedin. Euthanasia was carried out by injection of sodium pentobarbital (Pentobarb 300 (300 mg/mL), Sigma-Aldrich, New Zealand) at a dose of 100 mg/kg-150 mg/kg.

All procedures involving sheep were approved by the University of Otago Animal Ethics Committee (Approval Number: 36/15, 19 June 2015).

3.4.3.3 Experimental design

3.4.3.3.1 The design of analysing US effect on spread.

In the post-mortem sheep experiment, the effects of different formulation types, injection volume and US exposure time were studied by a balanced factorial design. The levels of the factors are listed in the following table:

Table 3-1 Factorial design of US impacted spread.

Factor	***Factor level***		
	Low	Centre	High
Formulation type (F)	Solution	Suspension	SEDDS
Injection volume (V)	1.5 mL	N/A	4.5 mL
US duration (U)	0 min	5 min	10 min

In total, there were 3x3x2=18 different combinations of levels and factors. Each combination was tested as duplicated, the total injection number was 36. The 36 injections were randomly assigned to the backs of three sheep and the rumps of the same three sheep as shown in Figure 3.2 and Table 3.2. Thus back and rump were two blocks. Three levels of US treatment (0, 5 or 10 min) were then randomly assigned to each formulation-volume combination in a balanced fashion (see Table 3.2)

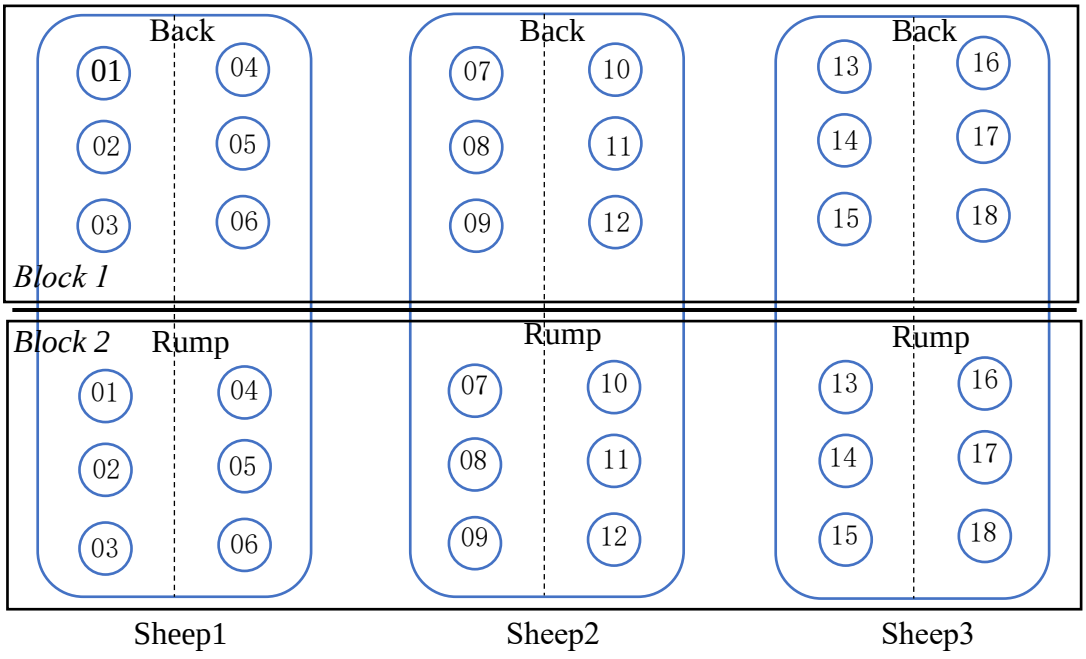

Figure 3-2 Block design and injection sites

Table 3-2 The randomly assignment of combinations.

Combination #	***Factor1: Formulation***	***Factor2: Injection volume (mL)***	***Factor3: US exposure duration (mins)***	***Block1 position (Back)***	***Block2 position (Rump)***
1	Solution	1.5	0	B17	R04
2	Solution	1.5	5	B09	R09
3	Solution	1.5	10	B05	R13
4	Solution	4.5	0	B07	R18
5	Solution	4.5	5	B04	R10
6	Solution	4.5	10	B13	R03
7	Suspension	1.5	0	B14	R11
8	Suspension	1.5	5	B11	R12
9	Suspension	1.5	10	B08	R06
10	Suspension	4.5	0	B02	R02
11	Suspension	4.5	5	B15	R16
12	Suspension	4.5	10	B18	R15
13	SEDDS	1.5	0	B12	R01
14	SEDDS	1.5	5	B16	R14

Combination #	*Factor1: Formulation*	*Factor2: Injection volume (mL)*	*Factor3: US exposure duration (mins)*	*Block1 position (Back)*	*Block2 position (Rump)*
15	SEDDS	1.5	10	B03	R05
16	SEDDS	4.5	0	B10	R07
17	SEDDS	4.5	5	B06	R08
18	SEDDS	4.5	10	B01	R17

In this design, due to the duplicated test was on a different block (back vs rump), the difference between blocks was tested. The ANOVA design for US impact on spread is shown in Table 3-3:

Table 3-3 Design of ANOVA for US impacted spread

Factor	***Degree of freedom***
Formulation	2
Injection volume	1
US duration	2
Block	1
Formulation x Injection volume	2
Formulation x US duration	4
Injection volume x US duration	2
Formulation x injection volume x US duration	4
Error	17
Total	35

From literature, interactions with block are included within the error term

3.4.3.3.2 The design for analysing initial spread

Initial spread was assessed by carrying out CT scans soon after (see Table 3.7 for timings) all injections listed in Table 3-2 were finished, but before any application of US. Thus the factors involved in the analysis of initial spread were formulation type and injection volume. Table 3-4 shows the factors and their levels for the experiment of initial spread.

Table 3-4 Factorial design of initial spread

Factor	***Factor level***		
	Low	Centre	High
Formulation type (F)	Solution	Suspension	SEDDS
Injection volume (V)	1.5 mL	N/A	4.5 mL

There were totally 3 x 2 = 6 combinations of factors and levels. The randomly assignment of injection site is shown in Table 3-5 which is the same as Table 3-2 but without the column of US exposure duration.

Table 3-5 The randomly assignment of combinations for initial spread.

Combination #	***Factor1: Formulation***	***Factor2: Injection volume (mL)***	***Block1 position (Back)***	***Block2 position (Rump)***
1	Solution	1.5	B17	R04
			B09	R09
			B05	R13
2	Solution	4.5	B07	R18
			B04	R10
			B13	R03
3	Suspension	1.5	B14	R11
			B11	R12
			B08	R06
4	Suspension	4.5	B02	R02
			B15	R16
			B18	R15

Combination #	*Factor1: Formulation*	*Factor2: Injection volume (mL)*	*Block1 position (Back)*	*Block2 position (Rump)*
5	SEDDS	1.5	B12	R01
			B16	R14
			B03	R05
6	SEDDS	4.5	B10	R07
			B06	R08
			B01	R17

Each combination was tested six times. The total number of injections (36) was divided into two blocks, one block being the back of three sheep and the other block being the rump of the three sheep. The analysis of variance (ANOVA) of initial spread is shown in Table 3-6:

Table 3-6 Design of ANOVA for initial spread

Factor	***Degree of freedom***
Formulation	2
Injection volume	1
Block	1
Formulation x Injection volume	2
Error	29
Total	35

From literature, interactions with block are included within the error term.

3.4.3.4 IM injection protocol

Following euthanasia, the carcasses were fixed on a moveable operating table and the entire rumps and backs shaved in preparation for IM injections. A total of 12 injections were made into each carcass (6 in the rump and 6 in the back) using BD® 5 mL Tuberculin Syringes and BD® PrecisionGlide needles (21G 1 1/2TW). Injections were made 10 min after euthanasia at an angle of 90° to skin surface and a depth of 25 mm. The location of injections into the muscle groups is shown in Figure 3-3.

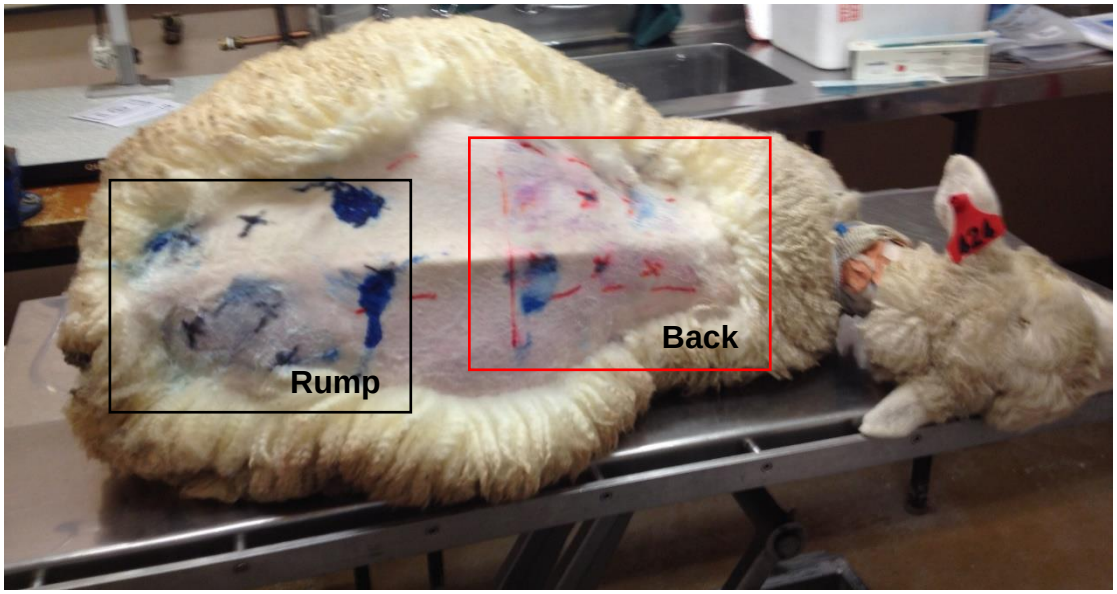

Figure 3-3 The location of the 12 injections in the rump (6) and back (6) muscles of a post-mortem sheep.

A summary of the procedures and the timeline involved is given in Table 3-7.

Table 3-7 Timeline for each sheep in the post-mortem experiment

Time (min)	**Event (for each sheep)**
0	Animal euthanasia and shave
10	Total 12 IM injections, 6 on back and 6 on rump
20	Injection finished, start the 1st CT scan
30	1st CT scan finished, start US treatments
65	All US treatments finished
70	2nd CT scan starts

There were three levels for US duration: 0, 5 and 10 min. But the gap between the 1st and 2nd CT scan was 40 min and it took 35 min to finish all 12 randomly assigned US

treatments. The reason is during the experiment, there were only two US transducers available so it was impossible to carry all 12 treatments simultaneously. In order to keep the gap between two CT scans the same, the 2nd CT scan was set 40 min after the 1st one. This procedure means for 0 min US group, during the 40 min gap between two CT scans, the IM injected formulation received 0 min US treatment. For the 5 and 10 min US groups, they received 5 and 10 US treatment, respectively, during the same time period.

3.4.3.5 CT imaging and US protocol

Following IM injections, animals were moved to the CT scanner (GE Lightspeed CT Scanner, General Electric, USA). Two rounds of whole body CT scan were applied to each animal. Each CT scan captured a series of images of various positions in a transverse plane. The distance between each image slice was 1.25 mm.

First an image was captured showing the general condition of spread of the injected formulations in the whole animal in the sagittal plane. Subsequently the first whole body CT scan was carried out to capture the situation before US treatment and provide a measure of the initial spread. The term “initial spread” used here is of passive spread of injectate, that is prior to application of US. Then US was applied for various times (0, 5 or 10 min) to the injection sites using a TGS-7c Ultrasound Device (TGS Electronics Pty. Ltd, Australia). The surface temperature before and after exposure to US was also recorded using an infrared laser thermal detector (Mini IR Thermometer 42500, Extech, USA).

After US application, sheep were subjected to the second whole body CT scan in the transverse plane to capture the resulting spread pattern.

3.4.3.6 CT image analysis

CT images were imported into ImageJ (version 1.50b) software for analysis. The images in the transverse plane were sorted as an image sequence for each pair of injections. Each image slice of 250 mm x 250 mm had 512 x 512 resolution which is approximately 0.48 x 0.48 mm/pixel.

First, all slices in the transverse plane were stacked up by a plugin 3D viewer of ImageJ to rebuild an image in the 3D mode. Each image slice in the transverse plane was processed by adjusting the threshold to reduce the signal from muscle. Then the whole image sequence was adjusted to 8-bit images. Next, areas of bone in the images were manually coloured black. Finally, the contrast from the injected formulation was the only visible part in the image allowing its area to be measured by ImageJ. The areas in each image slice were summed and multiplied by the distance between each slice to calculate the volume of spread Vspread using Equation 3.1:

$$V_{spread} = \sum Area_{each\ slice} \times 1.25\ (mm^3) \qquad \text{Equation 3.1}$$

Here $Area_{\text{each slice}}$ is the area (mm^2) of the contrast pattern in each CT slice and 1.25 mm is the distance between each slice. The percentage increase in volume of spread between two CT scans is given by Equation 3.2.

$$\text{Ratio} = \frac{V_{spread\ 2nd\ CT\ scan}}{V_{spread\ 1st\ CT\ scan}} \times 100\% \qquad \text{Equation 3.2}$$

3.4.4 Statistical analysis

Data were analyzed using two-way analysis of variance (two-way ANOVA) in Minitab software (version 17.0). The factorial design of the ANOVA was first to identify any difference in the initial spread associated with injection volume and type of formulation. Secondly, the ANOVA determined any difference in the increase in spread resulting from US exposure time, injection volume and formulation type. Post-hoc analysis was performed using the Tukey test and statistically significant differences were those for which $p \leq 0.05$.

3.4.5 Characterization of the formulations for post-mortem study

3.4.5.1 Determination of particle size of the oily suspension

The particle size of original barium sulfate suspension (from Section 3.4.3.1) was unable to be measured as it was too cloudy. In order to dilute the suspension without changing the particle size, saturated barium sulfate in Miglyol 821 was prepared. Excess barium sulfate was added to Miglyol 812 (100 ml) and stirred overnight to make a saturated solution. It was then allowed to settle for 1 h and the supernatant transferred

to a glass vial. An aliquot (0.5 mL) of milled 30% barium sulfate suspension (from section 3.5.1) was diluted 1:100 by adding 49.5 mL barium sulfate-saturated Miglyol 812.

The diluted barium sulfate suspension was filled into the quartz sample container (fraction cell) of the laser diffraction particle size analyser (Horiba Instruments, Irvine, CA). The relative refractive index was set at 1.44 (Cable, 2012) and the cell recirculation speed at 2. Samples were prepared in duplicate and results were the mean of at least 10 measurements.

3.4.5.2 Rheology of suspension and SEDDS

The viscosities of the barium sulfate oily suspension and SEDDS were measured in triplicate using a TA rheometer HR3 (TA instruments, U.S.A) with cone-plate geometry (Cone SST ST 60MM 2DEG SAMRT-SWAP, ref. 996902). The shear stress and viscosity of samples were measured at increasing shear rate (ramp up) from 0 s^{-1} to 200 s^{-1} followed by measurements at decreasing shear rate (ramp down) from 200 s^{-1} to 0 s^{-1}. The test duration was 480 s. The temperature of tests was set at 37°C and 42°C. Data were recorded every 3 s.

3.4.6 Dissection of muscle to study spread

Approximately 2 hours after the second CT scan, dissection of sheep muscle at the injection sites was carried out in the Department of Anatomy, University of Otago. The whole back and rump muscles were dissected into pieces each containing at least one injection site and then snap frozen in liquid nitrogen. Frozen muscle was then stored at -85°C until processed seven months later. The frozen muscle pieces were then cut into cross-sectional slices approximately 15 mm thick and the spread pattern (dye) captured using an Iphone 6 camera (Apple, USA).

3.4.7 Effect of US on muscle temperature

A piece of lamb rump (100 mm x 50 mm x 50 mm) with skin (4 mm) and a thin layer of wool was obtained from a local butcher and fixed in a plastic container with skin side up. The container had two openings, one on top for the US probe and another on the side for thermocouples (Digitech QM1323, China) placed at various depths (4, 20

and 30 mm) below the skin surface (Figure 3-2). US (1. MHz, 3 W/cm^2, 10 min continuous) was applied and the surface temperature measured at 0, 10, 15 20, 25, 30 and 35 min using an infrared laser thermal meter (Mini IR Thermometer 42500, Extech, USA). Thermocouples measured temperature at various depths every minute for the first 15 min and then every 5 min up to 35 min.

3.5 RESULTS

3.5.1 Preliminary study I: Spread in porcine muscle phantoms

The effect of US on the spread of an aqueous solution of Nile blue dye injected into porcine muscle was assessed using fluorescence imaging. The site of injection was marked by a bright fluorescent spot the intensity of which was constant over a 10 min period. Following the application of US, the brightly labelled spot dissipated and the area covered by dye within muscle increased (Figure 3-4) indicating spread.

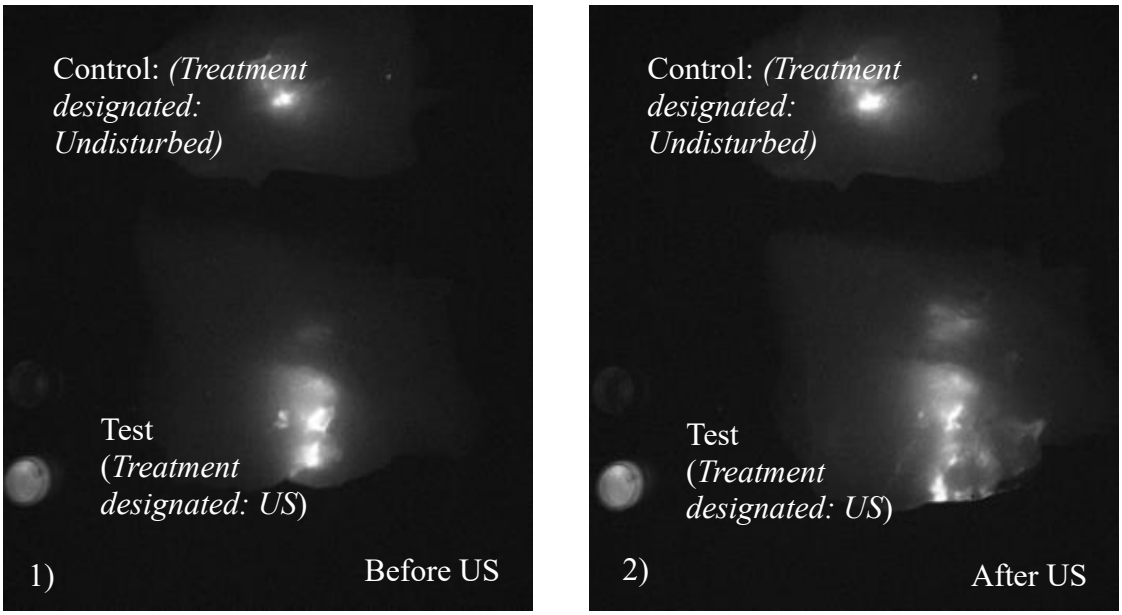

Figure 3-4 Effect of US on the spread of an aqueous solution of Nile blue dye (0.5 mL 0.001% w/w) injected into a porcine muscle phantom and imaged with an FX pro imager. The control site (top) was left undisturbed while the test site (bottom) was exposed to US (1.1 MHz, 3 W/cm^2 for 3 min, 100% duty cycle).

The effect of US on the spread of an oily suspension within porcine muscle was assessed using fluorescent imaging of MF-FluoRed particles (0.1% w/w). As shown in Figure 3-5, the oily formulation did not spread outward from the initial site of injection in control tissue. After exposure to US, the fluorescent spot disappeared but the nearby edge of the tissue was illuminated. Whether this is indicative of spread is complicated by the proximity of the muscle boundary.

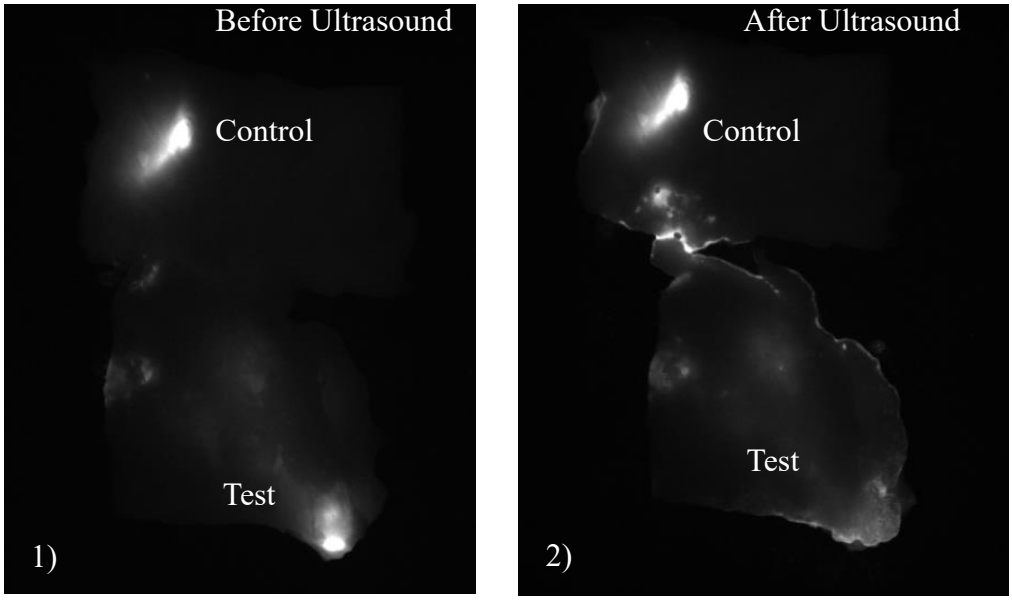

Figure 3-5 Effect of US on the spread of fluorescence labelled particles in an oily suspension (0.3 mL 0.1% w/w) injected into a porcine muscle phantom and imaged with an FX pro imager.. The control site (top) was left undisturbed while the test site (bottom) was exposed to US (1 MHz, 3 W/cm^2 for 3 min on 100% duty cycle).

3.5.2 Preliminary study II: Contrast agent concentration in the post-mortem sheep study

Figure 3-6 shows the results of injecting formulations (0.1 mL of injection volume with 2 cm of injection depth) containing various concentrations of contrast agents into four pieces of sheep muscle (10 x 8 cm in size). The Figure shows that Lipiodol (48% w/v) provides the most intense contrast which is sufficient to distinguish it from muscle and bone. For the barium sulfate suspension, both the 30% and 40% concentrations are distinguishable from muscle but the 40% suspension was too viscous to allow facile delivery from the syringe. The presence of Oil Blue dye (meats 3 and 4) did not interfere with the contrast displayed by both Lipiodol and barium sulfate.

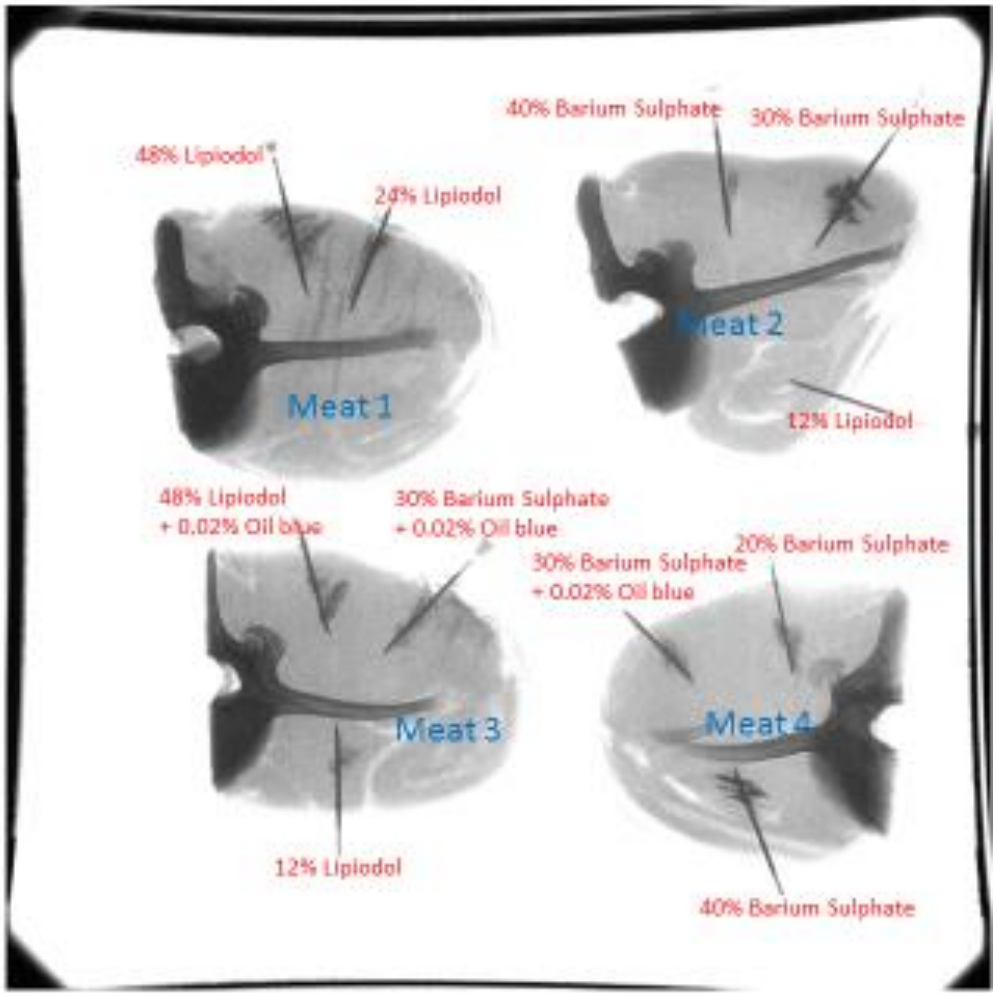

Figure 3-6 Pieces of lamb loin chops injected with oily formulations containing various concentrations of Lipiodol and barium sulfate contrast agents together with Oil Blue dye. The needles used for injection were left in the muscle to identify the injection sites.

3.5.3 Spread in post-mortem sheep

Figure 3-7 shows a CT scan of the spread of formulations containing contrast agents injected into the rump and back muscle of a post-mortem sheep. The formulations displayed sufficient contrast to show that the spread occurred along the muscle fascia.

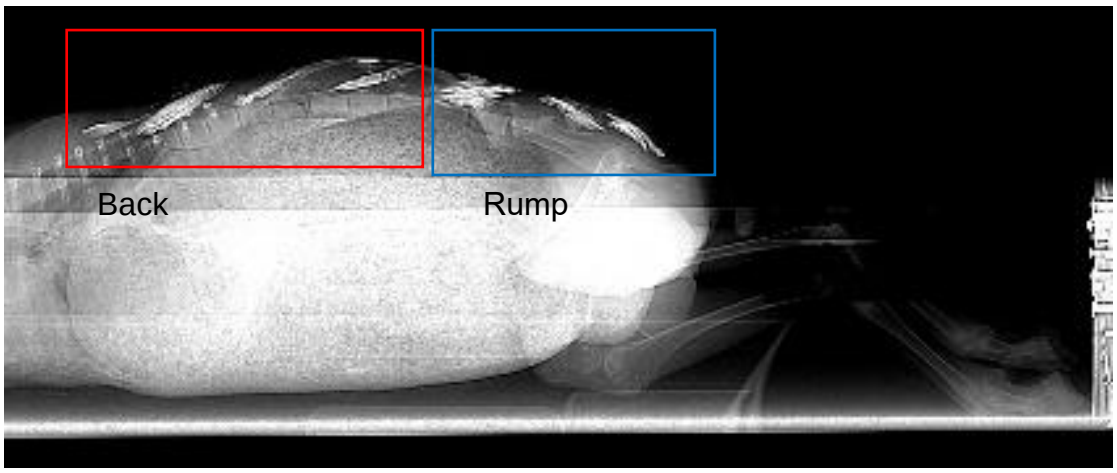

Figure 3-7 General condition of spread of formulations containing contrast agents injected into the back muscle (red box) and rump muscle (blue box) of a post-mortem sheep as observed by CT scan in the transverse plane.

3.5.3.1 Initial spread of oily formulations

The initial spread was the volume of spread of the injected formulations in the post-mortem sheep after 10 min calculated using Equation 3.1. The results from ANOVA of initial spread are shown in the Fig 3-8, Fig 3-9 and Table 3-8:

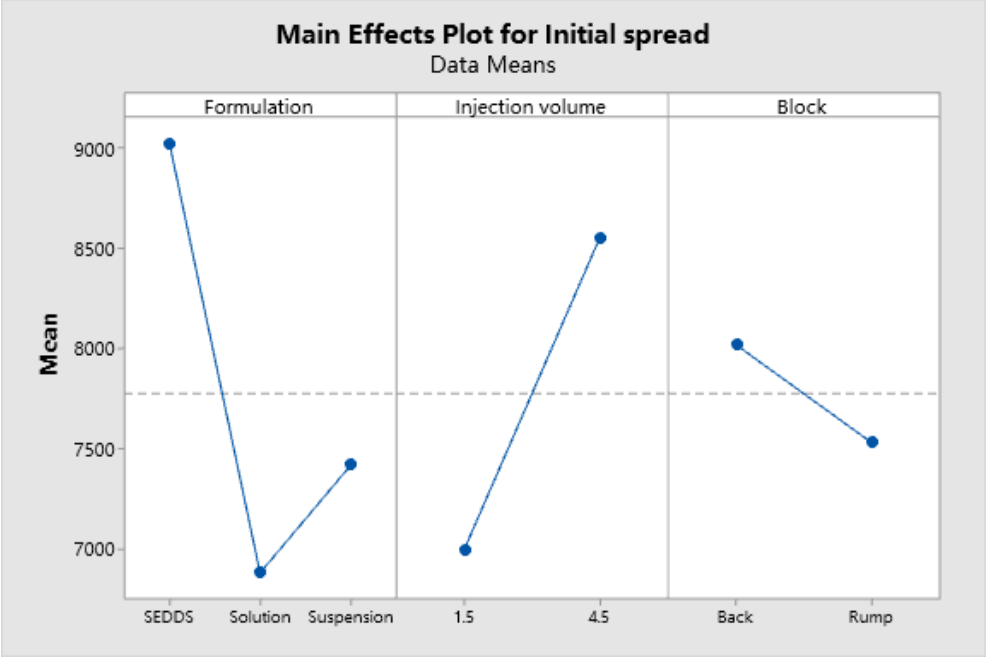

Figure 3-8 Main effects plot for initial spread.

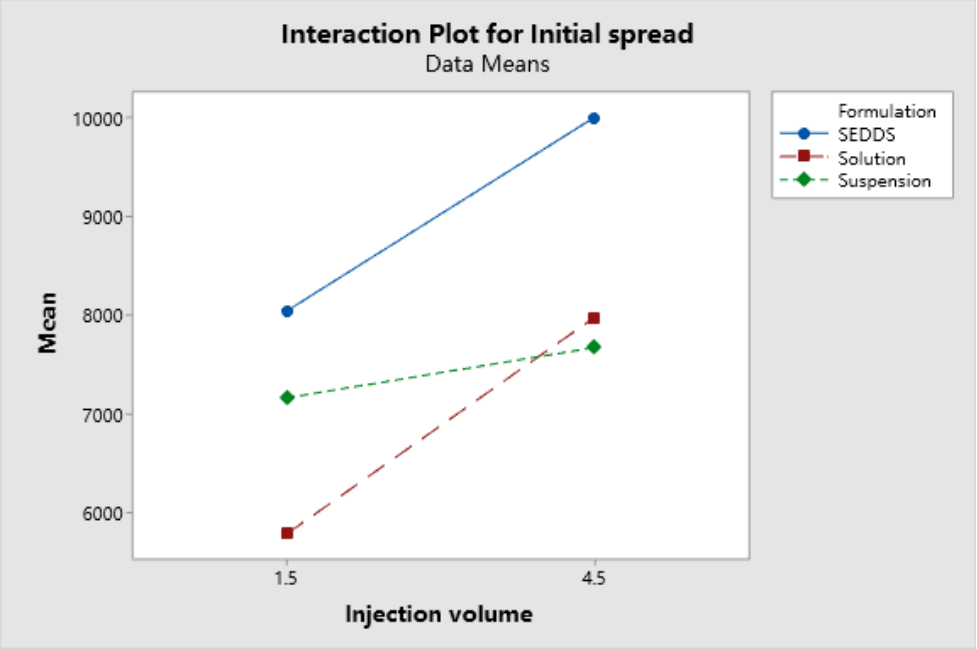

Figure 3-9 Interaction plot (formulation x injection volume) for initial spread.

Table 3-8 ANOVA for initial spread

Source	DF	Adj SS	Adj MS	F-valve	P-value
Formulation	2	29809510	14904755	0.74	0.488
Injection volume	1	21840044	21840044	1.08	0.307
Block	1	2150133	2150133	0.11	0.747
Formulation x Injection volume	2	5018098	2509049	0.12	0.884
Error	29	586905530	20238122		
Lack-of-fit	5	150644437	30128887	1.66	0.183
Pure	24	436261093	18177546		
Total	35	645723315			

There was no significant difference (p>0.05) in the volume of spread between formulations, injection volumes and blocks. The p-value for block (back vs rump) of 0.747 meaning there was no significant difference between back and rump and in future studies blocking in this way would be unnecessary. The interaction plot (Fig 3-9) showed non-parallel lines suggesting an interaction between injection volume and formulation type; however the interaction was not significant (P = 0.884). Although the mean square values for factors were large, they were not significant because of the high variability of the data. The mean square value of error in Table 3-8 suggested high variation of volume of spread of IM injected formulations. The full ANOVA report of initial spread is attached as Appendix-2.

Since there is no significant difference between blocks, the data from back and rump were combined then each combination of F x V had six repeats. The volume of spread for injections of the 1.5 mL was in the order SEDDS > suspension > solution but the differences were again not significant (p>0.05) (Figure 3-10)

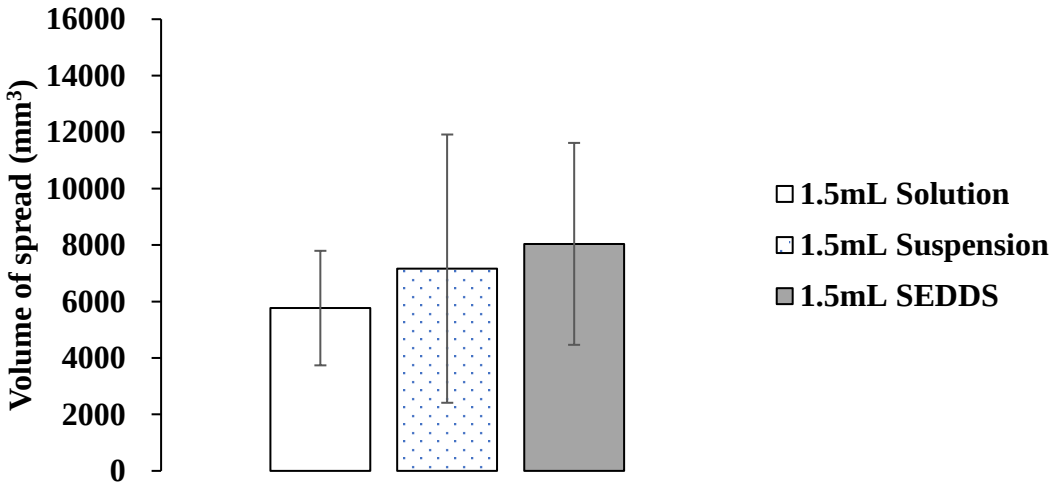

Figure 3-10 Initial spread of intramuscular injections of different formulations (1.5 mL) obtained from the 1st CT scan (data are means ± SD, n=6).

Similarly there was no significant difference (p>0.05) in the spread of the 4.5 mL injections of the three formulations (Figure 3-11).

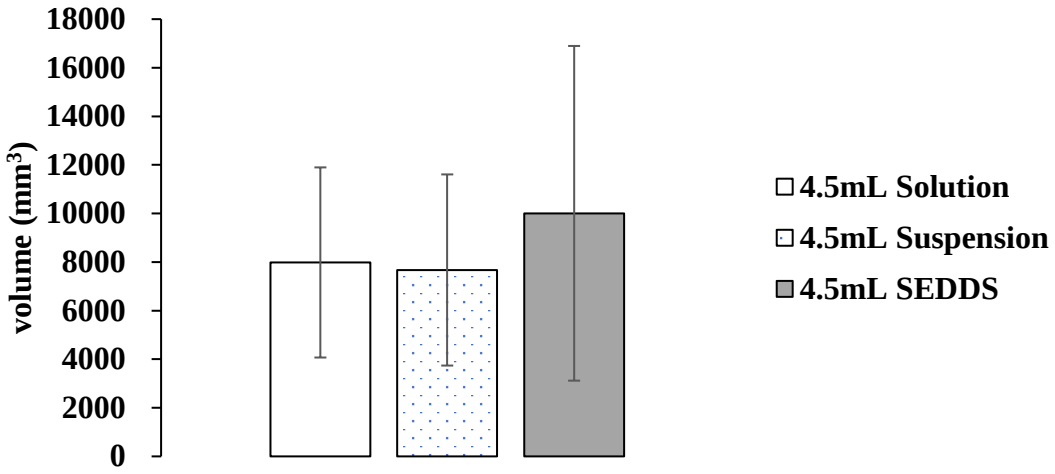

Figure 3-11 Initial spread of intramuscular injections of different formulations (4.5 mL) obtained from the 1st CT scan (data are means ± SD, n=6).

3.5.3.2 Effect of US on the ratio of change in volume of spread

The ratio of the volumes of spread of the 2nd to the 1st CT scan was calculated using Equation 3.2. As described in Section 3.4.3.4, the time between the two CT scans was around 40 min. The results from ANOVA analysis are shown in Fig 3-12, Fig 3-13 and Table 3-9.

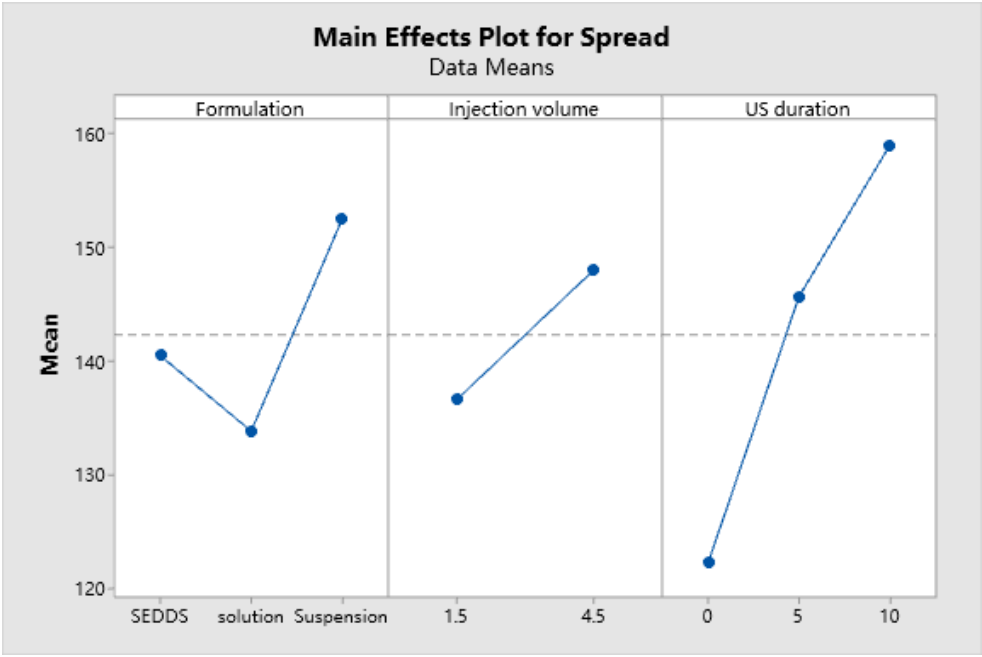

Figure 3-12 Main effects plot for the US impacted spread of IM injected formulations.

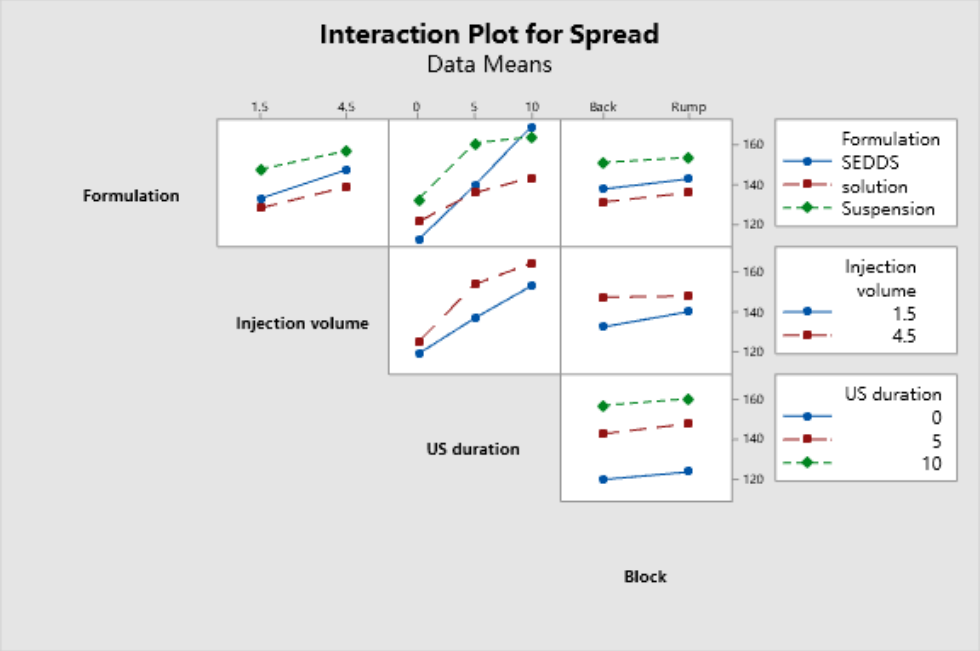

Figure 3-13 Interaction plot for the US impacted spread of IM injected formulations.

Table 3-9 ANOVA for US impacted spread

Source	DF	Adj SS	Adj MS	F-value	P-value
Formulation	2	2161.9	1080.95	21.84	0.000
Injection volume	1	1166.2	1166.22	23.57	0.000
US duration	2	8357.6	4178.80	84.45	0.000
Block	1	150.1	150.06	3.03	0.100
Formulation x Injection volume	2	42.3	21.16	0.43	0.659
Formulation x US duration	4	1555.8	388.95	7.86	0.001
Injection volume x US duration	2	185.4	92.69	1.87	0.184
Formulation x Injection volume x US duration	4	552.9	138.23	2.79	0.060
Error	17	841.2	49.48		
Total	35	15013.4			

Significant differences ($p \leq 0.05$) were observed across all three factors: formulation type, injection volume and US exposure time. The only significant interaction is the formulation x US durations. However, there were no significant differences for the interactions between formulation type and injection volume, injection volume and US exposure time nor for the interaction between formulation type, injection volume and US exposure time ($p=0.060$). The p-value for block (back vs rump) of 0.100 meaning there was no significant difference between back and rump and in future studies blocking in this way would be unnecessary. The detailed data of ratio of volumes of spread of each formulation were attached in Appendix-3.

3.5.4 Post-hoc statistical analysis: Tukey's test

The adjusted p-values from post-hoc Tukey's tests are shown in the Table 3-10. There was no significant difference across all combinations between injection volumes and US exposure times on the spread of oily solution. Details of Post-hoc statistical analysis report was attached in Appendix-4.

On the other hand, US significantly ($p<0.05$) enhanced the spread of oily suspensions and SEDDS. For the 1.5 ml injection of the oily suspension, exposure to US for 5 min did not affect spread but exposure for 10 min significantly increased spread of both oily suspensions ($p = 0.0025$) and SEDDS ($p = 0.0011$).

For the 4.5 mL injection of the oily suspension, exposure to US for 5 min significantly increased spread ($p = 0.0186$). However, exposure to US for 10 min did not lead to any further increase in spread ($p>0.05$). For the 4.5 mL injection of SEDDS, exposure to US for 5 min increased spread significantly ($p = 0.0073$) and increase in exposure to 10 min resulted in a further increase in spread ($p = 0.001$).

Table 3-10 Adjusted p-values from post-hoc Tukey's test

Formulation type & injection volume	**US exposure time**	**Adjusted p-value**	**Significant difference**
Solution 1.5 mL	0 min vs 5 min	0.9907	N
	0 min vs 10 min	0.3842	N
	5 min vs 10 min	0.9846	N
Solution 4.5 mL	0 min vs 5 min	0.4141	N

Formulation type & injection volume	US exposure time	Adjusted p-value	Significant difference
	0 min vs 10 min	0.1399	N
	5 min vs 10 min	1	N
Suspension 1.5 mL	0 min vs 5 min	0.1321	N
	0 min vs 10 min	0.0025	Y
	5 min vs 10 min	0.7746	N
Suspension 4.5 mL	0 min vs 5 min	0.0186	Y
	0 min vs 10 min	0.1756	N
	5 min vs 10 min	0.9964	N
SEDDS 1.5 mL	0 min vs 5 min	0.4003	N
	0 min vs 10 min	0.0011	Y
	5 min vs 10 min	0.1822	N

Formulation type & injection volume	US exposure time	Adjusted p-value	Significant difference
SEDDS 4.5 mL	0 min vs 5 min	0.0073	Y
	0 min vs 10 min	0.0001	Y
	5 min vs 10 min	0.0079	Y

3.5.5 Characterization of the formulations for post-mortem study

3.5.5.1 Particle size of the oily suspension

The mean particle size of 30% barium sulfate suspension was 13.8 ± 0.01 μm (D90 = 30 μm).

3.5.5.2 Rheology characterization

For rheological measurements, different shear rates were applied to simulate the shear stress during storage (1 s^{-1} on standing), on mild shaking before injection (10 s^{-1}) and during injection itself (100 s^{-1}). Figs 3-14 and 3-15 show the dependence of shear stress on shear rate at 37°C and 42°C for 30% barium sulfate suspension and SEDDS respectively. Table 3-11 shows the viscosities for barium sulfate suspension and SEDDS at the two temperatures.

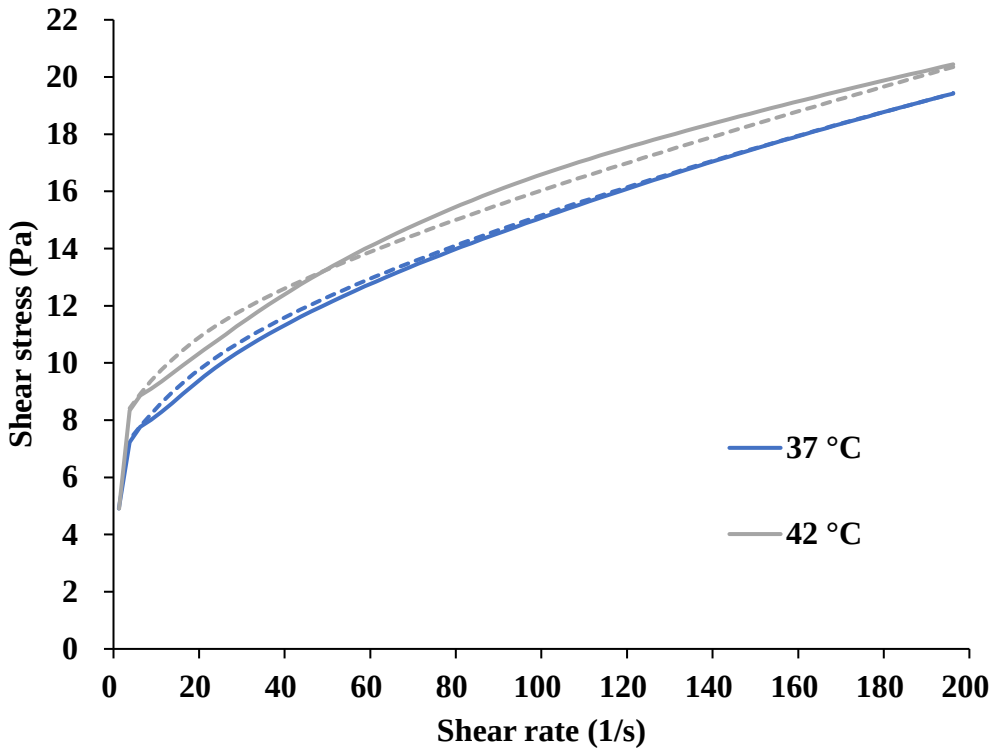

Figure 3-14 Dependence of shear stress on shear rate for an oily suspension of 30% (w/w) barium sulfate at 37°C and 42°C. Ramp up and ramp down of shear rate is shown as solid and dashed lines respectively.

The plots of shear stress vs shear rate for the 30% (w/w) barium sulfate oily suspension tentatively suggest plastic or pseudoplastic behaviour. The curves do not pass through the origin but rather intersect the shear stress axis at around 5 Pa which can be taken as the yield point. Above the yield point, the curves are indicative of pseudoplastic flow. The ramp up and ramp down curves overlap. The similarity of the curves at 37°C and 42°C indicate temperature has only limited influence on the rheological properties of barium sulfate suspension.

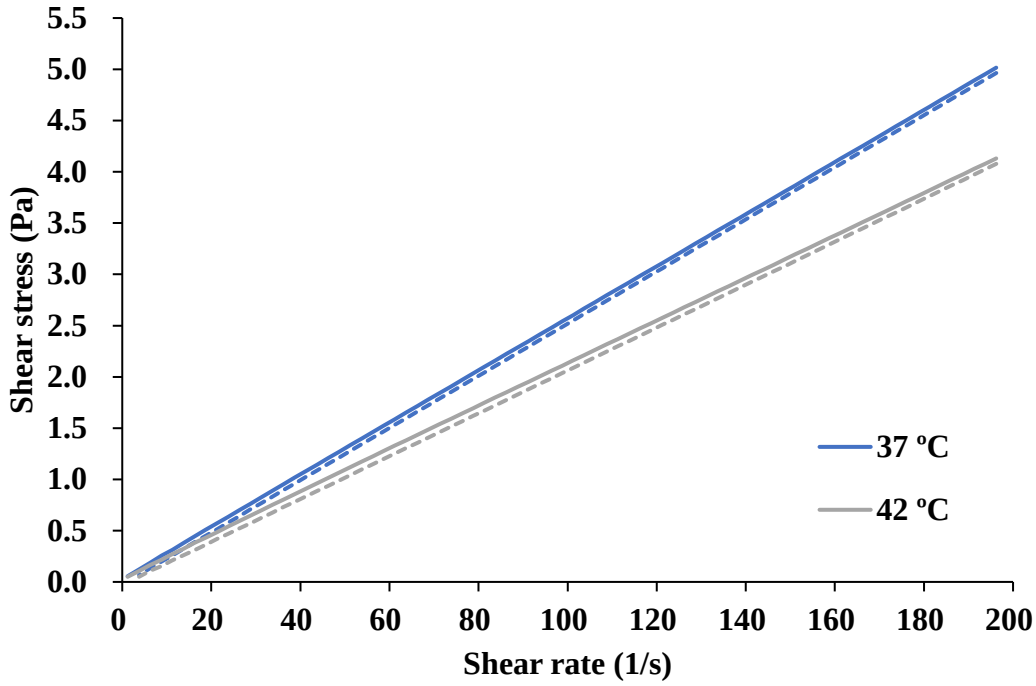

Figure 3-15 Dependence of shear stress on shear rate for an oily suspension of SEDDS at 37°C and 42°C. Ramp up and ramp down of shear rate is shown as solid and dashed lines respectively

As shown in Figure 3-15, the shear stress-shear rate plots for SEDDS at both 37°C and 42°C are indicative of Newtonian flow behaviour. The ramp up and ramp down curves overlap. No thixotropy was detected. Again, the influence of temperature was limited.

Determination of viscosity revealed the barium sulfate suspension shows high viscosity at low shear rate (Table 3-11) and decreasing viscosity as shear rate increased. There was no significant difference in viscosity at the two temperatures. The viscosity of SEDDS was low at all shear rates and again it was little influenced by temperature.

Table 3-11 Viscosities of oily suspensions of 30% (w/w) barium sulfate and SEDDS at different shear stresses and temperatures (data are means ± SD, n=2).

Barium sulfate oily suspension (30% w/w)		
Shear rate (s^{-1})	**Viscosity (Pa.s) at 37°C**	**Viscosity (Pa.s) at 42°C**
1	4.01 ± 0.12	3.90 ± 0.09
10	0.87± 0.06	0.87 ± 0.05
100	0.16 ± 0.01	0.16 ± 0.02
SEDDS		
Shear rate (s^{-1})	**Viscosity (Pa.s) at 37°C**	**Viscosity (Pa.s) at 42°C**
1	0.05 ± 0.01	0.04 ± 0.02
10	0.03± 0.01	0.02 ± 0.01
100	0.03 ± 0.00	0.02 ± 0.00

3.5.6 Post-mortem dissection of rump and back muscles

In total 83 pieces (5 cm x 5 cm x 2 cm) of muscle were collected from the rump and back of post-mortem sheep. Initially, the purpose of the study was to calculate the volumes of spread and compare them with the volumes of spread obtained in the CT scan study. However, due to the difference in the thickness (1.25 mm) of the CT slices and manually cut slices (15 mm), it was not possible to match the volumes of spread measured by the two techniques. Therefore the spreading patterns based on cross-section of each slice were photographed and analyzed.

Based on the observed spreading patterns at the injection site, the spreading patterns could be divided into three types: Spread pattern A where spread was confined to a restricted area; spread pattern B where the formulation spread along the fascial sheaths of the muscles; and spread pattern C where the formulation mainly spread along the fat layer between the muscle bundles. Figure 3-16 (a-c) shows typical examples of each group.

(a)

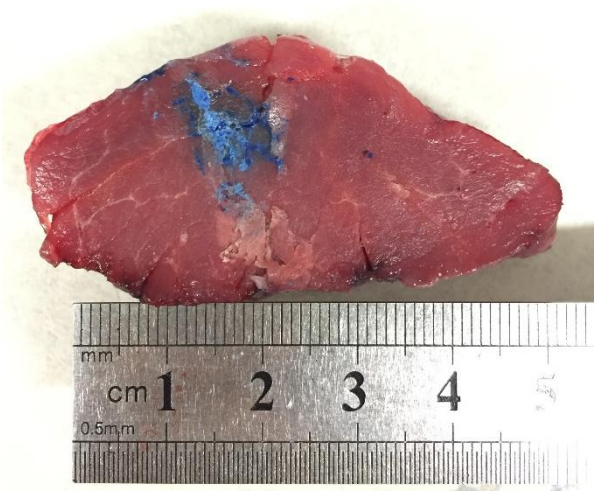

(b)

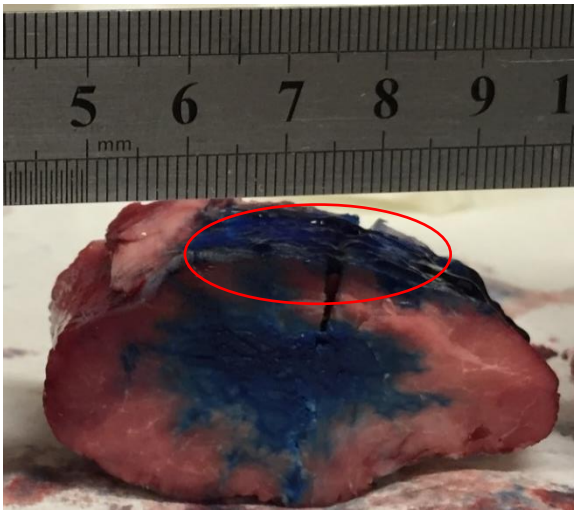

(c) 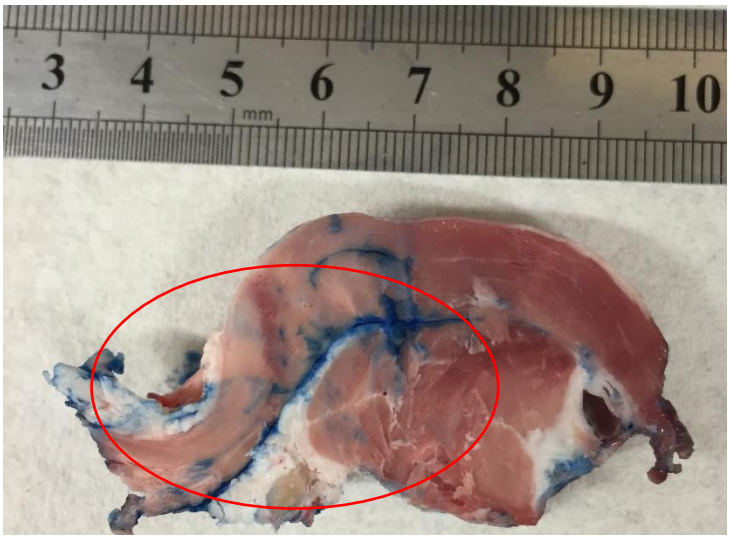

Figure 3-16 Spreading patterns observed by dissection of injection sites in muscle from post-mortem sheep. (a) Spread of 1.5 ml injection of 30% barium sulfate suspension containing oil blue dye (0.01%)); spread is mainly within the muscle bundle and confined to a restricted area. (b) Spread of 1.5 mL Lipiodol containing oil blue dye (0.01%); spread is outside the muscle bundle along the sheath. (c) Spread of 4.5 mL Lipiodol containing oil blue dye (0.01%); dye accumulated in fat layer between the muscle bundles.

The three types of spreading patterns (Figure 3-16) were found in both rump and back muscle of post-mortem sheep and across all factors (formulation type, injection volume and US exposure time).

Figure 3-17 shows a comparison between the spread observed after dissection and the image obtained by CT scan. Spread observed after dissection (Figure 3-17a) is mainly along the fascial sheaths and confined in a muscle bundle. Spread observed in the CT scan (Figure 3-17b) reveals only a bright spot covering the whole spreading area.

a)

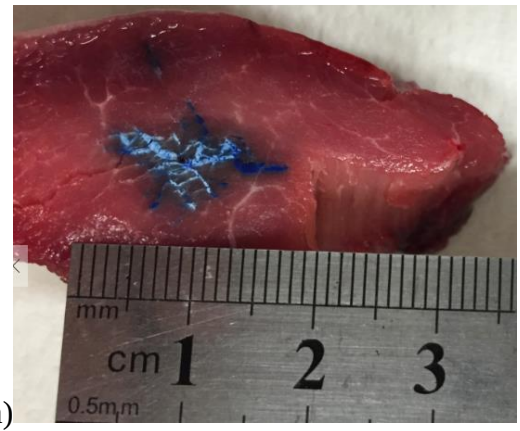

b)

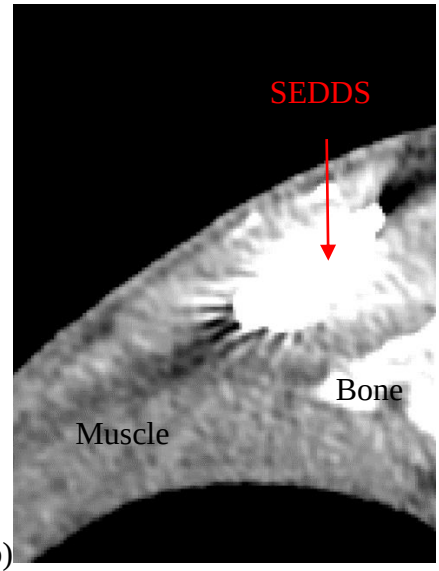

Figure 3-17 Spread of an IM injection of an oily suspension of SEDDS (4.5 mL) containing Oil Blue dye observed (a) after dissection and (b) by CT scan where the red arrow indicates the area of spread.

This result suggests the resolution of the CT imaging system (0.48 x 0.48 mm per pixel) is not sufficient to distinguish spread along the primysial and epimysial septae.

3.5.7 Measurement of thermal response to US in muscle phantom

Figure 3-18 and Table 3-12 show the temperature rise in response to US at the surface and at various depths from the surface in the sheep rump muscle phantom with and without skin respectively.

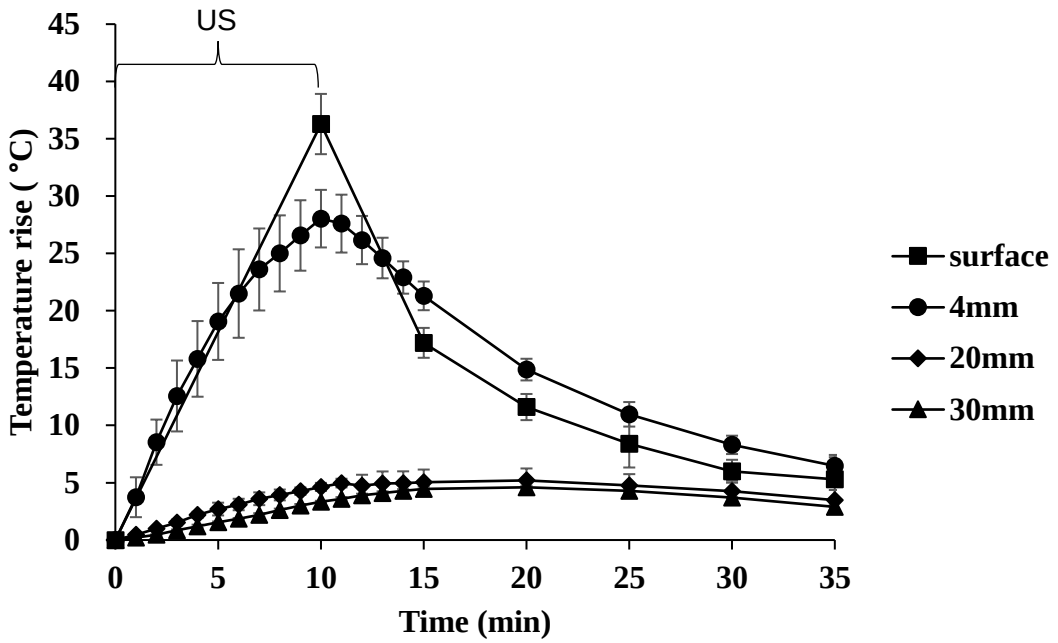

Figure 3-18 Effect of US (3 W/cm^2, 1.1 MHz, 10 min) on temperature rise at the surface and at various depths from the surface of a sheep muscle phantom with skin attached (data are means ± SD, n=9 for surface, n=3 for below surface).

The temperature at the surface of rump muscle with skin attached (Figure 3-18) increased by 36°C from 24.6 ± 1.3°C to 60.9 ± 2.6°C. At a depth of 4 mm from the skin surface, the temperature increased by 28°C; at depths of 20 mm and 30 mm which are representative of the depths to which injectates were delivered, only a rise of ~5°C was observed.

The temperature on the skin surface of sheep used in the post-mortem study exposed to US (1 MHz, 3 W, 100% duty cycle, 10 min) was also recorded. The results show that the temperature increased to 58 ± 2°C.

Table 3-12 Surface temperature after US exposure (1MHz, 3W, 10 min with 100% duty cycle). Data points are means ± SD. (ex vivo: n = 9, post – mortem study: n = 6)

	Muscle phantom (n = 9)	Post-mortem study (n = 6)
Surface temperature (°C)	61 ± 3	58 ± 2

As shown in Figure 3-18 and Table 3-12, the thermal effect of US at the skin surface was dramatic. Even in the post-mortem sheep, the temperature below the surface increased by 5°C. However, temperature increase in live animals would probably be less due to the blood circulation.

3.6 Discussion

In this Chapter, the effects of formulation type, injection volume and US exposure on the spread of IM injections were evaluated. Experiments focused on spread in large muscle groups (back and rump) of and post-mortem sheep immediately after euthanasia. All formulations contained an oily base and a contrast agent for image analysis. The formulations included an oily solution of Lipiodol, a suspension of barium sulfate (30%) and SEDDS (composed of 40% Lipiodol, 40% medium chain triglycerides and 20% Cremophor). Two injection volumes,1.5 and 4.5 mL, were used and injected into a muscular region at a total of 36 sites each separated by at least 10 cm. After approximately 10 min, US (1.1 MHz, 3 W/cm^2, 100% duty cycle) was applied to a total of 24 injection sites for either 5 min or 10 min duration.

As a proof-of-concept, a preliminary study was performed using a porcine muscle phantom and fluorescence imaging. This study aimed to evaluate the effect of formulation type (oily vs. aqueous) and US exposure on IM spread. To enable image analysis, the oily suspension contained Nile blue coated particles and the aqueous solution contained solubilized Nile blue. The results of the preliminary study showed that exposure to US (1.1 MHz, 6 min, 100% DC, 3 W/cm^2) enhanced the spread of both formulations. Moving to studies in post-mortem sheep, an imaging protocol for CT

scanning was optimized using lamb loin chops. The aim was to determine the optimum concentration of contrast agent for imaging. For solutions, sufficient contrast was observed for the stock Lipiodol solution containing 48% w/v fatty acid. For suspensions, a barium sulfate concentration of 30% w/w was found to provide good contrast specificity without increasing the viscosity to a point where injection was difficult.

The spread of an IM injectate within living tissue is a dynamic process that depends on how the formulation is expelled from a syringe and the local tissue heterogeneity. To evaluate this, an initial characterization of spread was required. This was defined as the spread of an oily formulation within the first 10 min of an IM injection in post-mortem sheep as evaluated by CT scan. Surprisingly, despite a 3-fold difference in injection volume (1.5 mL vs 4.5 mL), no significant difference in the volume of spread was observed for any of the three formulations (Section 3.5.4.1). Accordingly, the underlying reason(s) for this surprising lack of correlation was explored by dissecting the muscle tissue at the injection sites. It was observed that three types of spread occurred depending on the tissue structure: (i) within the muscle bundle, (ii) around the surface of the muscle bundle, and (iii) along the fat layer(s). Variable spreading profiles have also been reported in previous studies (Kaye et al. 1974, Austin et al. 1980a, Austin et al. 1980b). For example, spread on the surface of the muscle bundle was reported by Bjerregaard et al (2001) and Brown et al (1944) concluded that an oily formulation spreads along the fat layer rather than undergoing penetration.

The above results suggest that the spread of injectable formulations significantly depends on the interaction between the formulation and the structure of the muscle tissue. Some researchers have suggested it is critical to distinguish between intramuscular spread and extramuscular spread. In addition, when injecting a large volume, leakage from the intended target can occur due to the injectate exceeding the elasticity of the muscle tissue. For example, Gehling (2018) reported extensive extramuscular spread on injection of 200 µL of iohexol into the thigh muscle of mice. In this case, the injectate was found to spread between the muscle bundle where fat layers are usually present. Combined with other research, it suggests that injecting a large volume can lead to both intramuscular and extramuscular spread. Because the

absorption profiles are quite different (Zuidema et al. 1988), it could explain the erratic absorption of some IM injections.

The influence of US on the spread of IM injections of oily formulations was studied by taking post-injection CT scans at the injection site. For IM injections of the oily suspension, the spread of the 1.5 mL and 4.5 mL injections was significantly greater after exposure to US for 10 min and 5 min respectively. As mentioned previously, even with the lower injection volume, some intramuscular spread turns into extramuscular spread due to elasticity of the muscle. Once the injectate spreads outside the muscle bundle, it normally encounters layers of fat which is less elastic than muscle and therefore poses less resistance to spread. Application of US then applies a shear force at the injection site to further spread the injectate both intramuscularly and along the fat layers. It does this by (i) the high shear rate applied by US thinning the oily suspension as the it showed pseudoplastic and its viscosity was lower at higher shear rate (Table 3-11) and (ii) deceasing the particle size of the suspension through breaking down aggregates. Previous studies have shown that smaller particles (< 2-3 μm) pass more easily through the fibrous network of muscle (Zuidema et al. 1994). US also causes heating and this is discussed below.

With regard to the significant increase in spread caused by the shorter exposure to US for the 4.5 mL injection, it could be due to the greater probability of the formulation lying within the focal point of the US beam, since the diameter of the focal point of TSG – 7c US transducer is 26 mm. But the maximum length observed of spreading patterns was 120 mm in back muscle of post – mortem sheep. Apparently only a part of injected formulation was overlaid with US. The effect of a different vehicle used in oily suspension (Miglyol) and oily solution (poppy seed oil) is considered as minimal. Schultz, et al, injected 400 μL sesame oil and fractionated coconut oil into vastus lateralis of rabbits and studied the spread profile (Schultz et al. 1998). No significant difference was found in Schultz's study.

For SEDDS, the spread of the 1.5 mL injection was significantly increased only by the 10 min exposure to US as found for the oily suspension. In contrast, the spread of the 4.5 mL injection was significantly increased by exposure to US for both 5 min and 10 min duration. US caused about a about 5 °C (Figure 3.21) temperature rise at the

depth of the injections. This would have only a small effect on the viscosity of SEDDS (Table 3-11). Also, the viscosity of SEDDS dropped only slightly (from 0.05 Pa.s to 0.03 Pa.s) with increasing shear rate (Table 3-11) suggesting that US would have little effect on the viscosity of SEDDS. Therefore it is unlikely that US affected the spread of SEDDS by shear thinning of the formulation. Although the heating effect of US on viscosity is concluded to be minimal, the heating could lead to some flow due to thermal gradients but this was not investigated. Also, it is possible that the increasing spread is the result of the ability of US to increase the emulsification of the formulation by providing energy for the increasing surface area (Luque de Castro et al. 2007). The smaller the oil globules are, the better they can disperse throughout the aqueous medium in the surrounding muscle.

In literature, 3 MHz, 1.5 W/cm^2 US for 3.4 min exposure caused 4.5°C increase of temperature at a depth of 2.5 cm in muscle of human volunteers (Hayes et al. 2004). In this study, 28°C temperature increasement was observed at 4 cm depth in post-mortem experiment (Fig 3-18). The much higher raise of temperature in post-mortem model could be due to the lack of blood circulation. This is a critical difference between the post-mortem model to live model. As the heating may not occur the same effect, the thermal gradient in live model is expected smaller than post-mortem model. The effect of US on spread of IM injection in live model still needs more investigation.

No significant effect of US was found following the injection of both 1.5 mL and 4.5 mL volumes of oily solution for both 5 min and 10 min duration. The literature suggests there are two possible mechanisms of spread of oily solutions in muscle: (i) the solubilized contrast agent can spread by partitioning from the oily vehicle into the surrounding fluid (Hirano et al. 1981b), and (ii) the contrast agent can spread with its vehicle if the droplet size is sufficiently small (Weng Larsen et al. 2009). With respect to the oily solution, the lack of effect on US on spread may be explained by (i) the low partition coefficient of the contrast agent (ethyl esters of iodized fatty acids) that compose Lipiodol and (ii) the large droplet size of the oily formulation. With the chosen parameters of US, the log P of fatty acids and the droplet size of the formulation would not be altered because the heating effect was minimal (from 37°C to 42°C) and mechanical actuation due to cavitation was absent (Mujoo et al. 2016). It is possible

that with more energy deposition into tissue via US actuation, the heating and shearing effects could accelerate the spread of oily solutions. This requires further investigation.

3.7 Conclusion

In this chapter, the initial spread of all formulation types and injection volumes were measured and shown to be highly variable probably due to the heterogeneity of muscle tissue. Exposure to US for 10 min was found to significantly increase the spread of 1.5 mL and 4.5 mL volumes of oily suspensions and SEDDS. For the suspensions, this increase in spread is probably facilitated by the shear force of the applied US which reduces the viscosity. For the SEDDS, the viscosity was not changed too much due to the shear force from US application, neither the temperature increasement. The potential explanation was the US enhanced the emulsification, and the small oil globules from the emulsification could disperse throughout the aqueous medium faster. The heating effect of US also created a thermal gradient from the surface of skin to deep muscle. This thermal gradient may lead to convective flow but requires more investigation.

The use of CT scanning to visualize the spread of IM injections of oily formulations was shown to be a suitable strategy. In this study, the spread of IM injected oily formulations showed as a bulk from the CT scans. Shape of most bulk of injections were thin and long, which is different to sphere from some previous research (Tanaka et al. 1974, Hirano et al. 1981a). One major limitation of CT scanning used in this study was the resolution was too low. According to Section 1.2, the thickness of perimysium in muscle is 30 μm -40 μm. The CT scanning used in this study provided a resolution about 0.48 x 0.48 mm/pixel, which suggested this resolution was not sufficient to neither visualise the perimysium, nor the spread of IM injected formulation through the perimysium. This results showed consistency to another study focused on visualizing the pattern and volume of spread of IM injected oily formulation by using magnetic resonance imaging (MRI) technology (Kalicharan et al. 2016). Kailicharan's study also suggested resolution was a major limitation to improve the outcome of studies related to the spread of IM injections.

Aside from the imaging system, there was another limitation in this experimental system: the US transducer. The spread of IM injected formulation covered various depths and lengths which exceded the area of the US. As showed in Fig 3-18(c), the length of some bulk of injection was longer than 30 mm, whereas the diameter of US transducer was 26 mm. It is impossible to apply US on the whole bulk of injection evenly and simultaneously. Due to the variations in shape and size of the bulk of injection, it was hard to determine whether the US transducer covered the whole bulk of injection or not. This limitation could increase the error in the results. A real-time imaging-guiding system may improve the performance but future tests are required.

CHAPTER FOUR
CONCLUSION AND FUTURE WORK

4.1 GENERAL DISCUSSION

Two experimental models were tested in this study. In the gel phantom study (Chapter 2), oily and aqueous solutions were injected into agarose gel and tested with or without exposure to US. In the post-mortem sheep study (Chapter 3), an oily solution, suspension and a self-emulsifying drug delivery system (SEDDS) were injected into the back and rump muscles of lambs. Three durations of exposure to US (0, 5 and 10 min) were applied to the injection sites and the volume of spread measured after each injection. In Chapter 1, the following research questions were posed:

- Does US influence the spread of IM injections?
- Which factors determine the spread of IM injections in model systems and animals?

Referring to the first research question, significantly increased spread of 1.5 mL and 4.5 mL IM injections of the oily suspension and SEDDS was found in post-mortem sheep after exposure to US (1 MHz, 3 W/cm^2, 100% duty cycle) for 10 min. No influence of US on the spread of the oily solution was found in either the animal or gel phantom study. Also there was no effect of US on the spread of the aqueous solution in the gel study.

Referring to the second research question, the following factors were considered critical in determining the spread of IM injections:

Formulation type

The spread of the oily suspension and SEDDS was significantly enhanced by exposure to US at the injection site but the spread of the oily and aqueous solutions showed no response to US. For the oily solution, its hydrophobic nature makes it difficult to spread into an aqueous system such as the agarose gel or animal muscle. In contrast, in testing the aqueous solution in the gel study, the Nile blue dye diffused rapidly into the aqueous gel.

Temperature

A rise in temperature resulted from exposure to US in both the gel and post-mortem animal studies. For example, the temperature at the injection site in post-mortem sheep was found to increase by about 5°C after exposure to US (10 min, 1 MHz and 3W/cm^2). However, the influence of temperature on the spread of IM injections was not clear particularly in the absence of blood flow in post-mortem animals. Further research into the influence of temperature on spread in live animals is needed.

Viscosity and shear force

In theory, a lower viscosity can enhance the convection of an IM injection. In the post-mortem animal study, the viscosity of oily suspension was measured by a viscometer at various shear rate. The higher shear rate reduced the viscosity of oily suspension dramatically. It is speculated that US might cause shear thinning to the oily suspension and increased the spread of IM injection oily suspension in the post-mortem sheep.

Injection volume and duration of US exposure

There was no significant interaction between injection volume and the duration of US crossing all three types of formulation. Noticeably, from Table 3-10, for both SEDDS and the oily suspension, a significant increase in spread was observed for the small injection volume (1.5 mL) after 10 min exposure to US. For both SEDDS and the oily suspension, significant increases in spread were observed for the large injection volume (4.5 mL) after only 5 min exposure. These results suggest a large injection volume may require a shorter duration of US exposure to enhance spread.

The hypothesis of this thesis

The hypothesis of this thesis was that US can enhance the spread of formulations administered by IM injection in artificial models or animal muscle. The results show that exposure to US (1 MHz 3 W/cm^2, 100% duty cycle) for 10 min can enhance the spread of an oily suspension and SEDDS. The results also show that temperature,

injection volume, viscosity and hydrophilic/hydrophobic properties of the injected formulation are important for IM spread.

Comparing the agarose gel model with post-mortem sheep

In this thesis, two experimental models were used to study the influence of US on the spread of formulations administered by IM injection. Considering the agarose gel model, the transparency of agarose gel makes it easy to measure spread using a coloured dye. However, gels were unable to withstand injection of large volumes and cracked easily. Using premade cavities allowed injection of higher volumes but did not properly mimic an IM injection since pressure was not applied. Similarly, although the acoustic and thermal properties of agarose gel approximately match those of real muscle, agarose gel has neither skin nor a fat layer. In summary, agarose gel is a simple and cost-effective means to study IM injections of small volumes but has major deficiencies.

The post-mortem animal model provides the opportunity to study real muscle but suffers from the limitations of no blood flow and no muscle contraction. Blood flow provides two different effects on the spread of IM injected formulations. The first one is a sink condition to allow efficient partitioning of an oily formulation by providing sufficient solvent (Anissimov et al. 1999) and can be enhanced by the temperature rise induced by US (Robinson et al. 1995) to further increase the spread of an IM injection. On the other hand, the blood circulation carries the heat causing by US exposure away from the injection area. Then the thermal gradient created by US is supposed to be smaller than post-mortem model. It still enhances the convective flow but not as strongly as the in post-mortem model. The final impact from blood flow on US increased spread of IM injections needs more study. Apart from blood flow, muscle contraction and muscle elasticity can add extra shear stress to the injected formulation (Havas et al. 1997, Koo et al. 2013). Finally, the selection of an efficient imaging technique poses a significant challenge for a post-mortem animal study.

4.2 FUTURE DIRECTIONS

Due to limitations on instrumentation, time and budget, only a few physicochemical properties related to the effect of US on the spread of IM injections were studied in this thesis. In the future, other physicochemical properties would be worthy of study. For example, convective spread could be influenced by the surface tension of an injected fluid (Martin 2006) and is worth exploring. Other physicochemical properties such as particle size and HLB value are also of interest.

In terms of US, only the influence of duration of exposure was studied here. The frequency and intensity of US are critical for its biological effects and thus the influence of different frequencies and intensity of US would be of interest in future studies. This is particularly true given that previous research has shown that pulsed high intensity and high frequency US (HIFU) enhances penetration of substances into tissue and widens the intercellular spaces between epithelial cells (Frenkel 2008). The influence of pulsed HIFU on intramuscular spread is also of interest. Acoustic pressure was not measured in this study so it was difficult to evaluate the non-thermal effects of US on tissue. In future work, a hydrophone could be used to measure the acoustic pressure induced by US and thereby illuminate the interaction between US and convective spread. Finally, as stated earlier, spread of IM injections in live animals would move research in this area to the next level.

REFERENCE

Anissimov, Y. G. and M. S. Roberts (1999). "Diffusion modeling of percutaneous absorption kinetics. 1. Effects of flow rate, receptor sampling rate, and viable epidermal resistance for a constant donor concentration." Journal of Pharmaceutical Sciences 88(11): 1201-1209.

Austin, K. L., J. V. Stapleton and L. E. Mather (1980a). "Multiple intramuscular injections: A major source of variability in analgesic response to meperidine." PAIN 8(1): 47-62.

Austin, K. L., J. V. Stapleton and L. E. Mather (1980b). "Relationship between blood meperidine concentrations and analgesic response: a preliminary report." Anesthesiology 53(6): 460-466.

Aymard, P., D. R. Martin, K. Plucknett, T. J. Foster, A. H. Clark and I. T. Norton (2001). "Influence of thermal history on the structural and mechanical properties of agarose gels." Biopolymers 59(3): 131-144.

Baker, K. G., V. J. Robertson and F. A. Duck (2001). "A review of therapeutic ultrasound: Biophysical effects." Physical Therapy 81(7): 1351-1358.

Barnett, S. B. (1998). "WFUMB Symposium on Safety of Ultrasound in Medicine. Conclusions and recommendations on thermal and non-thermal mechanisms for biological effects of ultrasound. Kloster-Banz, Germany. 14-19 April, 1996. World Federation for Ultrasound in Medicine and Biology." Ultrasound in medicine & biology 24 Suppl 1: i-xvi, S1-58.

Behrendt, F. F., P. Bruners, J. Kalafut, A. H. Mahnken, S. Keil, C. Plumhans, M. Das, S. Stanzel, J. E. Wildberger, J. Pfeffer, R. W. Günther and G. Mühlenbruch (2008). "Introduction of a dedicated circulation phantom for comprehensive in vitro analysis of intravascular contrast material application." Investigative Radiology 43(10): 729-736.

Bjerregaard, S., H. Pedersen, H. Vedstesen, C. Vermehren, I. Soderberg and S. Frokjaer (2001). "Parenteral water/oil emulsions containing hydrophilic compounds with enhanced in vivo retention: formulation, rheological characterisation and study of in vivo fate using whole body gamma-scintigraphy." Int J Pharm 215(1-2): 13-27.

Chen, X., G. W. Astary, H. Sepulveda, T. H. Mareci and M. Sarntinoranont (2008). "Quantitative assessment of macromolecular concentration during direct infusion into an agarose hydrogel phantom using contrast-enhanced MRI." Magnetic Resonance Imaging 26(10): 1433-1441.

Cortela, G. A., M. A. Von Krüger, C. A. Negreira and W. C. A. Pereira (2016). "Influence of ultrasonic scattering in the calculation of thermal dose in ex-vivo bovine muscular tissues." Ultrasonics 65: 121-130.

Darville, N., M. van Heerden, D. Mariën, M. De Meulder, S. Rossenu, A. Vermeulen, A. Vynckier, S. De Jonghe, P. Sterkens, P. Annaert and G. Van den Mooter (2016). "The effect of macrophage and angiogenesis inhibition on the drug release and absorption from an intramuscular sustained-release paliperidone palmitate suspension." Journal of Controlled Release 230: 95-108.

Dauffenbach, J., M. J. Pingree, S. J. Wisniewski, N. Murthy and J. Smith (2014). "Distribution pattern of sonographically guided iliopsoas: Injections cadaveric investigation using coned beam computed tomography." Journal of Ultrasound in Medicine 33(3): 405-414.

Davis, S. S., C. Washington, P. West, L. Illum, G. Liversidge, L. Sternson and R. Kirsh (1987). "Lipid Emulsions as Drug Delivery Systems." Annals of the New York Academy of Sciences 507(1): 75-88.

Dayton, P., A. Klibanov, G. Brandenburger and K. Ferrara (1999). "Acoustic radiation force in vivo: A mechanism to assist targeting of microbubbles." Ultrasound in Medicine and Biology 25(8): 1195-1201.

Dayton, P. A., J. S. Allen and K. W. Ferrara (2002). "The magnitude of radiation force on ultrasound contrast agents." Journal of the Acoustical Society of America 112(5 I): 2183-2192.

Divkovic, G. W., M. Liebler, K. Braun, T. Dreyer, P. E. Huber and J. W. Jenne (2007). "Thermal properties and changes of acoustic parameters in an egg white phantom during heating and coagulation by high intensity focused ultrasound." Ultrasound Med Biol 33(6): 981-986.

Draper, D. O., J. C. Castel and D. Castel (1995). "Rate of temperature increase in human muscle during 1 MHz and 3 MHz continuous ultrasound." Journal of Orthopaedic and Sports Physical Therapy 22(4): 142-150.

Dutt, G. B., S. Doraiswamy and N. Periasamy (1991). "Molecular-Reorientation Dynamics of Polar Dye Probes in Tertiary-Butyl Alcohol Water Mixtures." Journal of Chemical Physics 94(8): 5360-5368.

Fang, S. H., T. Nishimura and K. Takahashi (1999). "Relationship between development of intramuscular connective tissue and toughness of pork during growth of pigs." Journal of Animal Science 77(1): 120-130.

Foroughi, J., G. M. Spinks, G. G. Wallace, J. Oh, M. E. Kozlov, S. Fang, T. Mirfakhrai, J. D. W. Madden, M. K. Shin, S. J. Kim and R. H. Baughman (2011). "Torsional Carbon Nanotube Artificial Muscles." Science 334(6055): 494-497.

Fratzl, P. (2008). Collagen: Structure and Mechanics, Springer US.

Frenkel, V. (2008). "Ultrasound mediated delivery of drugs and genes to solid tumors." Advanced Drug Delivery Reviews 60(10): 1193-1208.

Frenkel, V., R. Gurka, A. Liberzon, U. Shavit and E. Kimmel (2001). "Preliminary investigations of ultrasound induced acoustic streaming using particle image velocimetry." Ultrasonics 39(3): 153-156.

Frenkel, V., E. Kimmel and Y. Iger (2000a). "Ultrasound-facilitated transport of silver chloride (AgCl) particles in fish skin." Journal of Controlled Release 68(2): 251-261.

Frenkel, V., E. Kimmel and Y. Iger (2000b). "Ultrasound-induced intercellular space widening in fish epidermis." Ultrasound in Medicine & Biology 26(3): 473-480.

Gammell, P. M., D. H. Le Croissette and R. C. Heyser (1979). "Temperature and frequency dependence of ultrasonic attenuation in selected tissues." Ultrasound in Medicine & Biology 5(3): 269-277.

Gehling, A. M., K. Kuszpit, E. J. Bailey, K. H. Allen-Worthington, D. P. Fetterer, P. J. Rico, T. M. Bocan and C. C. Hofer (2018). "Evaluation of Volume of Intramuscular Injection into the Caudal Thigh Muscles of Female and Male BALB/c Mice (Mus musculus)." J Am Assoc Lab Anim Sci 57(1): 35-43.

Gordon L. Amidon, P. I. L., Elizabeth M. Topp (2000). Transport processes in pharmaceutical systems. New York, Marcel Dekker.

Havas, E., T. Parviainen, J. Vuorela, J. Toivanen, T. Nikula and V. Vihko (1997). "Lymph flow dynamics in exercising human skeletal muscle as detected by scintography." The Journal of Physiology 504(1): 233-239.

Hayes, B. T., M. A. Merrick, M. A. Sandrey and M. L. Cordova (2004). "Three-MHz ultrasound heats deeper into the tissues than originally theorized." Journal of Athletic Training 39(3): 230-234.

Hirano, K., T. Ichihashi and H. Yamada (1981a). "Studies on the absorption of practically water-insoluble drugs following injection. I. Intramuscular absorption from water-immiscible oil solutions in rats." Chem Pharm Bull (Tokyo) 29(2): 519-531.

Hirano, K., T. Ichihashi and H. Yamada (1981b). "Studies on the absorption of practically water-insoluble drugs following injection. II. Intramuscular absorption from aqueous suspensions in rats." Chem Pharm Bull (Tokyo) 29(3): 817-827.

Hirano, K. and H. Yamada (1981c). "Studies on the absorption of practically water-insoluble drugs following injection. IV. An approach for predicting relative intramuscular absorption rates of a drug in oily solution, aqueous suspension and aqueous surfactant solution in rats." Chem Pharm Bull (Tokyo) 29(5): 1410-1415.

Howard, J. R. and J. Hadgraft (1983). "The clearance of oily vehicles following intramuscular and subcutaneous injections in rabbits." International Journal of Pharmaceutics 16(1): 31-39.

Hynynen, K., N. McDannold, N. A. Sheikov, F. A. Jolesz and N. Vykhodtseva (2005). "Local and reversible blood-brain barrier disruption by noninvasive focused ultrasound at frequencies suitable for trans-skull sonications." NeuroImage 24(1): 12-20.

Kalicharan, R. W., P. Baron, C. Oussoren, L. W. Bartels and H. Vromans (2016). "Spatial distribution of oil depots monitored in human muscle using MRI." International Journal of Pharmaceutics 505(1-2): 52-60.

Kaye, D., M. E. Levison and E. D. Labovitz (1974). "The Unpredictability of Serum Concentrations of Gentamicin: Pharmacokinetics of Gentamicin in Patients with

Normal and Abnormal Renal Function." Journal of Infectious Diseases 130(2): 150-154.

Koo, T. K., J.-Y. Guo, J. H. Cohen and K. J. Parker (2013). "Relationship between shear elastic modulus and passive muscle force: An ex-vivo study." Journal of Biomechanics 46(12): 2053-2059.

López-Haro, S. A., M. I. Gutiérrez, A. Vera and L. Leija (2015). "Modeling the thermo-acoustic effects of thermal-dependent speed of sound and acoustic absorption of biological tissues during focused ultrasound hyperthermia." Journal of Medical Ultrasonics 42(4): 489-498.

Larsen, C., K. Schultz, A. N. Fisher and L. Illum (1998). "Intramuscular fate of C-14- and I-131-labelled triglycerides." International Journal of Pharmaceutics 166(2): 227-230.

Lele, P. P., A. B. Mansfield, A. I. Murphy, J. Namery and N. Senapati (1975). "TISSUE CHARACTERIZATION BY ULTRASONIC FREQUENCY-DEPENDENT ATTENUATION AND SCATTERING." Natl Bur Stand Spec Publ(453): 167-196.

Liu, Y., S. Paliwal, K. S. Bankiewicz, J. R. Bringas, G. Heart, S. Mitragotri and M. R. Prausnitz (2010). "Ultrasound-enhanced drug transport and distribution in the brain." AAPS PharmSciTech 11(3): 1005-1017.

Luque de Castro, M. D. and F. Priego-Capote (2007). "Ultrasound-assisted crystallization (sonocrystallization)." Ultrason Sonochem 14(6): 717-724.

Martin, P. J. S. A. N. (2006). Martin's physical pharmacy and pharmaceutical sciences : physical chemical and biopharmaceutical principles in the pharmaceutical sciences. Philadelphia, Lippincott Williams & Wilkins.

McCabe, M. (1972). "The diffusion coefficient of caffeine through agar gels containing a hyaluronic acid-protein complex. A model system for the study of the permeability of connective tissues." Biochemical Journal 127(1): 249-253.

Miller, D. L., S. V. Pislaru and J. F. Greenleaf (2002). "Sonoporation: Mechanical DNA delivery by ultrasonic cavitation." Somatic Cell and Molecular Genetics 27(1-6): 115-134.

Miller, D. L., N. B. Smith, M. R. Bailey, G. J. Czarnota, K. Hynynen and I. R. S. Makin (2012). "Overview of therapeutic ultrasound applications and safety considerations." Journal of Ultrasound in Medicine 31(4): 623-634.

Morrissey, V. P. J. (2011). Practical and Professional Clinical Skills. New York, Oxford University Press.

Mujoo, H., J. N. J. Reynolds and I. G. Tucker (2016). "The influence of bile salts on the response of liposomes to ultrasound." Journal of Liposome Research 26(2): 87-95.

Narayanan, J., J. Y. Xiong and X. Y. Liu (2006). "Determination of agarose gel pore size: Absorbance measurements vis a vis other techniques." International Conference on Materials for Advanced Technologies (ICMAT 2005) 28: 83-86.

Neslihan Gursoy, R. and S. Benita (2004). "Self-emulsifying drug delivery systems (SEDDS) for improved oral delivery of lipophilic drugs." Biomedicine & Pharmacotherapy 58(3): 173-182.

Nguyen, A. T., C. Wong, A. Mojallal and M. Saint-Cyr (2011). "Lateral supragenicular pedicle perforator flap: clinical results and vascular anatomy." J Plast Reconstr Aesthet Surg 64(3): 381-385.

Nowak, R. M., S. K. Fleshman and G. K. Lewis (2015). Acoustic and thermal outputs of commercially available therapeutic ultrasound devices. 2015 41st Annual Northeast Biomedical Engineering Conference, NEBEC 2015.

O'Brien Jr, W. D. (2007). "Ultrasound-biophysics mechanisms." Progress in Biophysics and Molecular Biology 93(1-3): 212-255.

Offer, G. and J. Trinick (1983). "On the mechanism of water holding in meat: The swelling and shrinking of myofibrils." Meat Science 8(4): 245-281.

Ortega, R., A. Téllez, L. Leija and A. Vera (2010). Measurement of ultrasonic properties of muscle and blood biological phantoms. Physics Procedia.

Pearce, K. L., K. Rosenvold, H. J. Andersen and D. L. Hopkins (2011). "Water distribution and mobility in meat during the conversion of muscle to meat and ageing and the impacts on fresh meat quality attributes--a review." Meat Sci 89(2): 111-124.

Pernodet, N., M. Maaloum and B. Tinland (1997). "Pore size of agarose gels by atomic force microscopy." Electrophoresis 18(1): 55-58.

Pilkington, B., S. Goodhew and P. Dewilde (2010). "In situ thermal conductivity measurements of building materials with a thermal probe." Journal of Testing and Evaluation 38(3).

Pluen, A., P. A. Netti, R. K. Jain and D. A. Berk (1999). "Diffusion of macromolecules in agarose gels: comparison of linear and globular configurations." Biophys J 77(1): 542-552.

Rajanayagam, V., M. E. Fabry and J. C. Gore (1991). "In vivo quantitation of water content in muscle tissues by NMR imaging." Magnetic Resonance Imaging 9(4): 621-625.

Robert Schleip, T. W. F., Leon Chaitow, Peter Huijing (2012). Churchill Livingstone.

Robinson, S. E. and M. J. Buono (1995). "Effect of Continuous-Wave Ultrasound on Blood Flow in Skeletal Muscle." Physical Therapy 75(2): 145-149.

Schmalbruch, H. and Z. Kamieniecka (1974). "Fiber types in the human brachial biceps muscle." Experimental Neurology 44(2): 313-328.

Schultz, K., B. Møllgaard, A. N. Fisher, L. Illum and C. Larsen (1998). "Intramuscular rate of disappearance of oily vehicles in rabbits investigated by gamma-scintigraphy." International Journal of Pharmaceutics 169(1): 121-126.

Seo, E., J. H. Lim, S. J. Seo and S. J. Lee (2015). "Whole-body imaging of a hypercholesterolemic female zebrafish by using synchrotron X-ray micro-CT." Zebrafish 12(1): 11-20.

Takegami, K., Y. Kaneko, T. Watanabe, T. Maruyama, Y. Matsumoto and H. Nagawa (2004). "Polyacrylamide gel containing egg white as new model for irradiation experiments using focused ultrasound." Ultrasound Med Biol 30(10): 1419-1422.

Tanaka, T., H. Kobayashi, K. Okumura, S. Muranishi and H. Sezaki (1974). "Intramuscular absorption of drugs from oily solutions in the rat." Chem Pharm Bull (Tokyo) 22(6): 1275-1284.

ter Haar, G. (2007). "Therapeutic applications of ultrasound." Progress in Biophysics and Molecular Biology 93(1-3): 111-129.

Torr, G. R. (1984). "The acoustic radiation force." American Journal of Physics 52(5): 402-408.

Wells, P. N. T. (1977). "Ultrasonics in medicine and biology." Physics in Medicine and Biology 22(4): 629-669.

Weng Larsen, S. and C. Larsen (2009). "Critical Factors Influencing the In Vivo Performance of Long-acting Lipophilic Solutions—Impact on In Vitro Release Method Design." The AAPS Journal 11(4): 762-770.

Westrin, P., C. Jonmarker and O. Werner (1992). "Dissolving methohexital in a lipid emulsion reduces pain associated with intravenous injection." Anesthesiology 76(6): 930-934.

Wust, P., J. Nadobny, M. Szimtenings, E. Stetter and J. Gellermann (2007). "Implications of clinical RF hyperthermia on protection limits in the RF range." Health Physics 92(6): 565-573.

Ye, F., S. W. Larsen, A. Yaghmur, H. Jensen, C. Larsen and J. Østergaard (2012). "Drug release into hydrogel-based subcutaneous surrogates studied by UV imaging." Journal of Pharmaceutical and Biomedical Analysis 71: 27-34.

Zelman, S. (1961). "Notes on techniques of intramuscular injection. The avoidance of needless pain and morbidity." The American journal of the medical sciences 241: 563-574.

Zhang, L., X. Qian, K. Zhang, Q. Cui, Q. Zhao and Z. Liu (2013). "Three-dimensional reconstruction of blood vessels in the rabbit eye by X-ray phase contrast imaging." Biomed Eng Online 12: 30.

Zhi-Jian, C., W. C. Broaddus, R. R. Viswanathan, R. Raghavan and G. T. Gillies (2002). "Intraparenchymal drug delivery via positive-pressure infusion: experimental and modeling studies of poroelasticity in brain phantom gels." Biomedical Engineering, IEEE Transactions on 49(2): 85-96.

Zuidema, J., F. Kadir, H. A. C. Titulaer and C. Oussoren (1994). "Release and absorption rates of intramuscularly and subcutaneously injected pharmaceuticals (II)." International Journal of Pharmaceutics 105(3): 189-207.

Zuidema, J., F. A. J. M. Pieters and G. S. M. J. E. Duchateau (1988). "Release and absorption rate aspects of intramuscularly injected pharmaceuticals." International Journal of Pharmaceutics 47(1–3): 1-12.

APPENDIX-1

Imaging processing for measuring the area of spread

Setting scale

All images captured in gel phantom experiments were processed by software ImageJ (Version 1.49, National Institutes of Health, U.S.A). A ruler was included in each image to set the scale. For instance, in ImageJ a line equalling 10 mm on the ruler was drawn. Then, using the "set scale" function of ImageJ, the "known distance" and the "unit of distance" were typed in. Then, "OK" was clicked to finish setting the scale.

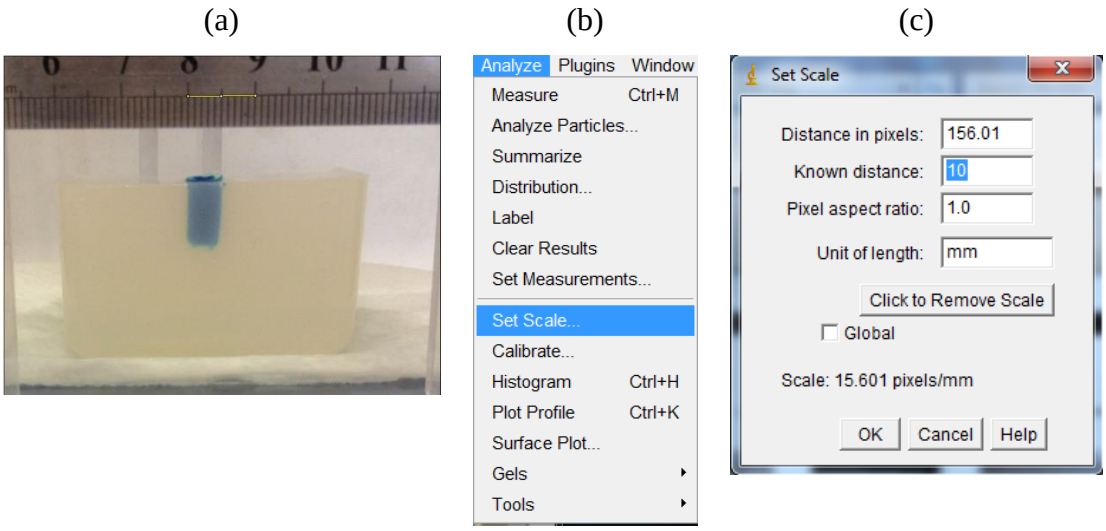

Figure 6-1 Using the Set Scale function in ImageJ. (a) The original picture showing the phantom gel and the Nile blue dye injectate; a ruler above the gel provides a reference for scale; (b) and (c) The user interfaces of ImageJ used to set the scale.

Selecting the area of interest

The distribution area of an injection needs to be correctly selected. Before selecting and measuring the area of interest, the background noise was reduced by the "subtract background" function of ImageJ. The injection area can be selected by "adjusting the threshold", and then using the "binary" function of ImageJ. Finally, the area of interest can be set and managed by the "ROI manager" function of ImageJ. In order to ensure a

consistent threshold and reduce the variance during image processing, a fixed level of threshold was used for all images. The process is shown in the following Figures:

(a)

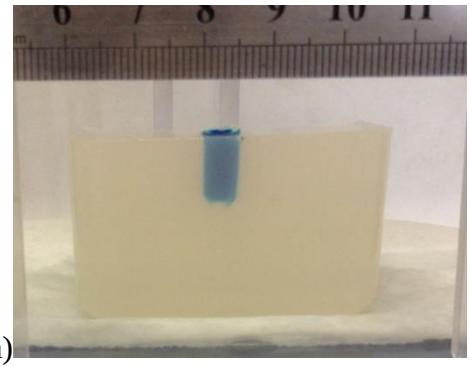

(b)

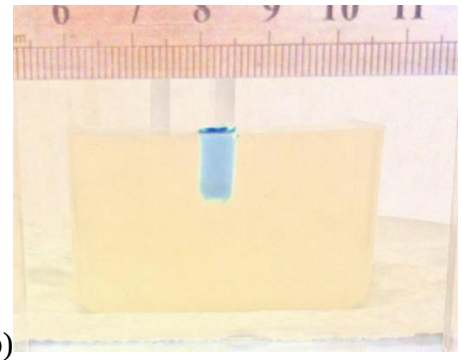

(c)

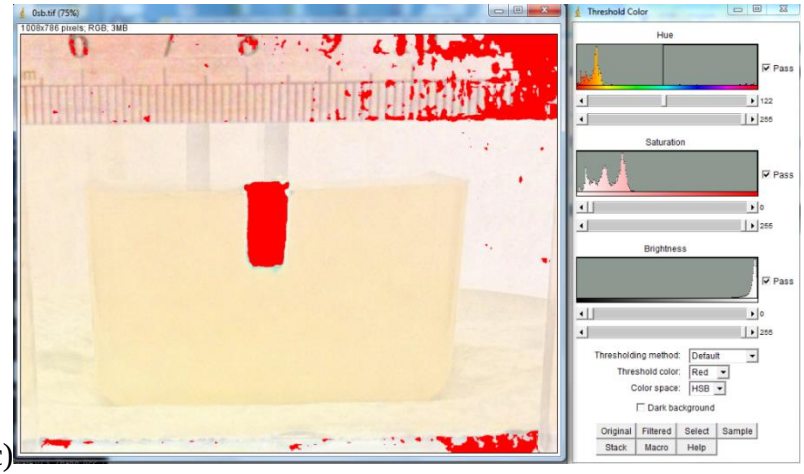

(d)

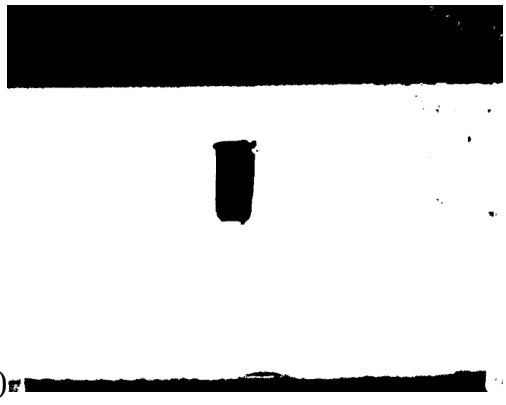

Figure 6-2 Processing images using ImageJ. (a) The original picture showing the phantom gel and the Nile blue injectate; (b) reducing background noise by subtracting the background; (c) adjusting the threshold; and (d) select Binary to convert the picture to a white/black image.

Area of distribution measurement

The distribution area of an injectate is selected from Binary images as follows:

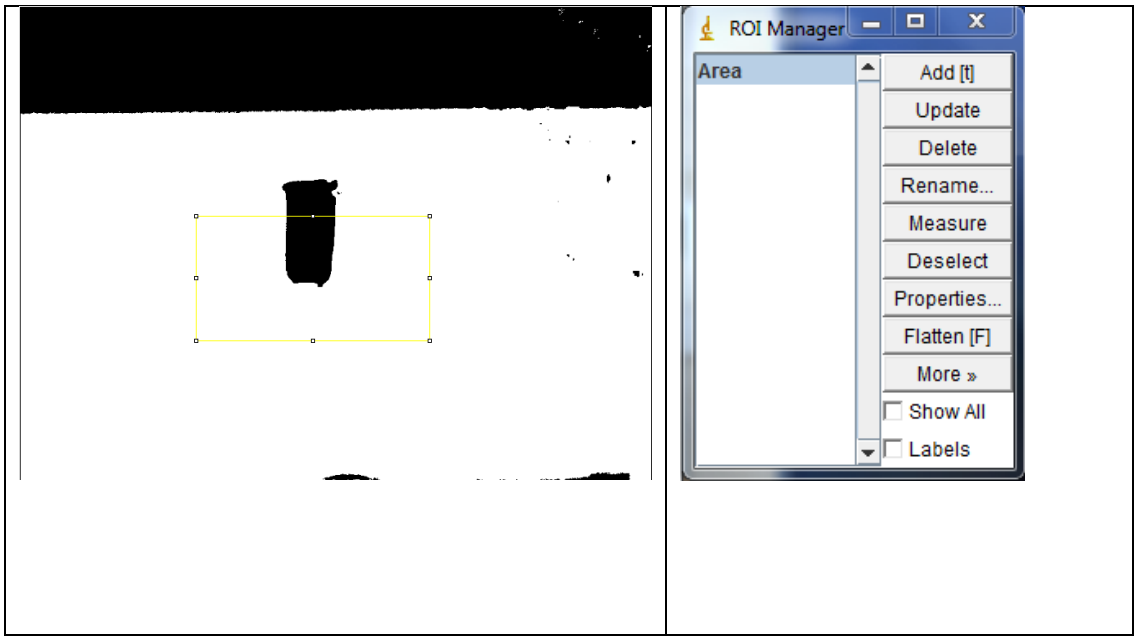

Figure 6-3. Select the area of interest.

The distribution area of an injectate can be measured in ImageJ. The "Region of interest" (ROI) manager is used to create consistent measurements (yellow block in Figure 6-3) in each image. Then the area of the black colour inside the "Region of interest" is measured by the "Analysis particles" function in ImageJ.

Grayscale measurement

The grayscale of each injection was measured using the following method:

The original images were set to scale as described in Appendix. Then each image was chopped into a consistent size and a line set as region of interest and kept consistent in each picture as shown in Figure 6-4 (a).

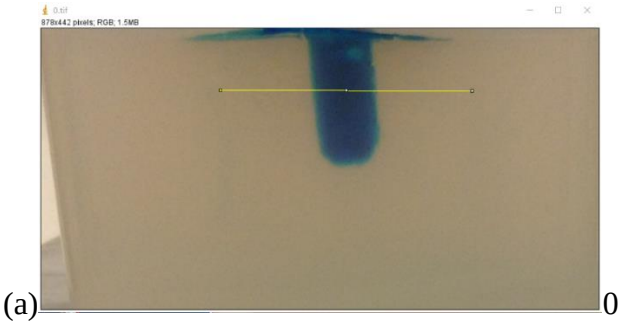

Figure 6-4 Grayscale measurement. (a) The yellow line indicates the consistent region of interest in images taken at various times (0, 30 and 60 mins); (b) selecting the function “Multiple plot” in the ROI manager of ImageJ; (c) a typical multiple plot which can be exported to Microsoft Excel.

The grayscale was then measured by the function “Multiple Plot” in the ROI manager of ImageJ as shown in Figure 6-4 (b). Finally, all plots (a typical one shown in Figure 6-4 (c)) were exported to Microsoft Excel.

APPENDIX-2

General Linear Model: Initial spread versus Formulation, Injection volume, Block

Method

Factor coding (-1, 0, +1)

Factor Information

Factor	Type	Levels	Values
Formulation	Fixed	3	SEDDS, Solution, Suspension
Injection volume	Fixed	2	1.5, 4.5
Block	Fixed	2	Back, Rump

Analysis of Variance

Source	DF	Adj SS	Adj MS	F-Value	P-Value
Formulation	2	29809510	14904755	0.74	0.488
Injection volume	1	21840044	21840044	1.08	0.307
Block	1	2150133	2150133	0.11	0.747
Formulation*Injection volume	2	5018098	2509049	0.12	0.884
Error	29	586905530	20238122		
Lack-of-Fit	5	150644437	30128887	1.66	0.183
Pure Error	24	436261093	18177546		
Total	35	645723315			

Model Summary

S	R-sq	R-sq(adj)	R-sq(pred)
4498.68	9.11%	0.00%	0.00%

Coefficients

Term	Coef	SE Coef	T-Value	P-Value	VIF
Constant	7775	750	10.37	0.000	
Formulation					
SEDDS	1249	1060	1.18	0.248	1.33
Solution	-893	1060	-0.84	0.407	1.33
Injection volume					
1.5	-779	750	-1.04	0.307	1.00
Block					
Back	244	750	0.33	0.747	1.00
Formulation*Injection volume					
SEDDS 1.5	-204	1060	-0.19	0.849	1.33
Solution 1.5	-320	1060	-0.30	0.765	1.33

Regression Equation

Initial spread = 7775 + 1249 Formulation_SEDDS - 893 Formulation_Solution
- 356 Formulation_Suspension - 779 Injection volume_1.5
+ 779 Injection volume_4.5 + 244 Block_Back - 244 Block_Rump
- 204 Formulation*Injection volume_SEDDS 1.5
+ 204 Formulation*Injection volume_SEDDS 4.5
- 320 Formulation*Injection volume_Solution 1.5
+ 320 Formulation*Injection volume_Solution 4.5
+ 524 Formulation*Injection volume_Suspension 1.5
- 524 Formulation*Injection volume_Suspension 4.5

Comparisons for Initial spread

Tukey Pairwise Comparisons: Formulation

Grouping Information Using the Tukey Method and 95% Confidence

Formulation	N	Mean	Grouping
SEDDS	12	9024.50	A
Suspension	12	7419.17	A
Solution	12	6882.67	A

Means that do not share a letter are significantly different.

Tukey Pairwise Comparisons: Injection volume

Grouping Information Using the Tukey Method and 95% Confidence

Injection volume	N	Mean	Grouping
4.5	18	8554.33	A
1.5	18	6996.56	A

Means that do not share a letter are significantly different.

Tukey Pairwise Comparisons: Block

Grouping Information Using the Tukey Method and 95% Confidence

Block	N	Mean	Grouping
Back	18	8019.83	A
Rump	18	7531.06	A

Means that do not share a letter are significantly different.

Tukey Pairwise Comparisons: Formulation*Injection volume

Grouping Information Using the Tukey Method and 95% Confidence

Formulation*Injection volume	N	Mean	Grouping
SEDDS 4.5	6	10007.2	A
SEDDS 1.5	6	8041.8	A
Solution 4.5	6	7981.5	A
Suspension 4.5	6	7674.3	A
Suspension 1.5	6	7164.0	A
Solution 1.5	6	5783.8	A

Means that do not share a letter are significantly different.

Tukey Pairwise Comparisons: Formulation*Block

Grouping Information Using the Tukey Method and 95% Confidence

Formulation*Block	N	Mean	Grouping
SEDDS Back	6	11442.2	A
Suspension Rump	6	9535.5	A
Solution Back	6	7314.5	A
SEDDS Rump	6	6606.8	A
Solution Rump	6	6450.8	A
Suspension Back	6	5302.8	A

Means that do not share a letter are significantly different.

Tukey Pairwise Comparisons: Injection volume*Block

Grouping Information Using the Tukey Method and 95% Confidence

Injection volume*Block	N	Mean	Grouping
4.5 Back	9	9396.22	A
4.5 Rump	9	7712.44	A
1.5 Rump	9	7349.67	A
1.5 Back	9	6643.44	A

Means that do not share a letter are significantly different.

Tukey Pairwise Comparisons: Formulation*Injection volume*Block

Grouping Information Using the Tukey Method and 95% Confidence

Formulation*Injection volume*Block	N	Mean	Grouping
SEDDS 4.5 Back	3	12543.7	A
Suspension 1.5 Rump	3	10752.7	A
SEDDS 1.5 Back	3	10340.7	A
Solution 4.5 Back	3	8614.7	A
Suspension 4.5 Rump	3	8318.3	A
SEDDS 4.5 Rump	3	7470.7	A
Solution 4.5 Rump	3	7348.3	A
Suspension 4.5 Back	3	7030.3	A
Solution 1.5 Back	3	6014.3	A
SEDDS 1.5 Rump	3	5743.0	A
Solution 1.5 Rump	3	5553.3	A
Suspension 1.5 Back	3	3575.3	A

Means that do not share a letter are significantly different.

Main Effects Plot for Initial spread

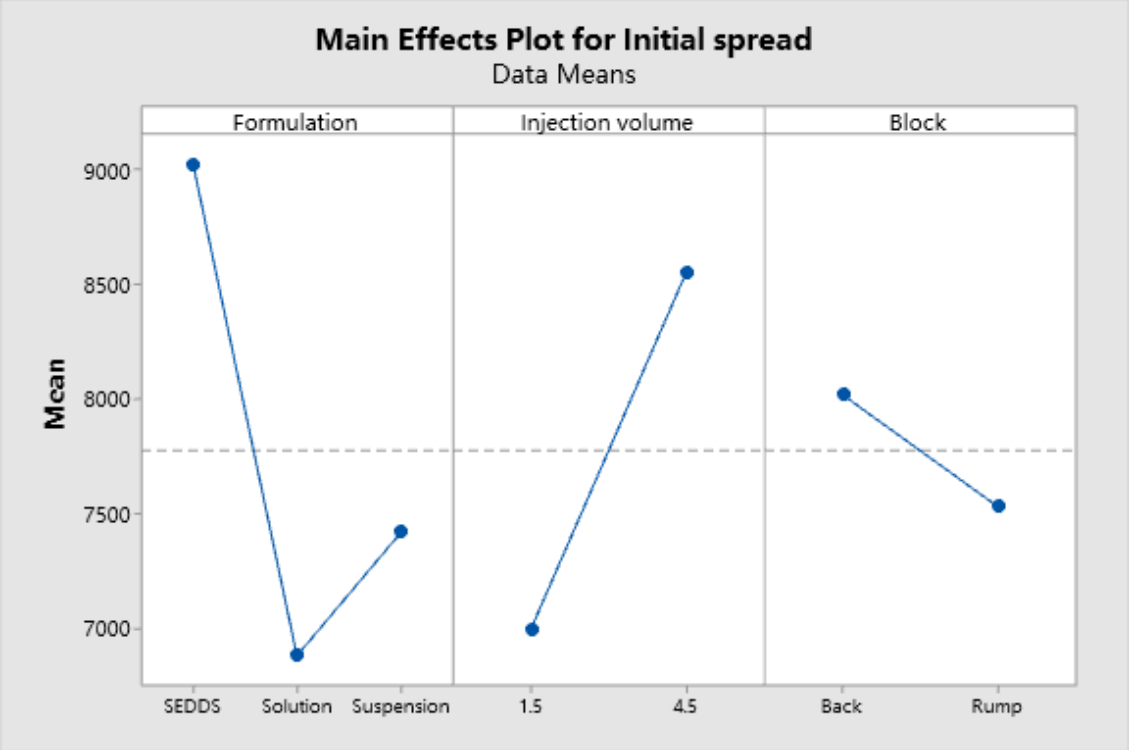

Interaction Plot for Initial spread

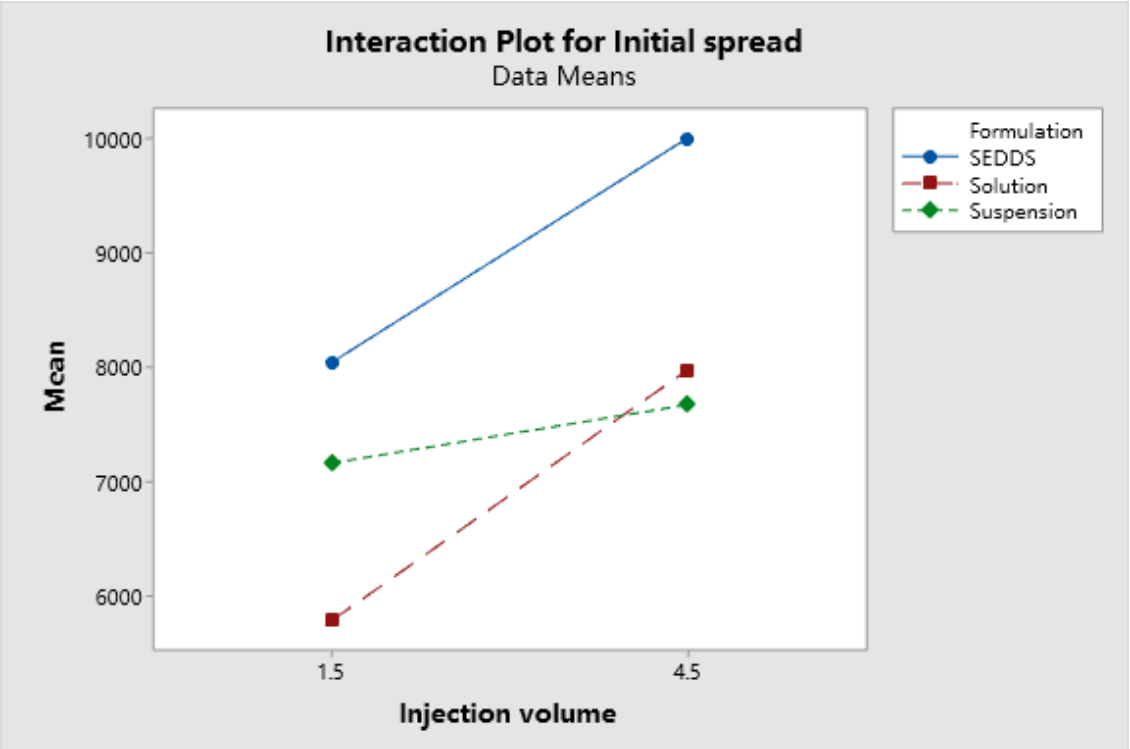

APPENDIX-3

On exposure to US, the mean spread of the 1.5 mL injections increased by 28% and 39% with exposure to US for 5 and 10 min respectively. The 4.5 mL injections showed a trend of being more sensitive to US showing increases in spread of 44% and 49% with exposure to US for 5 and 10 min respectively but this interaction between volume and US exposure was not statistically significant (P=0.184).

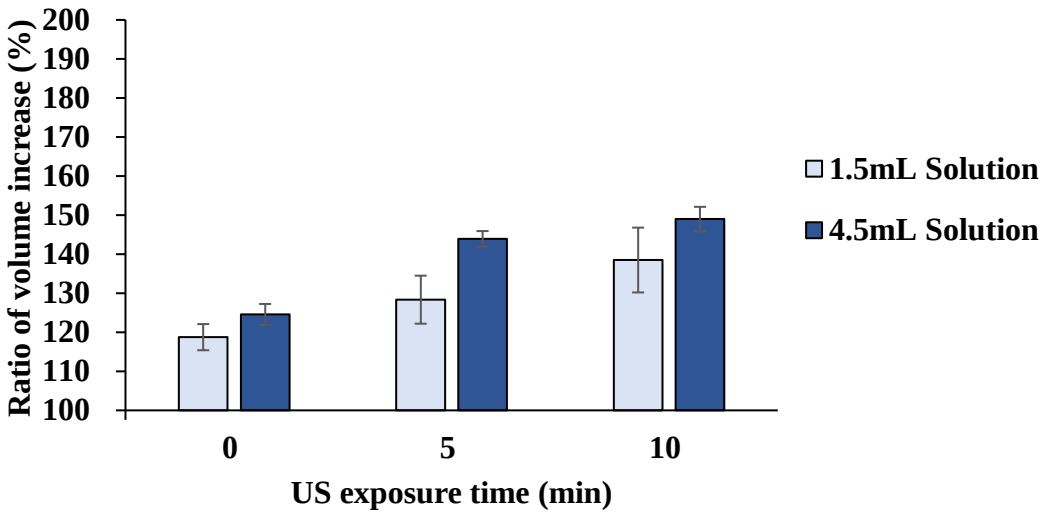

Figure 8-1 Ratio of volumes of spread of oily solutions for the 2 CT scans after exposure to no US (0) and to US for 5 and 10 min (data are means ± SD, n=2).

Turning to the oily suspensions, the spread of the control group increased by 27% and 39% for the 1.5 mL and 4.5 mL injection volumes respectively (Figure 3-15). Corresponding increases after 5 and10 min exposure to US were 51% and 66% for the 1.5 mL injection and 71% and 62% for the 4.5 mL injection.

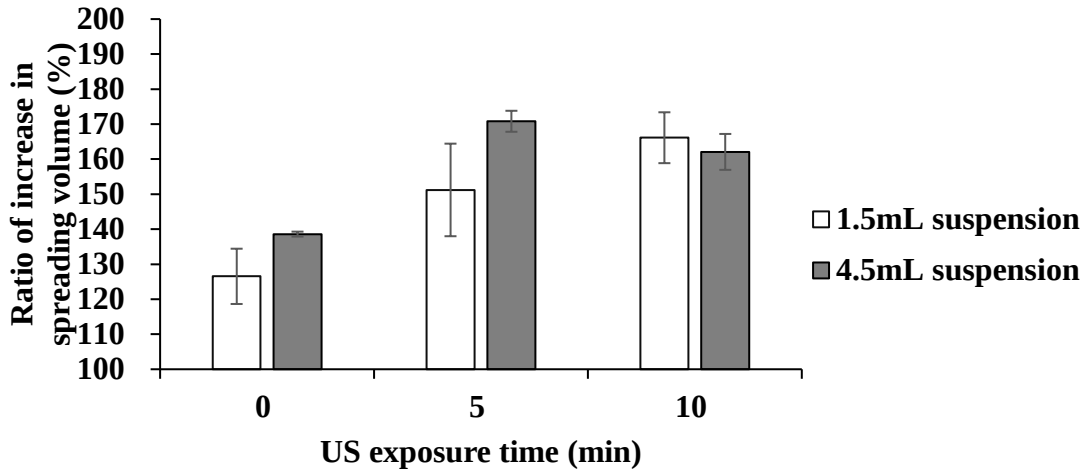

Figure 8-2 Ratio of volumes of spread of oily suspensions for the 2 CT scans after exposure to no US (0) and to US for 5 and 10 mins (data are means ± SD, n=2).

Turning to SEDDS, the spread of the control group increased by 13% and 12% for the 1.5 mL and 4.5 mL injection volumes respectively (Figure 3-16). Corresponding increases after 5 and10 min exposure to US were 33% and 54% for the 1.5 mL injections and 49 % and 84% for the 4.5 mL injections.

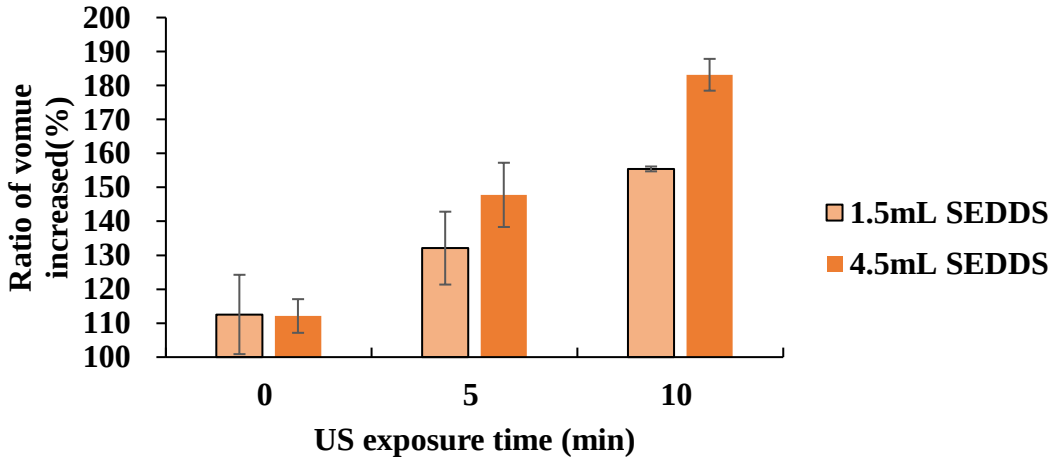

Figure 8-3 Ratio of volumes of spread of SEDDS for the 2 CT scans after exposure to no US (0) and to US for 5 and 10 mins (data are means ± SD, n=2).

APPENDIX–4

General Linear Model: Spread versus Formulation, Injection volume, US duration, Block

Method

Factor coding (-1, 0, +1)

Factor Information

Factor	Type	Levels	Values
Formulation	Fixed	3	SEDDS, solution, Suspension
Injection volume	Fixed	2	1.5, 4.5
US duration	Fixed	3	0, 5, 10
Block	Fixed	2	Back, Rump

Analysis of Variance

Source	DF	Adj SS	Adj MS	F-Value	P-Value
Formulation	2	2161.9	1080.95	21.84	0.000
Injection volume	1	1166.2	1166.22	23.57	0.000
US duration	2	8357.6	4178.80	84.45	0.000
Block	1	150.1	150.06	3.03	0.100
Formulation*Injection volume	2	42.3	21.16	0.43	0.659
Formulation*US duration	4	1555.8	388.95	7.86	0.001
Injection volume*US duration	2	185.4	92.69	1.87	0.184
Formulation*Injection volume*US duration	4	552.9	138.23	2.79	0.060
Error	17	841.2	49.48		
Total	35	15013.4			

Model Summary

S	R-sq	R-sq(adj)	R-sq(pred)
7.03442	94.40%	88.46%	74.87%

Coefficients

Term	Coef	SE Coef	T-Value	P-Value	VIF
Constant	142.31	1.17	121.39	0.000	
Formulation					
SEDDS	-1.80	1.66	-1.08	0.294	1.33
solution	-8.46	1.66	-5.10	0.000	1.33
Injection volume					
1.5	-5.69	1.17	-4.85	0.000	1.00
US duration					
0	-20.12	1.66	-12.14	0.000	1.33
5	3.39	1.66	2.04	0.057	1.33
Block					
Back	-2.04	1.17	-1.74	0.100	1.00
Formulation*Injection volume					
SEDDS 1.5	-1.48	1.66	-0.89	0.386	1.33
solution 1.5	0.37	1.66	0.23	0.824	1.33
Formulation*US duration					
SEDDS 0	-8.07	2.34	-3.44	0.003	1.78
SEDDS 5	-3.95	2.34	-1.69	0.110	1.78
solution 0	7.95	2.34	3.39	0.003	1.78
solution 5	-1.11	2.34	-0.47	0.642	1.78

Injection volume*US duration					
1.5 0	2.78	1.66	1.68	0.111	1.33
1.5 5	-2.78	1.66	-1.67	0.112	1.33
Formulation*Injection volume*US duration					
SEDDS 1.5 0	4.61	2.34	1.97	0.066	1.78
SEDDS 1.5 5	2.09	2.34	0.89	0.385	1.78
solution 1.5 0	-0.39	2.34	-0.17	0.869	1.78
solution 1.5 5	0.32	2.34	0.14	0.894	1.78

Regression Equation

Spread = 142.31 - 1.80 Formulation_SEDDS - 8.46 Formulation_solution
+ 10.26 Formulation_Suspension - 5.69 Injection volume_1.5
+ 5.69 Injection volume_4.5 - 20.12 US duration_0 + 3.39 US duration_5
+ 16.74 US duration_10 - 2.04 Block_Back + 2.04 Block_Rump
- 1.48 Formulation*Injection volume_SEDDS 1.5
+ 1.48 Formulation*Injection volume_SEDDS 4.5
+ 0.37 Formulation*Injection volume_solution 1.5
- 0.37 Formulation*Injection volume_solution 4.5
+ 1.10 Formulation*Injection volume_Suspension 1.5
- 1.10 Formulation*Injection volume_Suspension 4.5
- 8.07 Formulation*US duration_SEDDS 0 - 3.95 Formulation*US duration_SEDDS 5
+ 12.02 Formulation*US duration_SEDDS 10 + 7.95 Formulation*US duration_solution 0
- 1.11 Formulation*US duration_solution 5 - 6.84 Formulation*US duration_solution 10
+ 0.12 Formulation*US duration_Suspension 0
+ 5.06 Formulation*US duration_Suspension 5
- 5.19 Formulation*US duration_Suspension 10 + 2.78 Injection volume*US duration_1.5
0 - 2.78 Injection volume*US duration_1.5 5 - 0.01 Injection volume*US duration_1.5
10 - 2.78 Injection volume*US duration_4.5 0 + 2.78 Injection volume*US duration_4.5
5 + 0.01 Injection volume*US duration_4.5 10
+ 4.61 Formulation*Injection volume*US duration_SEDDS 1.5 0
+ 2.09 Formulation*Injection volume*US duration_SEDDS 1.5 5
- 6.70 Formulation*Injection volume*US duration_SEDDS 1.5 10
- 4.61 Formulation*Injection volume*US duration_SEDDS 4.5 0
- 2.09 Formulation*Injection volume*US duration_SEDDS 4.5 5
+ 6.70 Formulation*Injection volume*US duration_SEDDS 4.5 10
- 0.39 Formulation*Injection volume*US duration_solution 1.5 0
+ 0.32 Formulation*Injection volume*US duration_solution 1.5 5
+ 0.07 Formulation*Injection volume*US duration_solution 1.5 10
+ 0.39 Formulation*Injection volume*US duration_solution 4.5 0
- 0.32 Formulation*Injection volume*US duration_solution 4.5 5
- 0.07 Formulation*Injection volume*US duration_solution 4.5 10
- 4.22 Formulation*Injection volume*US duration_Suspension 1.5 0
- 2.41 Formulation*Injection volume*US duration_Suspension 1.5 5
+ 6.63 Formulation*Injection volume*US duration_Suspension 1.5 10
+ 4.22 Formulation*Injection volume*US duration_Suspension 4.5 0
+ 2.41 Formulation*Injection volume*US duration_Suspension 4.5 5
- 6.63 Formulation*Injection volume*US duration_Suspension 4.5 10

Fits and Diagnostics for Unusual Observations

Obs	Spread	Fit	Resid	Std Resid
15	160.60	149.21	11.39	2.36 R
16	141.90	153.29	-11.39	-2.36 R

R Large residual

Comparisons for Spread

Tukey Pairwise Comparisons: Formulation

Grouping Information Using the Tukey Method and 95% Confidence

Formulation	N	Mean	Grouping
Suspension	12	152.575	A
SEDDS	12	140.517	B
solution	12	133.850	B

Means that do not share a letter are significantly different.

Tukey Simultaneous Tests for Differences of Means

Difference of Formulation Levels	Difference of Means	SE of Difference	Simultaneous 95% CI	T-Value	Adjusted P-Value
solution - SEDDS	-6.67	3.03	(-14.40, 1.07)	-2.20	0.098
Suspension - SEDDS	12.06	3.03	(4.32, 19.79)	3.98	0.002
Suspension - solution	18.73	3.03	(10.99, 26.46)	6.18	0.000

Individual confidence level = 98.00%

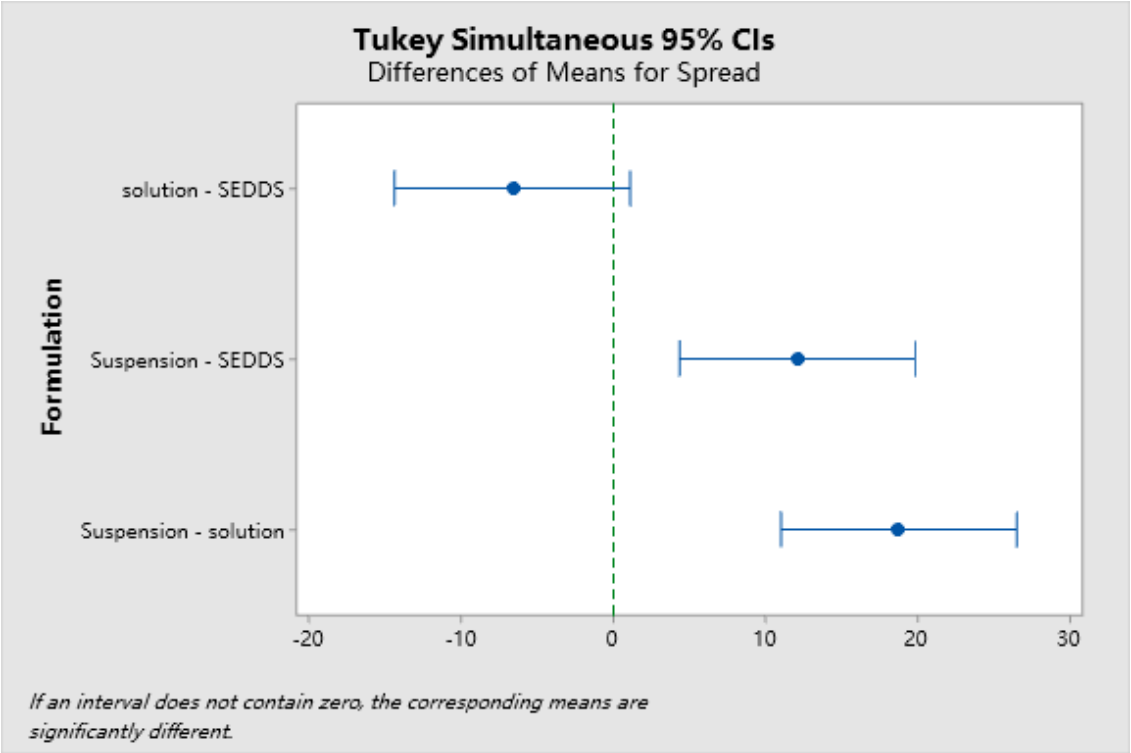

Tukey Pairwise Comparisons: Injection volume

Grouping Information Using the Tukey Method and 95% Confidence

Injection volume	N	Mean	Grouping
4.5	18	148.006	A
1.5	18	136.622	B

Means that do not share a letter are significantly different.

Tukey Simultaneous Tests for Differences of Means

Difference of Injection volume Levels	Difference of Means	SE of Difference	Simultaneous 95% CI	T-Value	Adjusted P-Value
4.5 - 1.5	11.38	2.47	(6.19, 16.58)	4.60	0.000

Individual confidence level = 95.00%

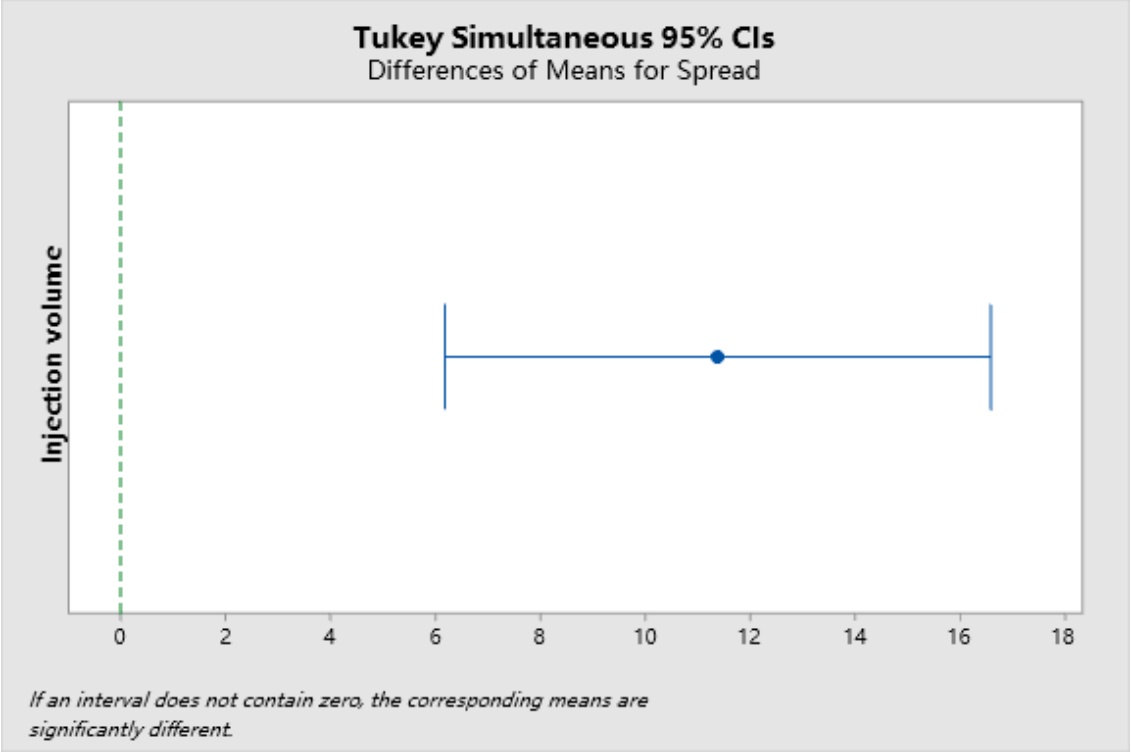

Tukey Pairwise Comparisons: US duration

Grouping Information Using the Tukey Method and 95% Confidence

US duration	N	Mean	Grouping		
10	12	159.050	A		
5	12	145.700		B	
0	12	122.192			C

Means that do not share a letter are significantly different.

Tukey Simultaneous Tests for Differences of Means

Difference of US duration Levels	Difference of Means	SE of Difference	Simultaneous 95% CI	T-Value	Adjusted P-Value
5 - 0	23.51	3.03	(15.77, 31.24)	7.76	0.000
10 - 0	36.86	3.03	(29.12, 44.59)	12.17	0.000
10 - 5	13.35	3.03	(5.62, 21.08)	4.41	0.001

Individual confidence level = 98.00%

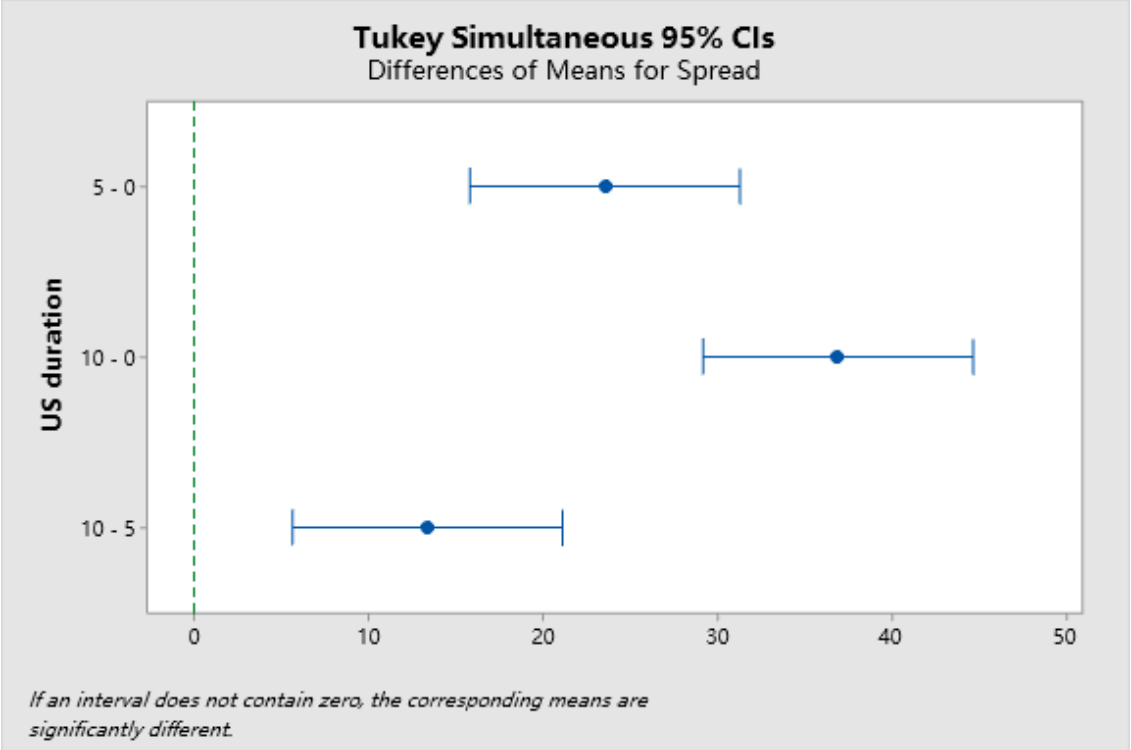

Tukey Pairwise Comparisons: Formulation*Injection volume

Grouping Information Using the Tukey Method and 95% Confidence

Formulation*Injection volume	N	Mean	Grouping		
Suspension 4.5	6	157.167	A		
Suspension 1.5	6	147.983	A	B	
SEDDS 4.5	6	147.683	A	B	
solution 4.5	6	139.167		B	C
SEDDS 1.5	6	133.350			C
solution 1.5	6	128.533			C

Means that do not share a letter are significantly different.

Tukey Simultaneous Tests for Differences of Means

Difference of Formulation*Injection volume Levels	Difference of Means	SE of Difference	Simultaneous 95% CI	T-Value
(SEDDS 4.5) - (SEDDS 1.5)	14.33	4.28	(0.73, 27.94)	3.35
(solution 1.5) - (SEDDS 1.5)	-4.82	4.28	(-18.42, 8.79)	-1.12
(solution 4.5) - (SEDDS 1.5)	5.82	4.28	(-7.79, 19.42)	1.36
(Suspension 1.5) - (SEDDS 1.5)	14.63	4.28	(1.03, 28.24)	3.42
(Suspension 4.5) - (SEDDS 1.5)	23.82	4.28	(10.21, 37.42)	5.56
(solution 1.5) - (SEDDS 4.5)	-19.15	4.28	(-32.75, -5.55)	-4.47
(solution 4.5) - (SEDDS 4.5)	-8.52	4.28	(-22.12, 5.09)	-1.99
(Suspension 1.5) - (SEDDS 4.5)	0.30	4.28	(-13.30, 13.90)	0.07
(Suspension 4.5) - (SEDDS 4.5)	9.48	4.28	(-4.12, 23.09)	2.21
(solution 4.5) - (solution 1.5)	10.63	4.28	(-2.97, 24.24)	2.48
(Suspension 1.5) - (solution 1.5)	19.45	4.28	(5.85, 33.05)	4.54
(Suspension 4.5) - (solution 1.5)	28.63	4.28	(15.03, 42.24)	6.68
(Suspension 1.5) - (solution 4.5)	8.82	4.28	(-4.79, 22.42)	2.06
(Suspension 4.5) - (solution 4.5)	18.00	4.28	(4.40, 31.60)	4.20

(Suspension 4.5) - (Suspension 1.5)	9.18	4.28	(-4.42, 22.79)	2.14

Difference of Formulation*Injection volume Levels	Adjusted P-Value
(SEDDS 4.5) - (SEDDS 1.5)	0.036
(solution 1.5) - (SEDDS 1.5)	0.865
(solution 4.5) - (SEDDS 1.5)	0.750
(Suspension 1.5) - (SEDDS 1.5)	0.031
(Suspension 4.5) - (SEDDS 1.5)	0.000
(solution 1.5) - (SEDDS 4.5)	0.003
(solution 4.5) - (SEDDS 4.5)	0.386
(Suspension 1.5) - (SEDDS 4.5)	1.000
(Suspension 4.5) - (SEDDS 4.5)	0.279
(solution 4.5) - (solution 1.5)	0.181
(Suspension 1.5) - (solution 1.5)	0.003
(Suspension 4.5) - (solution 1.5)	0.000
(Suspension 1.5) - (solution 4.5)	0.351
(Suspension 4.5) - (solution 4.5)	0.006
(Suspension 4.5) - (Suspension 1.5)	0.310

Individual confidence level = 99.48%

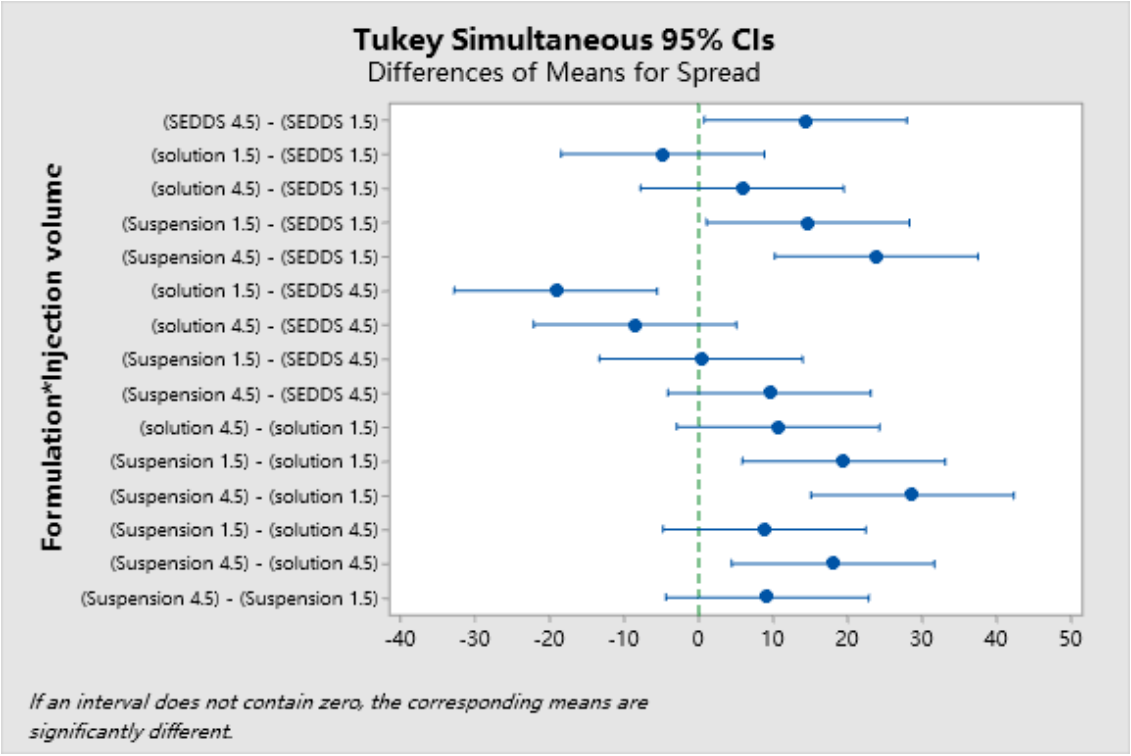

Tukey Pairwise Comparisons: Formulation*US duration

Grouping Information Using the Tukey Method and 95% Confidence

Formulation*US duration	N	Mean	Grouping		
SEDDS 10	4	169.275	A		
Suspension 10	4	164.125	A		
Suspension 5	4	161.025	A	B	
solution 10	4	143.750		B	C
SEDDS 5	4	139.950			C D
solution 5	4	136.125			C D

Suspension 0	4	132.575		C	D
solution 0	4	121.675			D	E
SEDDS 0	4	112.325				E

Means that do not share a letter are significantly different.

Tukey Simultaneous Tests for Differences of Means

Difference of Formulation*US duration Levels	Difference of Means	SE of Difference	Simultaneous 95% CI	T-Value	Adjusted P-Value
(SEDDS 5) - (SEDDS 0)	27.63	5.25	(9.22, 46.03)	5.26	0.001
(SEDDS 10) - (SEDDS 0)	56.95	5.25	(38.55, 75.35)	10.85	0.000
(solution 0) - (SEDDS 0)	9.35	5.25	(-9.05, 27.75)	1.78	0.693
(solution 5) - (SEDDS 0)	23.80	5.25	(5.40, 42.20)	4.54	0.006
(solution 10) - (SEDDS 0)	31.42	5.25	(13.02, 49.83)	5.99	0.000
(Suspension 0) - (SEDDS 0)	20.25	5.25	(1.85, 38.65)	3.86	0.025
(Suspension 5) - (SEDDS 0)	48.70	5.25	(30.30, 67.10)	9.28	0.000
(Suspension 10) - (SEDDS 0)	51.80	5.25	(33.40, 70.20)	9.87	0.000
(SEDDS 10) - (SEDDS 5)	29.32	5.25	(10.92, 47.73)	5.59	0.001
(solution 0) - (SEDDS 5)	-18.27	5.25	(-36.68, 0.13)	-3.48	0.052
(solution 5) - (SEDDS 5)	-3.83	5.25	(-22.23, 14.58)	-0.73	0.998
(solution 10) - (SEDDS 5)	3.80	5.25	(-14.60, 22.20)	0.72	0.998
(Suspension 0) - (SEDDS 5)	-7.38	5.25	(-25.78, 11.03)	-1.41	0.882
(Suspension 5) - (SEDDS 5)	21.07	5.25	(2.67, 39.48)	4.02	0.018
(Suspension 10) - (SEDDS 5)	24.17	5.25	(5.77, 42.58)	4.61	0.005
(solution 0) - (SEDDS 10)	-47.60	5.25	(-66.00, -29.20)	-9.07	0.000
(solution 5) - (SEDDS 10)	-33.15	5.25	(-51.55, -14.75)	-6.32	0.000
(solution 10) - (SEDDS 10)	-25.53	5.25	(-43.93, -7.12)	-4.86	0.003
(Suspension 0) - (SEDDS 10)	-36.70	5.25	(-55.10, -18.30)	-6.99	0.000
(Suspension 5) - (SEDDS 10)	-8.25	5.25	(-26.65, 10.15)	-1.57	0.807
(Suspension 10) - (SEDDS 10)	-5.15	5.25	(-23.55, 13.25)	-0.98	0.983
(solution 5) - (solution 0)	14.45	5.25	(-3.95, 32.85)	2.75	0.197
(solution 10) - (solution 0)	22.07	5.25	(3.67, 40.48)	4.21	0.012
(Suspension 0) - (solution 0)	10.90	5.25	(-7.50, 29.30)	2.08	0.516
(Suspension 5) - (solution 0)	39.35	5.25	(20.95, 57.75)	7.50	0.000
(Suspension 10) - (solution 0)	42.45	5.25	(24.05, 60.85)	8.09	0.000
(solution 10) - (solution 5)	7.62	5.25	(-10.78, 26.03)	1.45	0.862
(Suspension 0) - (solution 5)	-3.55	5.25	(-21.95, 14.85)	-0.68	0.999
(Suspension 5) - (solution 5)	24.90	5.25	(6.50, 43.30)	4.75	0.004
(Suspension 10) - (solution 5)	28.00	5.25	(9.60, 46.40)	5.34	0.001
(Suspension 0) - (solution 10)	-11.17	5.25	(-29.58, 7.23)	-2.13	0.485
(Suspension 5) - (solution 10)	17.28	5.25	(-1.13, 35.68)	3.29	0.075
(Suspension 10) - (solution 10)	20.38	5.25	(1.97, 38.78)	3.88	0.024
(Suspension 5) - (Suspension 0)	28.45	5.25	(10.05, 46.85)	5.42	0.001
(Suspension 10) - (Suspension 0)	31.55	5.25	(13.15, 49.95)	6.01	0.000
(Suspension 10) - (Suspension 5)	3.10	5.25	(-15.30, 21.50)	0.59	0.999

Individual confidence level = 99.75%

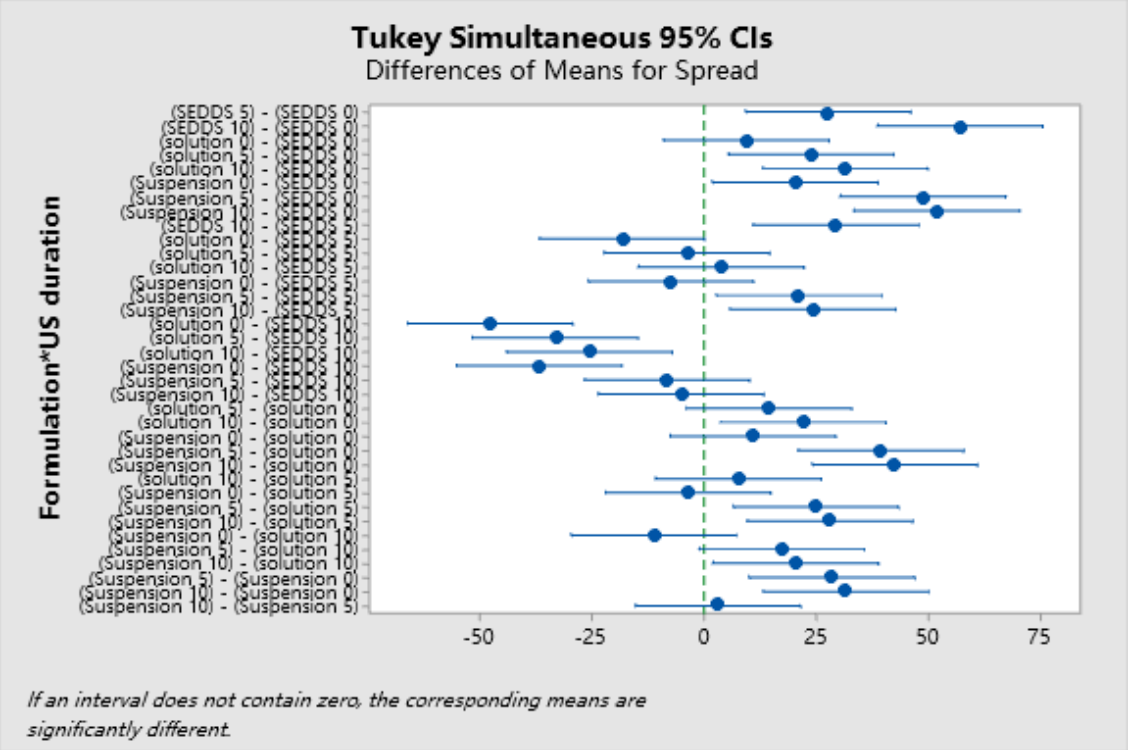

Tukey Pairwise Comparisons: Injection volume*US duration

Grouping Information Using the Tukey Method and 95% Confidence

Injection volume*US duration	N	Mean	Grouping		
4.5 10	6	164.750	A		
4.5 5	6	154.167	A		
1.5 10	6	153.350	A		
1.5 5	6	137.233		B	
4.5 0	6	125.100		B	C
1.5 0	6	119.283			C

Means that do not share a letter are significantly different.

Tukey Simultaneous Tests for Differences of Means

Difference of Injection volume*US duration Levels	Difference of Means	SE of Difference	Simultaneous 95% CI	T-Value	Adjusted P-Value
(1.5 5) - (1.5 0)	17.95	4.28	(4.35, 31.55)	4.19	0.006
(1.5 10) - (1.5 0)	34.07	4.28	(20.46, 47.67)	7.95	0.000
(4.5 0) - (1.5 0)	5.82	4.28	(-7.79, 19.42)	1.36	0.750
(4.5 5) - (1.5 0)	34.88	4.28	(21.28, 48.49)	8.14	0.000
(4.5 10) - (1.5 0)	45.47	4.28	(31.86, 59.07)	10.61	0.000
(1.5 10) - (1.5 5)	16.12	4.28	(2.51, 29.72)	3.76	0.015
(4.5 0) - (1.5 5)	-12.13	4.28	(-25.74, 1.47)	-2.83	0.097
(4.5 5) - (1.5 5)	16.93	4.28	(3.33, 30.54)	3.95	0.010
(4.5 10) - (1.5 5)	27.52	4.28	(13.91, 41.12)	6.42	0.000
(4.5 0) - (1.5 10)	-28.25	4.28	(-41.85, -14.65)	-6.59	0.000
(4.5 5) - (1.5 10)	0.82	4.28	(-12.79, 14.42)	0.19	1.000
(4.5 10) - (1.5 10)	11.40	4.28	(-2.20, 25.00)	2.66	0.133
(4.5 5) - (4.5 0)	29.07	4.28	(15.46, 42.67)	6.78	0.000

(4.5 10) - (4.5 0)	39.65	4.28	(26.05, 53.25)	9.25	0.000
(4.5 10) - (4.5 5)	10.58	4.28	(-3.02, 24.19)	2.47	0.185

Individual confidence level = 99.48%

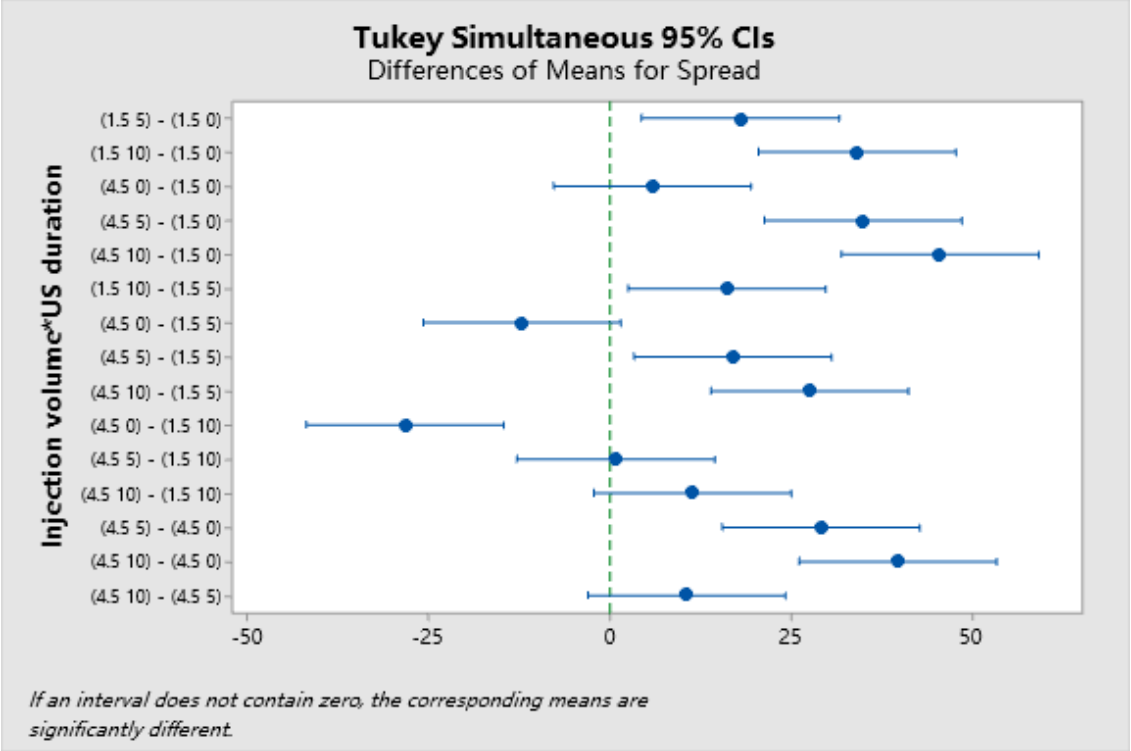

Tukey Pairwise Comparisons: Formulation*Injection volume*US duration

Grouping Information Using the Tukey Method and 95% Confidence

Formulation*Injection volume*US duration	N	Mean	Grouping					
SEDDS 4.5 10	2	183.15	A					
Suspension 4.5 5	2	170.80	A	B				
Suspension 1.5 10	2	166.15	A	B	C			
Suspension 4.5 10	2	162.10	A	B	C			
SEDDS 1.5 10	2	155.40	A	B	C	D		
Suspension 1.5 5	2	151.25		B	C	D	E	
solution 4.5 10	2	149.00		B	C	D	E	
SEDDS 4.5 5	2	147.80		B	C	D	E	F
solution 4.5 5	2	143.90		B	C	D	E	F
Suspension 4.5 0	2	138.60			C	D	E	F	G
solution 1.5 10	2	138.50			C	D	E	F	G
SEDDS 1.5 5	2	132.10				D	E	F	G
solution 1.5 5	2	128.35				D	E	F	G
Suspension 1.5 0	2	126.55				D	E	F	G
solution 4.5 0	2	124.60					E	F	G
solution 1.5 0	2	118.75						F	G
SEDDS 1.5 0	2	112.55							G
SEDDS 4.5 0	2	112.10							G

Means that do not share a letter are significantly different.

Tukey Simultaneous Tests for Differences of Means

Difference of Formulation*Injection volume*US duration Levels	Difference of Means	SE of Difference	Simultaneous 95% CI	T-Value
(SEDDS 1.5 5) - (SEDDS 1.5 0)	19.55	7.42	(-10.31, 49.41)	2.63
(SEDDS 1.5 10) - (SEDDS 1.5 0)	42.85	7.42	(12.99, 72.71)	5.77
(SEDDS 4.5 0) - (SEDDS 1.5 0)	-0.45	7.42	(-30.31, 29.41)	-0.06
(SEDDS 4.5 5) - (SEDDS 1.5 0)	35.25	7.42	(5.39, 65.11)	4.75
(SEDDS 4.5 10) - (SEDDS 1.5 0)	70.60	7.42	(40.74, 100.46)	9.51
(solution 1.5 0) - (SEDDS 1.5 0)	6.20	7.42	(-23.66, 36.06)	0.84
(solution 1.5 5) - (SEDDS 1.5 0)	15.80	7.42	(-14.06, 45.66)	2.13
(solution 1.5 10) - (SEDDS 1.5 0)	25.95	7.42	(-3.91, 55.81)	3.50
(solution 4.5 0) - (SEDDS 1.5 0)	12.05	7.42	(-17.81, 41.91)	1.62
(solution 4.5 5) - (SEDDS 1.5 0)	31.35	7.42	(1.49, 61.21)	4.22
(solution 4.5 10) - (SEDDS 1.5 0)	36.45	7.42	(6.59, 66.31)	4.91
(Suspension 1.5 0) - (SEDDS 1.5 0)	14.00	7.42	(-15.86, 43.86)	1.89
(Suspension 1.5 5) - (SEDDS 1.5 0)	38.70	7.42	(8.84, 68.56)	5.21
(Suspension 1.5 10) - (SEDDS 1.5 0)	53.60	7.42	(23.74, 83.46)	7.22
(Suspension 4.5 0) - (SEDDS 1.5 0)	26.05	7.42	(-3.81, 55.91)	3.51
(Suspension 4.5 5) - (SEDDS 1.5 0)	58.25	7.42	(28.39, 88.11)	7.85
(Suspension 4.5 10) - (SEDDS 1.5 0)	49.55	7.42	(19.69, 79.41)	6.68
(SEDDS 1.5 10) - (SEDDS 1.5 5)	23.30	7.42	(-6.56, 53.16)	3.14
(SEDDS 4.5 0) - (SEDDS 1.5 5)	-20.00	7.42	(-49.86, 9.86)	-2.70
(SEDDS 4.5 5) - (SEDDS 1.5 5)	15.70	7.42	(-14.16, 45.56)	2.12
(SEDDS 4.5 10) - (SEDDS 1.5 5)	51.05	7.42	(21.19, 80.91)	6.88
(solution 1.5 0) - (SEDDS 1.5 5)	-13.35	7.42	(-43.21, 16.51)	-1.80
(solution 1.5 5) - (SEDDS 1.5 5)	-3.75	7.42	(-33.61, 26.11)	-0.51
(solution 1.5 10) - (SEDDS 1.5 5)	6.40	7.42	(-23.46, 36.26)	0.86
(solution 4.5 0) - (SEDDS 1.5 5)	-7.50	7.42	(-37.36, 22.36)	-1.01
(solution 4.5 5) - (SEDDS 1.5 5)	11.80	7.42	(-18.06, 41.66)	1.59
(solution 4.5 10) - (SEDDS 1.5 5)	16.90	7.42	(-12.96, 46.76)	2.28
(Suspension 1.5 0) - (SEDDS 1.5 5)	-5.55	7.42	(-35.41, 24.31)	-0.75
(Suspension 1.5 5) - (SEDDS 1.5 5)	19.15	7.42	(-10.71, 49.01)	2.58
(Suspension 1.5 10) - (SEDDS 1.5 5)	34.05	7.42	(4.19, 63.91)	4.59
(Suspension 4.5 0) - (SEDDS 1.5 5)	6.50	7.42	(-23.36, 36.36)	0.88
(Suspension 4.5 5) - (SEDDS 1.5 5)	38.70	7.42	(8.84, 68.56)	5.21
(Suspension 4.5 10) - (SEDDS 1.5 5)	30.00	7.42	(0.14, 59.86)	4.04
(SEDDS 4.5 0) - (SEDDS 1.5 10)	-43.30	7.42	(-73.16, -13.44)	-5.83
(SEDDS 4.5 5) - (SEDDS 1.5 10)	-7.60	7.42	(-37.46, 22.26)	-1.02
(SEDDS 4.5 10) - (SEDDS 1.5 10)	27.75	7.42	(-2.11, 57.61)	3.74
(solution 1.5 0) - (SEDDS 1.5 10)	-36.65	7.42	(-66.51, -6.79)	-4.94
(solution 1.5 5) - (SEDDS 1.5 10)	-27.05	7.42	(-56.91, 2.81)	-3.65
(solution 1.5 10) - (SEDDS 1.5 10)	-16.90	7.42	(-46.76, 12.96)	-2.28
(solution 4.5 0) - (SEDDS 1.5 10)	-30.80	7.42	(-60.66, -0.94)	-4.15
(solution 4.5 5) - (SEDDS 1.5 10)	-11.50	7.42	(-41.36, 18.36)	-1.55
(solution 4.5 10) - (SEDDS 1.5 10)	-6.40	7.42	(-36.26, 23.46)	-0.86
(Suspension 1.5 0) - (SEDDS 1.5 10)	-28.85	7.42	(-58.71, 1.01)	-3.89
(Suspension 1.5 5) - (SEDDS 1.5 10)	-4.15	7.42	(-34.01, 25.71)	-0.56
(Suspension 1.5 10) - (SEDDS 1.5 10)	10.75	7.42	(-19.11, 40.61)	1.45
(Suspension 4.5 0) - (SEDDS 1.5 10)	-16.80	7.42	(-46.66, 13.06)	-2.26
(Suspension 4.5 5) - (SEDDS 1.5 10)	15.40	7.42	(-14.46, 45.26)	2.08
(Suspension 4.5 10) - (SEDDS 1.5 10)	6.70	7.42	(-23.16, 36.56)	0.90
(SEDDS 4.5 5) - (SEDDS 4.5 0)	35.70	7.42	(5.84, 65.56)	4.81
(SEDDS 4.5 10) - (SEDDS 4.5 0)	71.05	7.42	(41.19, 100.91)	9.57
(solution 1.5 0) - (SEDDS 4.5 0)	6.65	7.42	(-23.21, 36.51)	0.90

(solution 1.5 5) - (SEDDS 4.5 0)	16.25	7.42	(-13.61, 46.11)	2.19
(solution 1.5 10) - (SEDDS 4.5 0)	26.40	7.42	(-3.46, 56.26)	3.56
(solution 4.5 0) - (SEDDS 4.5 0)	12.50	7.42	(-17.36, 42.36)	1.68
(solution 4.5 5) - (SEDDS 4.5 0)	31.80	7.42	(1.94, 61.66)	4.29
(solution 4.5 10) - (SEDDS 4.5 0)	36.90	7.42	(7.04, 66.76)	4.97
(Suspension 1.5 0) - (SEDDS 4.5 0)	14.45	7.42	(-15.41, 44.31)	1.95
(Suspension 1.5 5) - (SEDDS 4.5 0)	39.15	7.42	(9.29, 69.01)	5.28
(Suspension 1.5 10) - (SEDDS 4.5 0)	54.05	7.42	(24.19, 83.91)	7.28
(Suspension 4.5 0) - (SEDDS 4.5 0)	26.50	7.42	(-3.36, 56.36)	3.57
(Suspension 4.5 5) - (SEDDS 4.5 0)	58.70	7.42	(28.84, 88.56)	7.91
(Suspension 4.5 10) - (SEDDS 4.5 0)	50.00	7.42	(20.14, 79.86)	6.74
(SEDDS 4.5 10) - (SEDDS 4.5 5)	35.35	7.42	(5.49, 65.21)	4.76
(solution 1.5 0) - (SEDDS 4.5 5)	-29.05	7.42	(-58.91, 0.81)	-3.91
(solution 1.5 5) - (SEDDS 4.5 5)	-19.45	7.42	(-49.31, 10.41)	-2.62
(solution 1.5 10) - (SEDDS 4.5 5)	-9.30	7.42	(-39.16, 20.56)	-1.25
(solution 4.5 0) - (SEDDS 4.5 5)	-23.20	7.42	(-53.06, 6.66)	-3.13
(solution 4.5 5) - (SEDDS 4.5 5)	-3.90	7.42	(-33.76, 25.96)	-0.53
(solution 4.5 10) - (SEDDS 4.5 5)	1.20	7.42	(-28.66, 31.06)	0.16
(Suspension 1.5 0) - (SEDDS 4.5 5)	-21.25	7.42	(-51.11, 8.61)	-2.86
(Suspension 1.5 5) - (SEDDS 4.5 5)	3.45	7.42	(-26.41, 33.31)	0.46
(Suspension 1.5 10) - (SEDDS 4.5 5)	18.35	7.42	(-11.51, 48.21)	2.47
(Suspension 4.5 0) - (SEDDS 4.5 5)	-9.20	7.42	(-39.06, 20.66)	-1.24
(Suspension 4.5 5) - (SEDDS 4.5 5)	23.00	7.42	(-6.86, 52.86)	3.10
(Suspension 4.5 10) - (SEDDS 4.5 5)	14.30	7.42	(-15.56, 44.16)	1.93
(solution 1.5 0) - (SEDDS 4.5 10)	-64.40	7.42	(-94.26, -34.54)	-8.68
(solution 1.5 5) - (SEDDS 4.5 10)	-54.80	7.42	(-84.66, -24.94)	-7.38
(solution 1.5 10) - (SEDDS 4.5 10)	-44.65	7.42	(-74.51, -14.79)	-6.02
(solution 4.5 0) - (SEDDS 4.5 10)	-58.55	7.42	(-88.41, -28.69)	-7.89
(solution 4.5 5) - (SEDDS 4.5 10)	-39.25	7.42	(-69.11, -9.39)	-5.29
(solution 4.5 10) - (SEDDS 4.5 10)	-34.15	7.42	(-64.01, -4.29)	-4.60
(Suspension 1.5 0) - (SEDDS 4.5 10)	-56.60	7.42	(-86.46, -26.74)	-7.63
(Suspension 1.5 5) - (SEDDS 4.5 10)	-31.90	7.42	(-61.76, -2.04)	-4.30
(Suspension 1.5 10) - (SEDDS 4.5 10)	-17.00	7.42	(-46.86, 12.86)	-2.29
(Suspension 4.5 0) - (SEDDS 4.5 10)	-44.55	7.42	(-74.41, -14.69)	-6.00
(Suspension 4.5 5) - (SEDDS 4.5 10)	-12.35	7.42	(-42.21, 17.51)	-1.66
(Suspension 4.5 10) - (SEDDS 4.5 10)	-21.05	7.42	(-50.91, 8.81)	-2.84
(solution 1.5 5) - (solution 1.5 0)	9.60	7.42	(-20.26, 39.46)	1.29
(solution 1.5 10) - (solution 1.5 0)	19.75	7.42	(-10.11, 49.61)	2.66
(solution 4.5 0) - (solution 1.5 0)	5.85	7.42	(-24.01, 35.71)	0.79
(solution 4.5 5) - (solution 1.5 0)	25.15	7.42	(-4.71, 55.01)	3.39
(solution 4.5 10) - (solution 1.5 0)	30.25	7.42	(0.39, 60.11)	4.08
(Suspension 1.5 0) - (solution 1.5 0)	7.80	7.42	(-22.06, 37.66)	1.05
(Suspension 1.5 5) - (solution 1.5 0)	32.50	7.42	(2.64, 62.36)	4.38
(Suspension 1.5 10) - (solution 1.5 0)	47.40	7.42	(17.54, 77.26)	6.39
(Suspension 4.5 0) - (solution 1.5 0)	19.85	7.42	(-10.01, 49.71)	2.67
(Suspension 4.5 5) - (solution 1.5 0)	52.05	7.42	(22.19, 81.91)	7.01
(Suspension 4.5 10) - (solution 1.5 0)	43.35	7.42	(13.49, 73.21)	5.84
(solution 1.5 10) - (solution 1.5 5)	10.15	7.42	(-19.71, 40.01)	1.37
(solution 4.5 0) - (solution 1.5 5)	-3.75	7.42	(-33.61, 26.11)	-0.51
(solution 4.5 5) - (solution 1.5 5)	15.55	7.42	(-14.31, 45.41)	2.10
(solution 4.5 10) - (solution 1.5 5)	20.65	7.42	(-9.21, 50.51)	2.78
(Suspension 1.5 0) - (solution 1.5 5)	-1.80	7.42	(-31.66, 28.06)	-0.24
(Suspension 1.5 5) - (solution 1.5 5)	22.90	7.42	(-6.96, 52.76)	3.09
(Suspension 1.5 10) - (solution 1.5 5)	37.80	7.42	(7.94, 67.66)	5.09

(Suspension 4.5 0) - (solution 1.5 5)	10.25	7.42	(-19.61, 40.11)	1.38
(Suspension 4.5 5) - (solution 1.5 5)	42.45	7.42	(12.59, 72.31)	5.72
(Suspension 4.5 10) - (solution 1.5 5)	33.75	7.42	(3.89, 63.61)	4.55
(solution 4.5 0) - (solution 1.5 10)	-13.90	7.42	(-43.76, 15.96)	-1.87
(solution 4.5 5) - (solution 1.5 10)	5.40	7.42	(-24.46, 35.26)	0.73
(solution 4.5 10) - (solution 1.5 10)	10.50	7.42	(-19.36, 40.36)	1.41
(Suspension 1.5 0) - (solution 1.5 10)	-11.95	7.42	(-41.81, 17.91)	-1.61
(Suspension 1.5 5) - (solution 1.5 10)	12.75	7.42	(-17.11, 42.61)	1.72
(Suspension 1.5 10) - (solution 1.5 10)	27.65	7.42	(-2.21, 57.51)	3.73
(Suspension 4.5 0) - (solution 1.5 10)	0.10	7.42	(-29.76, 29.96)	0.01
(Suspension 4.5 5) - (solution 1.5 10)	32.30	7.42	(2.44, 62.16)	4.35
(Suspension 4.5 10) - (solution 1.5 10)	23.60	7.42	(-6.26, 53.46)	3.18
(solution 4.5 5) - (solution 4.5 0)	19.30	7.42	(-10.56, 49.16)	2.60
(solution 4.5 10) - (solution 4.5 0)	24.40	7.42	(-5.46, 54.26)	3.29
(Suspension 1.5 0) - (solution 4.5 0)	1.95	7.42	(-27.91, 31.81)	0.26
(Suspension 1.5 5) - (solution 4.5 0)	26.65	7.42	(-3.21, 56.51)	3.59
(Suspension 1.5 10) - (solution 4.5 0)	41.55	7.42	(11.69, 71.41)	5.60
(Suspension 4.5 0) - (solution 4.5 0)	14.00	7.42	(-15.86, 43.86)	1.89
(Suspension 4.5 5) - (solution 4.5 0)	46.20	7.42	(16.34, 76.06)	6.23
(Suspension 4.5 10) - (solution 4.5 0)	37.50	7.42	(7.64, 67.36)	5.05
(solution 4.5 10) - (solution 4.5 5)	5.10	7.42	(-24.76, 34.96)	0.69
(Suspension 1.5 0) - (solution 4.5 5)	-17.35	7.42	(-47.21, 12.51)	-2.34
(Suspension 1.5 5) - (solution 4.5 5)	7.35	7.42	(-22.51, 37.21)	0.99
(Suspension 1.5 10) - (solution 4.5 5)	22.25	7.42	(-7.61, 52.11)	3.00
(Suspension 4.5 0) - (solution 4.5 5)	-5.30	7.42	(-35.16, 24.56)	-0.71
(Suspension 4.5 5) - (solution 4.5 5)	26.90	7.42	(-2.96, 56.76)	3.62
(Suspension 4.5 10) - (solution 4.5 5)	18.20	7.42	(-11.66, 48.06)	2.45
(Suspension 1.5 0) - (solution 4.5 10)	-22.45	7.42	(-52.31, 7.41)	-3.03
(Suspension 1.5 5) - (solution 4.5 10)	2.25	7.42	(-27.61, 32.11)	0.30
(Suspension 1.5 10) - (solution 4.5 10)	17.15	7.42	(-12.71, 47.01)	2.31
(Suspension 4.5 0) - (solution 4.5 10)	-10.40	7.42	(-40.26, 19.46)	-1.40
(Suspension 4.5 5) - (solution 4.5 10)	21.80	7.42	(-8.06, 51.66)	2.94
(Suspension 4.5 10) - (solution 4.5 10)	13.10	7.42	(-16.76, 42.96)	1.77
(Suspension 1.5 5) - (Suspension 1.5 0)	24.70	7.42	(-5.16, 54.56)	3.33
(Suspension 1.5 10) - (Suspension 1.5 0)	39.60	7.42	(9.74, 69.46)	5.34
(Suspension 4.5 0) - (Suspension 1.5 0)	12.05	7.42	(-17.81, 41.91)	1.62
(Suspension 4.5 5) - (Suspension 1.5 0)	44.25	7.42	(14.39, 74.11)	5.96
(Suspension 4.5 10) - (Suspension 1.5 0)	35.55	7.42	(5.69, 65.41)	4.79
(Suspension 1.5 10) - (Suspension 1.5 5)	14.90	7.42	(-14.96, 44.76)	2.01
(Suspension 4.5 0) - (Suspension 1.5 5)	-12.65	7.42	(-42.51, 17.21)	-1.70
(Suspension 4.5 5) - (Suspension 1.5 5)	19.55	7.42	(-10.31, 49.41)	2.63
(Suspension 4.5 10) - (Suspension 1.5 5)	10.85	7.42	(-19.01, 40.71)	1.46
(Suspension 4.5 0) - (Suspension 1.5 10)	-27.55	7.42	(-57.41, 2.31)	-3.71
(Suspension 4.5 5) - (Suspension 1.5 10)	4.65	7.42	(-25.21, 34.51)	0.63
(Suspension 4.5 10) - (Suspension 1.5 10)	-4.05	7.42	(-33.91, 25.81)	-0.55
(Suspension 4.5 5) - (Suspension 4.5 0)	32.20	7.42	(2.34, 62.06)	4.34
(Suspension 4.5 10) - (Suspension 4.5 0)	23.50	7.42	(-6.36, 53.36)	3.17
(Suspension 4.5 10) - (Suspension 4.5 5)	-8.70	7.42	(-38.56, 21.16)	-1.17

Difference of Formulation*Injection volume*US duration Levels	**Adjusted P-Value**
(SEDDS 1.5 5) - (SEDDS 1.5 0)	0.477
(SEDDS 1.5 10) - (SEDDS 1.5 0)	0.002
(SEDDS 4.5 0) - (SEDDS 1.5 0)	1.000
(SEDDS 4.5 5) - (SEDDS 1.5 0)	0.012

(SEDDS 4.5 10) - (SEDDS 1.5 0)	0.000
(solution 1.5 0) - (SEDDS 1.5 0)	1.000
(solution 1.5 5) - (SEDDS 1.5 0)	0.772
(solution 1.5 10) - (SEDDS 1.5 0)	0.130
(solution 4.5 0) - (SEDDS 1.5 0)	0.960
(solution 4.5 5) - (SEDDS 1.5 0)	0.034
(solution 4.5 10) - (SEDDS 1.5 0)	0.009
(Suspension 1.5 0) - (SEDDS 1.5 0)	0.884
(Suspension 1.5 5) - (SEDDS 1.5 0)	0.005
(Suspension 1.5 10) - (SEDDS 1.5 0)	0.000
(Suspension 4.5 0) - (SEDDS 1.5 0)	0.127
(Suspension 4.5 5) - (SEDDS 1.5 0)	0.000
(Suspension 4.5 10) - (SEDDS 1.5 0)	0.000
(SEDDS 1.5 10) - (SEDDS 1.5 5)	0.236
(SEDDS 4.5 0) - (SEDDS 1.5 5)	0.443
(SEDDS 4.5 5) - (SEDDS 1.5 5)	0.779
(SEDDS 4.5 10) - (SEDDS 1.5 5)	0.000
(solution 1.5 0) - (SEDDS 1.5 5)	0.915
(solution 1.5 5) - (SEDDS 1.5 5)	1.000
(solution 1.5 10) - (SEDDS 1.5 5)	1.000
(solution 4.5 0) - (SEDDS 1.5 5)	1.000
(solution 4.5 5) - (SEDDS 1.5 5)	0.966
(solution 4.5 10) - (SEDDS 1.5 5)	0.688
(Suspension 1.5 0) - (SEDDS 1.5 5)	1.000
(Suspension 1.5 5) - (SEDDS 1.5 5)	0.508
(Suspension 1.5 10) - (SEDDS 1.5 5)	0.017
(Suspension 4.5 0) - (SEDDS 1.5 5)	1.000
(Suspension 4.5 5) - (SEDDS 1.5 5)	0.005
(Suspension 4.5 10) - (SEDDS 1.5 5)	0.048
(SEDDS 4.5 0) - (SEDDS 1.5 10)	0.001
(SEDDS 4.5 5) - (SEDDS 1.5 10)	1.000
(SEDDS 4.5 10) - (SEDDS 1.5 10)	0.085
(solution 1.5 0) - (SEDDS 1.5 10)	0.008
(solution 1.5 5) - (SEDDS 1.5 10)	0.100
(solution 1.5 10) - (SEDDS 1.5 10)	0.688
(solution 4.5 0) - (SEDDS 1.5 10)	0.039
(solution 4.5 5) - (SEDDS 1.5 10)	0.973
(solution 4.5 10) - (SEDDS 1.5 10)	1.000
(Suspension 1.5 0) - (SEDDS 1.5 10)	0.064
(Suspension 1.5 5) - (SEDDS 1.5 10)	1.000
(Suspension 1.5 10) - (SEDDS 1.5 10)	0.985
(Suspension 4.5 0) - (SEDDS 1.5 10)	0.696
(Suspension 4.5 5) - (SEDDS 1.5 10)	0.800
(Suspension 4.5 10) - (SEDDS 1.5 10)	1.000
(SEDDS 4.5 5) - (SEDDS 4.5 0)	0.011
(SEDDS 4.5 10) - (SEDDS 4.5 0)	0.000
(solution 1.5 0) - (SEDDS 4.5 0)	1.000
(solution 1.5 5) - (SEDDS 4.5 0)	0.739
(solution 1.5 10) - (SEDDS 4.5 0)	0.117
(solution 4.5 0) - (SEDDS 4.5 0)	0.947
(solution 4.5 5) - (SEDDS 4.5 0)	0.030
(solution 4.5 10) - (SEDDS 4.5 0)	0.008
(Suspension 1.5 0) - (SEDDS 4.5 0)	0.860
(Suspension 1.5 5) - (SEDDS 4.5 0)	0.004

(Suspension 1.5 10) - (SEDDS 4.5 0)	0.000
(Suspension 4.5 0) - (SEDDS 4.5 0)	0.115
(Suspension 4.5 5) - (SEDDS 4.5 0)	0.000
(Suspension 4.5 10) - (SEDDS 4.5 0)	0.000
(SEDDS 4.5 10) - (SEDDS 4.5 5)	0.012
(solution 1.5 0) - (SEDDS 4.5 5)	0.061
(solution 1.5 5) - (SEDDS 4.5 5)	0.485
(solution 1.5 10) - (SEDDS 4.5 5)	0.996
(solution 4.5 0) - (SEDDS 4.5 5)	0.241
(solution 4.5 5) - (SEDDS 4.5 5)	1.000
(solution 4.5 10) - (SEDDS 4.5 5)	1.000
(Suspension 1.5 0) - (SEDDS 4.5 5)	0.355
(Suspension 1.5 5) - (SEDDS 4.5 5)	1.000
(Suspension 1.5 10) - (SEDDS 4.5 5)	0.572
(Suspension 4.5 0) - (SEDDS 4.5 5)	0.997
(Suspension 4.5 5) - (SEDDS 4.5 5)	0.251
(Suspension 4.5 10) - (SEDDS 4.5 5)	0.868
(solution 1.5 0) - (SEDDS 4.5 10)	0.000
(solution 1.5 5) - (SEDDS 4.5 10)	0.000
(solution 1.5 10) - (SEDDS 4.5 10)	0.001
(solution 4.5 0) - (SEDDS 4.5 10)	0.000
(solution 4.5 5) - (SEDDS 4.5 10)	0.004
(solution 4.5 10) - (SEDDS 4.5 10)	0.016
(Suspension 1.5 0) - (SEDDS 4.5 10)	0.000
(Suspension 1.5 5) - (SEDDS 4.5 10)	0.029
(Suspension 1.5 10) - (SEDDS 4.5 10)	0.681
(Suspension 4.5 0) - (SEDDS 4.5 10)	0.001
(Suspension 4.5 5) - (SEDDS 4.5 10)	0.951
(Suspension 4.5 10) - (SEDDS 4.5 10)	0.368
(solution 1.5 5) - (solution 1.5 0)	0.995
(solution 1.5 10) - (solution 1.5 0)	0.462
(solution 4.5 0) - (solution 1.5 0)	1.000
(solution 4.5 5) - (solution 1.5 0)	0.157
(solution 4.5 10) - (solution 1.5 0)	0.045
(Suspension 1.5 0) - (solution 1.5 0)	0.999
(Suspension 1.5 5) - (solution 1.5 0)	0.025
(Suspension 1.5 10) - (solution 1.5 0)	0.001
(Suspension 4.5 0) - (solution 1.5 0)	0.454
(Suspension 4.5 5) - (solution 1.5 0)	0.000
(Suspension 4.5 10) - (solution 1.5 0)	0.001
(solution 1.5 10) - (solution 1.5 5)	0.991
(solution 4.5 0) - (solution 1.5 5)	1.000
(solution 4.5 5) - (solution 1.5 5)	0.789
(solution 4.5 10) - (solution 1.5 5)	0.396
(Suspension 1.5 0) - (solution 1.5 5)	1.000
(Suspension 1.5 5) - (solution 1.5 5)	0.256
(Suspension 1.5 10) - (solution 1.5 5)	0.006
(Suspension 4.5 0) - (solution 1.5 5)	0.990
(Suspension 4.5 5) - (solution 1.5 5)	0.002
(Suspension 4.5 10) - (solution 1.5 5)	0.018
(solution 4.5 0) - (solution 1.5 10)	0.889
(solution 4.5 5) - (solution 1.5 10)	1.000
(solution 4.5 10) - (solution 1.5 10)	0.988
(Suspension 1.5 0) - (solution 1.5 10)	0.962

(Suspension 1.5 5) - (solution 1.5 10)	0.938
(Suspension 1.5 10) - (solution 1.5 10)	0.087
(Suspension 4.5 0) - (solution 1.5 10)	1.000
(Suspension 4.5 5) - (solution 1.5 10)	0.027
(Suspension 4.5 10) - (solution 1.5 10)	0.221
(solution 4.5 5) - (solution 4.5 0)	0.496
(solution 4.5 10) - (solution 4.5 0)	0.186
(Suspension 1.5 0) - (solution 4.5 0)	1.000
(Suspension 1.5 5) - (solution 4.5 0)	0.111
(Suspension 1.5 10) - (solution 4.5 0)	0.002
(Suspension 4.5 0) - (solution 4.5 0)	0.884
(Suspension 4.5 5) - (solution 4.5 0)	0.001
(Suspension 4.5 10) - (solution 4.5 0)	0.007
(solution 4.5 10) - (solution 4.5 5)	1.000
(Suspension 1.5 0) - (solution 4.5 5)	0.653
(Suspension 1.5 5) - (solution 4.5 5)	1.000
(Suspension 1.5 10) - (solution 4.5 5)	0.292
(Suspension 4.5 0) - (solution 4.5 5)	1.000
(Suspension 4.5 5) - (solution 4.5 5)	0.104
(Suspension 4.5 10) - (solution 4.5 5)	0.584
(Suspension 1.5 0) - (solution 4.5 10)	0.281
(Suspension 1.5 5) - (solution 4.5 10)	1.000
(Suspension 1.5 10) - (solution 4.5 10)	0.669
(Suspension 4.5 0) - (solution 4.5 10)	0.989
(Suspension 4.5 5) - (solution 4.5 10)	0.319
(Suspension 4.5 10) - (solution 4.5 10)	0.925
(Suspension 1.5 5) - (Suspension 1.5 0)	0.174
(Suspension 1.5 10) - (Suspension 1.5 0)	0.004
(Suspension 4.5 0) - (Suspension 1.5 0)	0.960
(Suspension 4.5 5) - (Suspension 1.5 0)	0.001
(Suspension 4.5 10) - (Suspension 1.5 0)	0.011
(Suspension 1.5 10) - (Suspension 1.5 5)	0.832
(Suspension 4.5 0) - (Suspension 1.5 5)	0.942
(Suspension 4.5 5) - (Suspension 1.5 5)	0.477
(Suspension 4.5 10) - (Suspension 1.5 5)	0.983
(Suspension 4.5 0) - (Suspension 1.5 10)	0.089
(Suspension 4.5 5) - (Suspension 1.5 10)	1.000
(Suspension 4.5 10) - (Suspension 1.5 10)	1.000
(Suspension 4.5 5) - (Suspension 4.5 0)	0.027
(Suspension 4.5 10) - (Suspension 4.5 0)	0.226
(Suspension 4.5 10) - (Suspension 4.5 5)	0.998

Individual confidence level = 99.92%

* NOTE * Cannot draw the interval plot for the Tukey procedure. Interval plots for comparisons are illegible with more than 45 intervals.

Main Effects Plot for Spread

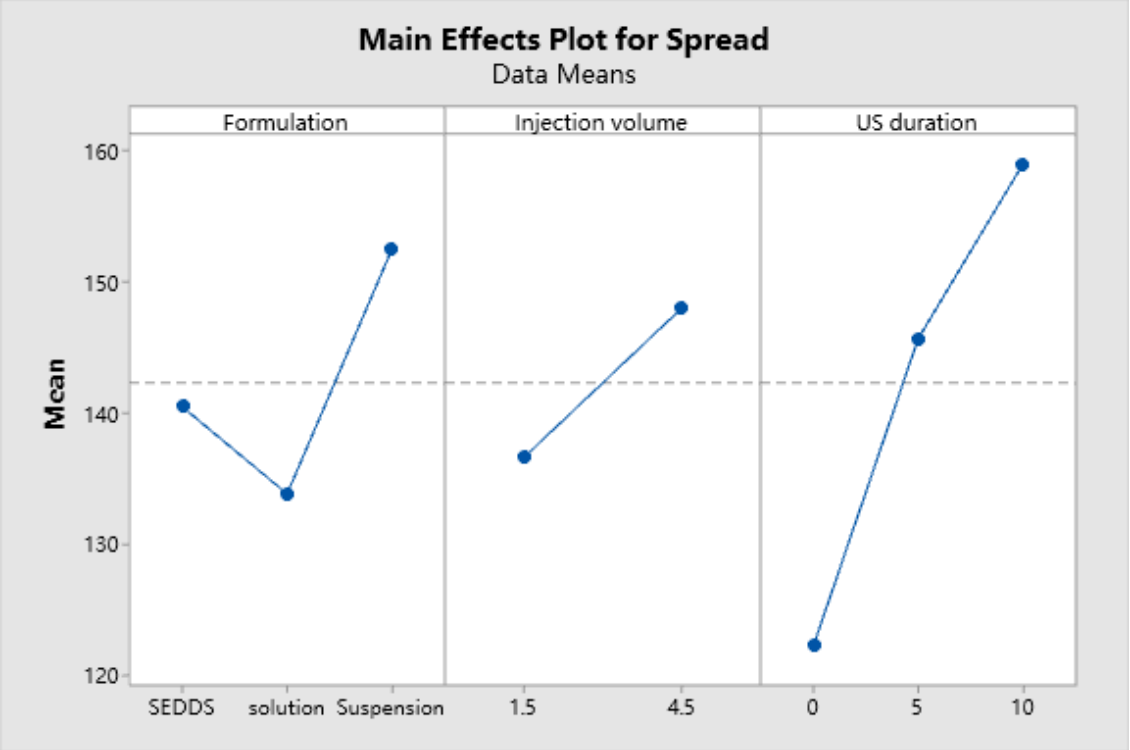

Interaction Plot for Spread